A Live Show in the Stomach

Monitoring *in vitro* and *in vivo* human gastric digestion with MRI

Ruoxuan Deng
邓若璇

A Live Show in the Stomach Monitoring *in vitro* and *in vivo* human gastric digestion with MRI Ruoxuan Deng

Propositions

1. Magnetic resonance markers have the potential to be used for monitoring food digestion at the molecular level. (this thesis)
2. In vitro digestion models are inaccurate but still essential. (this thesis)
3. Novel solutions in one domain often arise from existing knowledge in other domains.
4. Sales skills training may benefit scientists.
5. Holding strong opinions does not conflict with being open-minded.
6. During a pandemic, doing groceries is riskier than conducting human trials in a hospital.
7. You cannot blame others for their expectations that make you feel stressed.

Propositions belonging to the thesis entitled

A Live Show in the Stomach*: Monitoring in vitro and in vivo human gastric digestion with MRI*

Ruoxuan Deng

Wageningen, 11 May 2022

A LIVE SHOW IN THE STOMACH

Monitoring *in vitro* and *in vivo* human gastric digestion with MRI

Ruoxuan Deng

Thesis committee

Promotor

Prof. Dr Kees de Graaf

Professor of Sensory Science and Eating Behaviour

Wageningen University & Research

Co-promotors

Dr Anja E.M. Janssen

Associate professor, Food Process Engineering

Wageningen University & Research

Dr Paul A.M. Smeets

Senior Researcher, Division of Human Nutrition and Health

Wageningen University & Research

Dr Monica Mars

Associate professor, Division of Human Nutrition and Health

Wageningen University & Research

Other members

Prof. Dr Vincenzo Fogliano, Wageningen University & Research

Prof. Dr Alan Mackie, Leeds University, United Kingdom

Prof. Dr Ad Masclee, Maastricht University, The Netherlands

Dr Tim Lambers, FrieslandCampina, Wagningen, the Netherlands

This research was conducted under the auspices of the Graduate School VLAG (Advanced studies in Food Technology, Agrobiotechnology, Nutrition and Health Sciences)

A LIVE SHOW IN THE STOMACH

Monitoring *in vitro* and *in vivo* human gastric digestion with MRI

Ruoxuan Deng

Thesis

submitted in fulfilment of the requirements for the degree of doctor
at Wageningen University
by the authority of the Rector Magnificus,
Prof. Dr A.P.J. Mol
in the presence of the
Thesis Committee appointed by the Academic Board
to be defended in public
on Wednesday 11 May 2022 at 1:30 p.m.
in the Omnia Auditorium of Wageningen University

Ruoxuan Deng

A Live Show in the Stomach: Monitoring *in vitro* and *in vivo* human gastric digestion with MRI

PhD thesis, Wageningen University, Wageningen, the Netherlands (2022)

With references, with summary in English

ISBN: 978-94-6447-188-5

DOI: https://doi.org/10.18174/567833

Contents

Chapter 1

Introduction

Parts of this chapter have been published as:

Smeets, P. A. M., Deng, R., Van Eijnatten, E. J. M., & Mayar, M. (2021). Monitoring food digestion with magnetic resonance techniques. *Proceedings of the Nutrition Society*, 80(2), 148-158

Food is important to maintain human health. Modulating food intake can contribute to solving health issues, for example by reducing over-weight (Robinson et al., 2014). Food intake behavior can modulate total energy intake via affecting satiety, for example, a longer exposure period (because of the slower eating rate) usually leads to higher satiation effects (De Graaf & Kok, 2010). Food intake behavior is hugely influenced by food properties, from the perspectives of not only energy density (in other words: nutrient density) but also food structure. Moreover, food properties show also direct effects on food digestion and nutrient absorption and therefore physiology, food intake, nutritional status and health.

1.1 Food structure and protein

In recent years, research interest in food technology has increased in designing different food structures to modulate food digestibility and the release rate of nutrients (Capuano, Oliviero, Fogliano, & Pellegrini, 2018; Corstens et al., 2017; Foegeding, Stieger, & van de Velde, 2017; Sensoy, 2014). The food structure is a critical factor in the digestion rate (Bornhorst and Singh, 2014, Singh et al., 2015). The structure of dairy products shows a profound impact on the rate of nutrient digestibility, bioavailability and absorption (Mulet-Cabero, Mackie, Brodkorb, & Wilde, 2020). For example, the dense structure of a milk clot slows down casein digestion rate (Ye, Cui, Dalgleish, & Singh, 2016). In addition, another study showed that the structure of protein gels can be manipulated by varying the k-carrageenan concentration to encapsulate a health-promoting compound, and a denser gel structure delays digestion and thereby the release of the compound (Alavi et al., 2018).

Different food structures can be created by varying processing techniques and/or concentrations of ions or nutrients. For instance, a combination of constant shearing and heating on protein-gluten mixtures can create meat analogues (Schreuders et al., 2019); by adding different amount of acid and calcium ions, pectin solution can be transformed into a gel-like structure with different strength, since molecular interaction is changed due to the different electric charge on the molecules (Matia-Merino & Singh, 2007).

Protein is well known for its nutritional value as it is an important macro-nutrient for body metabolism, a good source of muscle builder, and an ingredient for providing satiation effects (Paddon-jones, Westman, Mattes, Wolfe, & Astrup, 2008). Protein is also an important structure contributor for many solid foods. Some examples of solid foods structured by protein are cheese, tofu and lean meat. Regarding the effect of food structure

on digestion, it is crucial to investigate the mechanisms underlying the digestion of protein-rich solid foods. For this purpose, protein gels have been widely used as model foods as these gels are easy-prepared and structure-alterable (Luo, Borst, Westphal, Boom, & Janssen, 2017; Remondetto, Beyssac, & Subirade, 2004; Sarkar et al., 2016).

1.2 Gastric digestion: the key for food structure breakdown

Digestion is the breakdown of food into small nutrient molecules that can be absorbed by human body. This important process takes place in our digestive system: the gastrointestinal tract (GI tract).

1.2.1 GI tract

The GI tract encompasses a series of complex physiological, mechanical and biochemical processing steps that lead to the breakdown of food structures, which ultimately allows absorption and utilization of nutrients (Mackie, 2019).

As shown in Fig. 1-1, digestion starts with the oral phase (ingestion) in the mouth. During oral processing, mastication and secretion of saliva lead to the formation of a food bolus that can be swallowed safely (Hutchings & Lillford, 1988). These oral processes are important not only for digestion, but also for the sensory perception of foods, eating enjoyment, and satiation (Krop et al., 2018). The second phase is gastric digestion, which involves the mixing of chyme and the addition of hydrochloric acid along with pepsin (a protease) and gastric lipase (Bornhorst, 2017). During gastric digestion, the food in the stomach is prepared for further digestion and absorption in the intestines. The small intestine comprises the duodenum, jejunum, and ileum. Food passes through the pyloric valve from the stomach into the small intestine, where pancreatic proteases, lipases, and amylases are added along with bile, resulting in mixed chyme. The chyme passes through the small intestine where most of the nutrients are absorbed. After that, it passes through the ileocecal valve into the last location: the large intestine. There, some of the remaining undigested food, such as dietary fiber, is fermented by bacteria into absorbable compounds such as short-chain fatty acids, and most of the remaining water is removed before defecation (Mackie, 2019).

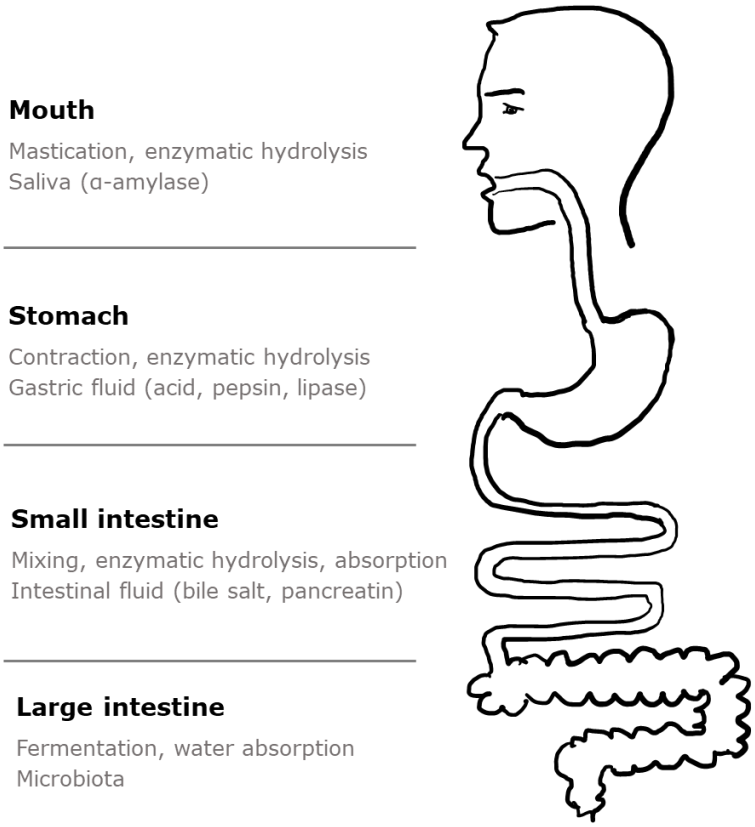

Fig.1-1 *Overview of the GI tract with the actions and key components.*

Across and within these different processing phases, there are numerous physiological signals (neural and hormonal) that feed forward and backwards, presumably to optimize digestion (Power & Schulkin, 2008). For example, the anticipation of food intake triggers several anticipatory physiological responses like increased salivation and production of gastric juice that prepare the body for the influx of nutrients (Smeets, Erkner, & De Graaf, 2010).

1.2.2 Gastric digestion

The stomach consists of four major parts: the fundus, corpus (or body), antrum, and pylorus (Fig. 1-2). For solid foods, especially protein-rich ones, gastric digestion is an important phase. As the stomach is the first organ where protein starts to be digested, by pepsin and gastric acid. Several processes are very important for food breakdown and optimal protein digestion in the stomach.

The first one is gastric motility: The stomach performs a wide variety of movements such as grinding, churning, kneading and propulsion. These motor activities that develop in response to the ingestion of a meal have a critical role in gastric digestion. The predominant movement is the regular peristaltic movement that originates from the distal part of the stomach (lower part of corpus and antrum) and develops towards the bottom (Ferrua & Singh, 2010). As a result of these movements, the particle size of food can be reduced so that the nutrients can be more efficiently accessed by the digestive enzymes.

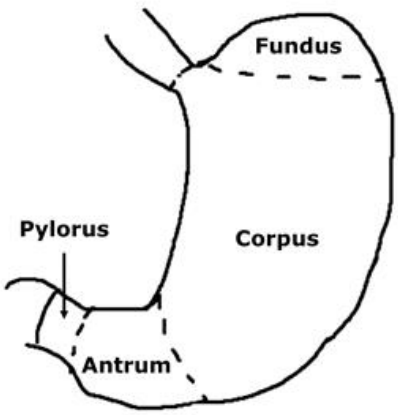

Fig. 1-2 *Illustration of a human stomach*

The second one is gastric secretion: different types of secretory cells are located in the stomach mucosa, and they are specialized to secrete different substances. For example, pepsinogen and gastric lipase are secreted by chief cells, hydrochloric acid (HCl) is from parietal cells, and mucus comes from mucus secreting cells (Schubert, 2010). The secretions help to break the food structure down via enzymatical hydrolysis; the low pH

created by the HCl guarantees the activity of pepsin to cleave the peptide bonds in protein (Piper & Fenton, 1965).

The third one is gastric emptying: after being processed in the stomach, the chyme is delivered to the duodenum. Gastric emptying is regulated by physiological feedback responses (hormones and neuro-systems) (Hellström, Grybäck, & Jacobsson, 2006). The emptying of food is affected by the nutrient density and rheological properties of the matrices (Mackie, 2019). Liquids are normally emptied faster than solid foods with equal nutrient density. For solid food, only the particles with sufficiently small size (less than 0.5–2 mm) can be squeezed through the pylorus (Kelly, 1980; Marciani et al., 2001; Meyer, 1980).

By virtue of these three processes, food is optimally digested, not only in a mechanical way (ground to smaller particles) but also in a biochemical way (hydrolyzed by gastric enzymes). Food properties play an important role in the gastric processes. The digestion rate of food particles in the stomach will likely influence the gastric emptying behavior directly and therefore affect satiety. For example, it was found that food with higher 'viscosity' suppressed appetite through reduced gastric emptying rate (Mackie, Rafiee, Malcolm, Salt, & van Aken, 2013). Therefore, it is important to understand how food structure affects gastric digestion and emptying.

1.3 In vitro digestion models: good tools to understand the mechanism

To understand gastric digestion, various approaches have been developed, including *in vivo* (human or animal) studies, *in silico* models, and *in vitro* digestion models.

In vivo human digestion research is essential, as it can demonstrate the physiological effects. However, it is also challenging due to biological complexity, practical constraints, and ethical obstacles. Notably, classic techniques to study gastric digestion *in vivo* are mostly indirect or invasive and involve, such as taking gastric aspirates through a nasogastric tube or monitoring gastric pressure or pH with sensors, measuring blood samples, or recording subjective satiety ratings (Fig. 1-3).

In the last years, *in silico* models are gaining interest to study the complex stream of mechanisms in the GI tract. These models can be used for modelling the enzymatic hydrolysis (Kondjoyan, Daudin, & Santé-Lhoutellier, 2015; Luo et al., 2019), gastric fluid dynamics (Ferrua & Singh, 2010; Li & Jin, 2021), and nutrient transit and absorption (Le Feunteun et al., 2014). However, the availability of *in silico* models remains limited and the models need to be further developed to be universally applicable.

In vitro model systems are widely used to study digestive processes under controlled and simplified conditions (Brodkorb et al., 2019). These model systems can be applied to acquire detailed information on the effects of enzymatic processes on the physical and chemical characteristics of food structures during digestion (Bornhorst & Singh, 2014; Luo, Boom, & Janssen, 2015).

With various *in vitro* digestion models, one or more digestion phases, such as gastric or intestinal digestion, can be mimicked (Muttakin, Moxon, & Gouseti, 2019). These models can also be applied to study the absorption of the digested material, by incorporating intestinal cell cultures (Marze, 2017). The models vary from simple static to highly sophisticated dynamic, computer-controlled gastrointestinal ones (Impact Food Bioact. Heal., 2015). In static models, the digestive fluid and food materials are constant, and hence, they are convenient for investigating the mechanisms of mass transport and structure breakdown under certain controlled conditions (Brodkorb et al., 2019; Kong & Singh, 2008; M. Minekus et al., 2014). Dynamic models, such as the TIM models (Mans Minekus, Marteau, Havenaar, & Veld, 1995) and the SHIME model (de Wiele et al.,, 2015), include

factors such as inflow of digestive fluid and gastric emptying (Guo et al., 2015). Therefore, such models are more physiologically realistic than static models.

With the use of *in vitro* models, multiple approaches can be combined to determine the progression of digestion by e.g. (bio-)chemical and physical analysis of digesta samples. Several chemical analysis approaches have been applied to measure food hydrolysis during digestion. For example, examining changes in the size of peptides or amount of free amino groups for protein digestion (Luo et al., 2015), glucose for starch digestion (Singh, Dartois, & Kaur, 2010), and free fatty acids for fat digestion (Golding & Wooster, 2010). From a physical perspective, rheology or texture analysis, sometimes combined with microscopy, are used to measure changes in physical properties such as viscosity, or in the structure of food particles (from macro to micro) during digestion (Fabek, Messerschmidt, Brulport, & Goff, 2014; Lorieau et al., 2018; Soukoulis, Fisk, Gan, & Hoffmann, 2016).

The advantages of using *in vitro* models include easy sampling, well-controlled and reproducible conditions, the ability to assess chemical processes in detail, and the absence of ethical restrictions. In addition, such simplified systems also make interpretation easier (within model boundaries), so multiple follow-up experiments can be readily done to further unravel observed phenomena. However, the validation of *in vitro* models remains a big challenge due to the inherent simplifications, such as the absence of physiological feedback mechanisms. For instance, secretion of digestive juices in response to a meal *in vivo* is regulated by the autonomic nervous system and several hormones, which is extremely challenging to replicate within *in vitro* models (Bornhorst & Singh, 2014). Moreover, *in vitro* studies often only provide the release of nutrients within the GI tract while *in vivo* (human) studies mostly measure biomarkers in blood, urine, or fecal. This displacement introduces difficulties to compare the *in vitro* and *in vivo* results. To aid the validation of *in vitro* models, it is of interest to investigate the potential of non-invasive and direct approaches feasible for both *in vivo* and *in vitro* monitoring of digestion.

1.4 MR: potential techniques to link in vitro and in vivo digestion research

Magnetic resonance (MR) techniques, for example time-domain nuclear magnetic resonance (TD-NMR) and magnetic resonance imaging (MRI), have shown potential as non-invasive approaches to examine gastric digestion. A central notion in this thesis is that MR techniques may be used to bridge the gap between *in vitro* and *in vivo* digestion research because they can be used to monitor relevant digestive processes both *in vitro* and *in vivo* (Fig. 1-3).

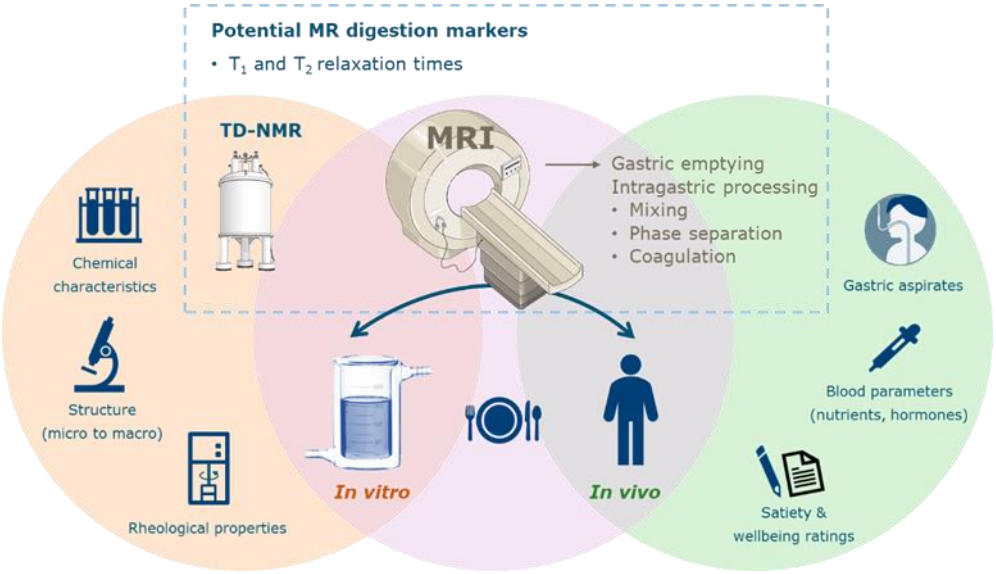

Fig. 1-3 *Overview of the proposed interdisciplinary approach to studying digestion by employing magnetic resonance (MR) techniques in combination with a variety of other measurements. Adapted from Smeets, Deng, Van Eijnatten, & Mayar (2020)*

TD-NMR provides information on the state of water protons in foods and has been widely used as a characterization and process quality control tool for different food systems (Hatzakis, 2019; van Duynhoven, Voda, Witek, & Van As, 2010). It is usually performed at relatively low magnetic field strengths (~0.5 Tesla) and can be used for measuring *in vitro* samples of digesta or gastric aspirates.

MRI is a commonly used related technique that, among numerous other applications e.g. in medical science, can be used to perform both *in vitro* and *in vivo* imaging measurements non-invasively (van Duynhoven et al., 2010). MRI is most commonly performed at 1.5 or 3 Tesla and yields two- or three-dimensional images. The images display areas with different

contrast due to different local physio-chemical properties (Hashemi, Bradley, & Lisanti, 2012; Kirtil & Oztop, 2016).

TD-NMR and MRI share the same underlying principles. They use magnetization in combination with radio-frequency (RF) pulses to obtain RF signals from nuclei of interest, usually water protons (1H) due to their natural abundance and sensitivity. For example, the contrast in MRI images is generated by the properties of the proton in different tissue types. Compared to MRI, the advantages of TD-NMR are low cost, ease of operation and detailed spectrum information, while the drawback is that TD-NMR can only be used to measure *in vitro* samples. MRI is capable to obtain *in vivo* or *in vitro* images which provides additional spatial information that cannot be acquired by TD-NMR. Therefore, they could supplement each other.

1.4.1 Anatomical changes

To date, in digestion research, MRI has mostly been used to observe macroscopic changes in the stomach contents throughout digestion by anatomical images (de Zwart & de Roos, 2010). Accordingly, MRI has been acknowledged as the best technique to provide a direct non-invasive measurement of gastric emptying. Moreover, by tweaking the sequences to be sensitive to different aspects of gastric contents, various targets can be reached, such as to measure the antral and small bowel motility and to observe the intragastric processes such as gastric mixing, phase separation, and coagulation (Marciani, 2011; Smeets et al., 2020).

Anatomical MRI images provide an abundance of straightforward information on what is taking place in the stomach at the macroscope level. In addition, other MR markers can be potential to indicate the change in molecular level during digestion (Smeets et al., 2020).

1.4.2 T_1 and T_2 relaxation times

Among several MR makers, longitudinal (T_1) and transverse (T_2) relaxation times are the most basic parameters measured with TD-NMR and MRI, but their use remains underexplored in digestion studies. Sometimes, the terms, longitudinal ($R_1 = T_1^{-1}$) and transverse ($R_2 = T_2^{-1}$) relaxation rates are used. In this section 1.4, the terms relaxation times will be used. T_1 and T_2 reflect how protons in a magnetic field relax back to their equilibrium position after excitation by an RF pulse. T_1 refers to the time it takes for the net magnetization to realign itself with the external magnetic field, Bo or z-axis while T_2

relaxation describes what happens in the x-y plane and is much shorter than T_1 relaxation (Blink, 2013). The main applications of T_1 and T_2 are based on the investigation of the relaxation behavior of water protons in different molecular environments (Mariette, 2009).

T_1 and T_2 measurements have been used to study various food properties *in vitro* such as moisture content, food structure, and macromolecule concentration (Kirtil et al., 2017). For instance, Ziegler et al. (2013) used T_1 measurements to predict water migration in starch-pectin gels during drying since T_1 decreases with the decrease of their moisture content. T_2 was used to predict the water holding capacity (WHC) of whey protein particles; a higher WHC is associated with a longer T_2. Similarly, T_2 has been used to study the swelling of hydrogels (Ozel et al., 2017; Peters et al., 2016). T_2 has also been used to study the local structure of cheese; due to the inhomogeneity of the cheese, three distinct T_2 relaxation components could be identified reflecting serum water (the water accumulated in the protein network), the water inside meshes of the casein gel-like network, and the water trapped within the casein matrix (Gianferri et al., 2007). In addition, T_2 can be used to determine the protein concentration in casein solutions; with increasing concentration the T_2 decreases (Le Dean et al., 2004). These examples show that T_1 and T_2 have the potential to be used to monitor changes in water migration, food structure, and the composition of food and digestive juice that take place during digestion.

Despite this, T_1 and T_2 measurements have only been carried out in a limited number of digestion studies. For instance, T_2 has been shown to be useful in detecting penetration of digestion fluid into the food matrix during *in vitro* digestion (Bordoni et al., 2014, 2011). Another study showed a linear association between the viscosity of locust bean gum meal and T_2 *in vitro*, and highlighted the possible application of T_2 to monitor changes in meal viscosity in the gastric lumen *in vivo* with the use of MRI (Marciani et al., 1998).

Because T_1 and T_2 are affected by many of such factors, careful validation is needed to be able to interpret changes in T_1 and T_2 in different digestion contexts. This requires further investigation under both *in vitro* and *in vivo* conditions with a combination of TD-NMR and MRI T_1 and T_2 measurements. As described previously, TD-NMR could provide detailed spectrum information and therefore may likely aid the interpretation of *in vitro* and *in vivo* relaxometry measurements with MRI. *In vivo* MRI may serve to validate and inform *in vitro* models, e.g., by using the same scan sequences for humans and *in vitro* digestion models.

In summary, anatomical MRI images can give a clear visualization of gastric content and serve as a 'camera' to indicate changes in the length scale of a few millimeters depending on the resolution. MR relaxation parameters might serve as markers to indicate changes on the molecular level. Their meaning in a digestion context needs to be further elucidated with *in vitro* and *in vivo* digestion studies. These markers have in theory a high potential to bridge *in vitro* and *in vivo* data, which could provide key insights in gastric protein digestion.

1.5 Aim and outline of the thesis

A better understanding of the gastric digestion of protein-rich solid food can help us to further explore the relationship between food properties and the physiological mechanisms underlying the digestion of nutrients and associated feelings of satiety. The breakdown of food structures has mainly been studied via *in vitro* models, which can provide detailed information about the effects of enzymatic processes on the physical and chemical characteristics of food structures. However, these results have been verified only to a limited extent *in vivo*. MRI is a promising tool to investigate gastric digestion in humans in more detail; T_1 and T_2 relaxation times are potentially well-suited to quantify changes in digestion over time in the stomach but require further development. Moreover, MRI may enable us to bridge the gap between *in vitro* and *in vivo* data as it is feasible for measuring *in vitro* samples and subsequently this information may contribute to interpreting the *in vivo* results.

The objective of this thesis is to obtain a better understanding of the breakdown of solid food by utilizing MR techniques to combine *in vitro* digestion data with *in vivo* digestion results.

Chapter 2 explores the potential of the MR parameter T_2 (or $R_2 = T_2^{-1}$) for monitoring the digestion of whey protein gels in a static *in vitro* digestion model. During digestion, the protein hydrolysis is measured by qualifying protein concentration in the supernatant; the change in R_2 of the supernatant is measured by TD-NMR and MRI. The relation between R_2 and protein concentrations during digestion is investigated.

Water plays an important role in T_2 measurements. We encountered water transportation (called swelling) during T_2 measurements. The effect of swelling on digestion is interesting to be understood. **Chapter 3** describes the effect of different swelling properties of whey protein gels differing in salt concentration on digestion rate in a static *in vitro* model. The acid and pepsin transportation are measured. The possible mechanism of how swelling would affect gastric digestion is discussed.

Towards the *in vivo* application of T_1 (or $R_1 = T_1^{-1}$) and T_2, in **Chapter 4,** an MRI compatible semi-dynamic *in vitro* gastric digestion model (MR-GAS) is developed; during digestion in MR-GAS, not only pH and protein concentration in the supernatant are

measured but also R_1 and R_2 of the supernatant are measured by TD-NMR and MRI. The use of R_1 and R_2 on monitoring digestion in MR-GAS is explored.

Chapter 5 moves forward to apply the MRI measurement on *in vivo* gastric digestion with a randomized cross-over human trial. Anatomical MRI scans and T_1 and T_2 scans are carried out to monitor the gastric digestion of different protein gels with human participants. The effect of nutrient density and food structure on oral processing and gastric emptying are studied. The extent of the feasibility of T_1 and T_2 on informing *in vivo* gastric digestion is investigated.

Chapter 6 provides a general discussion based on the results reported in this thesis and places the results in a broader perspective. The potential of MRI techniques on measuring gastric digestion and their contribution to bridging *in vitro* and *in vivo* digestion research is discussed. Moreover, directions for future research are suggested.

References

Alavi, F., Emam-Djomeh, Z., Yarmand, M. S., Salami, M., Momen, S., & Moosavi-Movahedi, A. A. (2018). Cold gelation of curcumin loaded whey protein aggregates mixed with k-carrageenan: Impact of gel microstructure on the gastrointestinal fate of curcumin. Food Hydrocolloids, 85(March), 267–280. https://doi.org/10.1016/j.foodhyd.2018.07.012

Blink, E. J. (2013). MRI : Physics. Version 1.3, 0–75. https://doi.org/10.1038/ni.2756-\rhttp://www.nature.com/ni/journal/v14/n12/abs/ni.2756.html#supplementary-information

Bordoni, A., Laghi, L., Babini, E., Di Nunzio, M., Picone, G., Ciampa, A., … Capozzi, F. (2014). The foodomics approach for the evaluation of protein bioaccessibility in processed meat upon *in vitro* digestion. Electrophoresis, 35(11), 1607–1614. https://doi.org/10.1002/elps.201300579

Bordoni, A., Picone, G., Babini, E., Vignali, M., Danesi, F., Valli, V., … Capozzi, F. (2011). NMR comparison of *in vitro* digestion of Parmigiano Reggiano cheese aged 15 and 30 months. Magnetic Resonance in Chemistry, 49(SUPPL. 1). https://doi.org/10.1002/mrc.2847

Bornhorst, G. M. (2017). Gastric mixing during food digestion: mechanisms and applications. Annual Review of Food Science and Technology, 8(1), 523–542. https://doi.org/10.1146/annurev-food-030216-025802

Bornhorst, G. M., & Singh, R. P. (2014). Gastric digestion *in vivo* and *in vitro*: how the structural aspects of food influence the digestion process. Annual Review of Food Science and Technology, 5(1), 111–132. https://doi.org/10.1146/annurev-food-030713-092346

Brodkorb, A., Egger, L., Alminger, M., Alvito, P., Assunção, R., Ballance, S., … Recio, I. (2019). INFOGEST static *in vitro* simulation of gastrointestinal food digestion. Nature Protocols, 14(4), 991–1014. https://doi.org/10.1038/s41596-018-0119-1

Capuano, E., Oliviero, T., Fogliano, V., & Pellegrini, N. (2018). Role of the food matrix and digestion on calculation of the actual energy content of food. Nutrition Reviews, 76(4), 274–289. https://doi.org/10.1093/NUTRIT/NUX072

Corstens, M. N., Berton-Carabin, C. C., de Vries, R., Troost, F. J., Masclee, A. A. M., & Schroën, K. (2017). Food-grade micro-encapsulation systems that may induce satiety via delayed lipolysis: A review. Critical Reviews in Food Science and Nutrition, 57(10), 2218–2244. https://doi.org/10.1080/10408398.2015.1057634

De Graaf, C., & Kok, F. J. (2010). Slow food, fast food and the control of food intake. Nature Reviews Endocrinology, 6(5), 290–293. https://doi.org/10.1038/nrendo.2010.41

de Wiele, T., den Abbeele, P., Ossieur, W., Possemiers, S., & Marzorati, M. (2015). The Simulator of the Human Intestinal Microbial Ecosystem (SHIME®). In K. Verhoeckx, P. Cotter, I. López-Expósito, C. Kleiveland, T. Lea, A. Mackie, … H. Wichers (Eds.), The Impact of Food Bioactives on Health: *in vitro* and ex vivo models (pp. 305–317). Cham: Springer International Publishing. https://doi.org/10.1007/978-3-319-16104-4_27

de Zwart, I. M., & de Roos, A. (2010). MRI for the evaluation of gastric physiology. European Radiology, 20(11), 2609–2616. https://doi.org/10.1007/s00330-010-1850-3

Fabek, H., Messerschmidt, S., Brulport, V., & Goff, H. D. (2014). The effect of invitro digestive processes on the viscosity of dietary fibres and their influence on glucose diffusion. Food Hydrocolloids, 35, 718–726. https://doi.org/10.1016/j.foodhyd.2013.08.007

Ferrua, M. J., & Singh, R. P. (2010). Modeling the fluid dynamics in a human stomach to gain insight of food digestion. Journal of Food Science, 75(7), 151–162. https://doi.org/10.1111/j.1750-3841.2010.01748.x

Foegeding, E. A., Stieger, M., & van de Velde, F. (2017). Moving from molecules, to structure, to

texture perception. Food Hydrocolloids, 68, 31–42. https://doi.org/10.1016/j.foodhyd-.2016.11.009

Gianferri, R., D'Aiuto, V., Curini, R., Delfini, M., & Brosio, E. (2007). Proton NMR transverse relaxation measurements to study water dynamic states and age-related changes in Mozzarella di Bufala Campana cheese. Food Chemistry, 105(2), 720–726. https://doi.org/10.1016/j.foodchem.2007.01.005

Golding, M., & Wooster, T. J. (2010). The influence of emulsion structure and stability on lipid digestion. Current Opinion in Colloid and Interface Science. https://doi.org/10.1016/j.cocis.2009.11.006

Guo, Q., Ye, A., Lad, M., Ferrua, M., Dalgleish, D., & Singh, H. (2015). Disintegration kinetics of food gels during gastric digestion and its role on gastric emptying: An *in vitro* analysis. Food and Function, 6(3), 756–764. https://doi.org/10.1039/c4fo00700j

Hashemi, R. H., Bradley, W. G., & Lisanti, C. J. (2012). MRI: The Basics: The Basics. Lippincott Williams & Wilkins.

Hatzakis, E. (2019). Nuclear Magnetic Resonance (NMR) Spectroscopy in Food Science: A Comprehensive Review. Comprehensive Reviews in Food Science and Food Safety, 18(1), 189–220. https://doi.org/10.1111/1541-4337.12408

Hellström, P. M., Grybäck, P., & Jacobsson, H. (2006). The physiology of gastric emptying. Best Practice and Research: Clinical Anaesthesiology, 20(3), 397–407. https://doi.org/10.1016/j.bpa.2006.02.002

Hutchings, J. B., & Lillford, P. J. (1988). The perception of food texture - the philosophy of the breakdown path. Journal of Texture Studies, 19(2), 103–115. https://doi.org/10.1111/j.1745-4603.1988.tb00928.x

Kelly, K. A. (1980). Gastric emptying of liquids and solids: Roles of proximal and distal stomach. American Journal of Physiology - Gastrointestinal and Liver Physiology, 2(2). https://doi.org/10.1152/ajpgi-.1980.239.2.g71

Kirtil, E., Cikrikci, S., McCarthy, M. J., & Oztop, M. H. (2017). Recent advances in time domain NMR & MRI sensors and their food applications. Current Opinion in Food Science, 17, 9–15. https://doi.org/10.1016/j.cofs.2017.07.005

Kirtil, E., & Oztop, M. H. (2016). 1H nuclear magnetic resonance relaxometry and magnetic resonance imaging and applications in food science and processing. Food Engineering Reviews, 8(1), 1–22. https://doi.org-/10.1007/s12393-015-9118-y

Kondjoyan, A., Daudin, J. D., & Santé-Lhoutellier, V. (2015). Modelling of pepsin digestibility of myofibrillar proteins and of variations due to heating. Food Chemistry, 172, 265–271. https://doi.org/10.1016/j.foodchem.2014.08.110

Kong, F., & Singh, R. P. (2008). A model stomach system to investigate disintegration kinetics of solid foods during gastric digestion. Journal of Food Science, 73(5), 202–210. https://doi.org/10.1111/j.1750-3841.2008.00745.x

Krop, E. M., Hetherington, M. M., Nekitsing, C., Miquel, S., Postelnicu, L., & Sarkar, A. (2018). Influence of oral processing on appetite and food intake – A systematic review and meta-analysis. Appetite, 125, 253–269. https://doi.org/10.1016/J.APPET.2018.01.018

Le Dean, A., Mariette, F., & Marin, M. (2004). 1H nuclear magnetic resonance relaxometry study of water state in milk protein mixtures. Journal of Agricultural and Food Chemistry, 52(17), 5449–5455. https://doi.org/10.1021/jf030777m

Le Feunteun, S., Barbé, F., Rémond, D., Ménard, O., Le Gouar, Y., Dupont, D., & Laroche, B. (2014). Impact of the dairy matrix structure on milk protein digestion kinetics: mechanistic

modelling based on mini-pig *in vivo* data. Food and Bioprocess Technology, 7(4), 1099–1113. https://doi.org/10.1007/s11947-013-1116-6

Li, C., & Jin, Y. (2021). A CFD model for investigating the dynamics of liquid gastric contents in human-stomach induced by gastric motility. Journal of Food Engineering, 296, 110461. https://doi.org/10.1016/j.-jfoodeng.2020.110461

Lorieau, L., Halabi, A., Ligneul, A., Hazart, E., Dupont, D., & Floury, J. (2018). Impact of the dairy product structure and protein nature on the proteolysis and amino acid bioaccessiblity during *in vitro* digestion. Food Hydrocolloids, 82, 399–411. https://doi.org/10.1016/j.foodhyd.2018.04.019

Luo, Q., Boom, R. M., & Janssen, A. E. M. (2015). Digestion of protein and protein gels in simulated gastric environment. LWT - Food Science and Technology, 63(1), 161–168. https://doi.org/10.1016-/j.lwt.2015.03.087

Luo, Q., Borst, J. W., Westphal, A. H., Boom, R. M., & Janssen, A. E. M. (2017). Pepsin diffusivity in whey protein gels and its effect on gastric digestion. Food Hydrocolloids, 66, 318–325. https://doi.org/10.1016/j.foodhyd.2016.11.046

Luo, Q., Sewalt, E., Borst, J. W., Westphal, A. H., Boom, R. M., & Janssen, A. E. M. (2019). Analysis and modeling of enhanced green fluorescent protein diffusivity in whey protein gels. Food Research International, 120, 449–455. https://doi.org/10.1016/j.foodres.2018.10.087

Mackie, A. (2019). The digestive tract: A complex system. In Interdisciplinary Approaches to Food Digestion (pp. 11–27). Cham: Springer International Publishing. https://doi.org/10.1007/978-3-030-03901-1_2

Mackie, A. R., Rafiee, H., Malcolm, P., Salt, L., & van Aken, G. (2013). Specific food structures supress appetite through reduced gastric emptying rate. AJP: Gastrointestinal and Liver Physiology, 304(11), G1038–G1043. https://doi.org/10.1152/ajpgi.00060.2013

Marciani, L. (2011). Assessment of gastrointestinal motor functions by MRI: A comprehensive review. Neurogastroenterology and Motility, 23(5), 399–407. https://doi.org/10.1111/j.1365-2982.2011.01670.x

Marciani, L., Manoj, P., Hills, B. P., Moore, R. J., Young, P., Fillery-Travis, A., … Gowland, P. A. (1998). Echo-Planar Imaging Relaxometry to Measure the Viscosity of a Model Meal. Journal of Magnetic Resonance, 135(1), 82–86. https://doi.org/10.1006/jmre.1998.1560

Marciani, L., Gowland, P. A., Fillery-Travis, A., Manoj, P., Wright, J., Smith, A., … Spiller, R. C. (2001). Assessment of antral grinding of a model solid meal with echo-planar imaging. American Journal of Physiology-Gastrointestinal and Liver Physiology, 280(5), G844–G849. https://doi.org/10.1152-/ajpgi.2001.280.5.G844

Mariette, F. (2009). Investigations of food colloids by NMR and MRI. Current Opinion in Colloid and Interface Science, 14(3), 203–211. https://doi.org/10.1016/j.cocis.2008.10.006

Marze, S. (2017). Bioavailability of nutrients and micronutrients: advances in modeling and *in vitro* approaches. Annual Review of Food Science and Technology, 8(1), 35–55. https://doi.org/10.1146/annurev-food-030216-030055

Matia-Merino, L., & Singh, H. (2007). Acid-induced gelation of milk protein concentrates with added pectin: Effect of casein micelle dissociation. Food Hydrocolloids, 21(5–6), 765–775. https://doi.org/10.1016-/j.foodhyd.2006.12.007

Meyer, J. H. (1980). Gastric emptying of ordinary food: effect of antrum on particle size. American Journal of Physiology - Gastrointestinal and Liver Physiology, 2(3), 133–135. https://doi.org/10.1152/ajpgi.-1980.239.3.g133

Minekus, M., Alminger, M., Alvito, P., Ballance, S., Bohn, T., Bourlieu, C., … Brodkorb, A. (2014).

A standardised static *in vitro* digestion method suitable for food-an international consensus. Food and Function, 5(6), 1113–1124. https://doi.org/10.1039/c3fo60702j

Minekus, Mans, Marteau, P., Havenaar, R., & Veld, J. H. J. H. in't. (1995). A multicompartmental dynamic computer-controlled model simulating the stomach and small Intestine. Alternatives to Laboratory Animals, 23(2), 197–209. https://doi.org/10.1177/026119299502300205

Mulet-Cabero, A. I., Mackie, A. R., Brodkorb, A., & Wilde, P. J. (2020). Dairy structures and physiological responses: a matter of gastric digestion. Critical Reviews in Food Science and Nutrition, 60(22), 3737–3752. https://doi.org/10.1080/10408398.2019.1707159

Muttakin, S., Moxon, T. E., & Gouseti, O. (2019). *In vivo*, *in vitro*, and *in silico* studies of the GI Tract. In O. Gouseti, G. M. Bornhorst, S. Bakalis, & A. Mackie (Eds.), Interdisciplinary Approaches to Food Digestion (pp. 29–67). Cham: Springer International Publishing. https://doi.org/10.1007/978-3-030-03901-1_3

Ozel, B., Uguz, S. S., Kilercioglu, M., Grunin, L., & Oztop, M. H. (2017). Effect of different polysaccharides on swelling of composite whey protein hydrogels: A low field (LF) NMR relaxometry study. Journal of Food Process Engineering, 40(3), 1–9. https://doi.org/-10.1111/jfpe.12465

Paddon-jones, D., Westman, E., Mattes, R. D., Wolfe, R. R., & Astrup, A. (2008). Protein, weight management, and satiety 1– 4. American Journal of Clinical Nutrition, 87, 1558–1561.

Peters, J. P. C. M., Vergeldt, F. J., Van As, H., Luyten, H., Boom, R. M., & van der Goot, A. J. (2016). Time domain nuclear magnetic resonance as a method to determine and characterize the water-binding capacity of whey protein microparticles. Food Hydrocolloids, 54, 170–178. https://doi.org/10.1016/j.foodhyd.2015.09.031

Piper, D. W., & Fenton, B. H. (1965). pH stability and activity curves of pepsin with special reference to their clinical importance. Gut, 6(5), 506–508. https://doi.org/10.1136/gut.6.5.506

Power, M. L., & Schulkin, J. (2008). Anticipatory physiological regulation in feeding biology: Cephalic phase responses. Appetite, 50(2–3), 194–206. https://doi.org/10.1016/-j.appet.2007.10.006

Remondetto, G. E., Beyssac, E., & Subirade, M. (2004). Iron availability from whey protein hydrogels: an *in vitro* study. Journal of Agricultural and Food Chemistry, 52(26), 8137–8143. https://doi.org/10.1021/jf040286h

Robinson, E., Almiron-Roig, E., Rutters, F., De Graaf, C., Forde, C. G., Smith, C. T., … Jebb, S. A. (2014). A systematic review and meta-analysis examining the effect of eating rate on energy intake and hunger. American Journal of Clinical Nutrition, 100(1), 123–151. https://doi.org/10.3945/ajcn.113.081745

Sarkar, A., Murray, B., Holmes, M., Ettelaie, R., Abdalla, A., & Yang, X. (2016). *In vitro* digestion of Pickering emulsions stabilized by soft whey protein microgel particles: influence of thermal treatment. Soft Matter, 12(15), 3558–3569. https://doi.org/10.1039/c5sm02998h

Schreuders, F. K. G., Dekkers, B. L., Bodnár, I., Erni, P., Boom, R. M., & van der Goot, A. J. (2019). Comparing structuring potential of pea and soy protein with gluten for meat analogue preparation. Journal of Food Engineering, 261(January), 32–39. https://doi.org/10.1016/-j.jfoodeng.2019.04.022

Schubert, M. L. (2010). Gastric secretion. Current Opinion in Gastroenterology, 26(6), 598–603. https://doi.org/-10.1097/MOG.0b013e32833f2010

Sensoy, I. (2014). A Review on the Relationship Between Food Structure, Processing, and Bioavailability. Critical Reviews in Food Science and Nutrition, 54(7), 902–909. https://doi.org/10.1080/10408398.2011.619016

Singh, J., Dartois, A., & Kaur, L. (2010). Starch digestibility in food matrix: a review. Trends in Food Science and Technology. https://doi.org/10.1016/j.tifs.2009.12.001

Smeets, P. A. M., Deng, R., Van Eijnatten, E. J. M., & Mayar, M. (2020). Monitoring food digestion with magnetic resonance techniques. Proceedings of the Nutrition Society, (3), 1–11. https://doi.org/10.1017-/S0029665120007867

Smeets, P. A. M., Erkner, A., & De Graaf, C. (2010). Cephalic phase responses and appetite. Nutrition Reviews, 68(11), 643–655. https://doi.org/10.1111/j.1753-4887.2010.00334.x

Soukoulis, C., Fisk, I. D., Gan, H. H., & Hoffmann, L. (2016). Intragastric structuring of anionic polysaccharide kappa-carrageenan filled gels under physiological *in vitro* digestion conditions. Journal of Food Engineering, 191, 105–114. https://doi.org/10.1016/j.jfoodeng.2016.07.009

The Impact of Food Bioactives on Health. (2015). The Impact of Food Bioactives on Health. https://doi.org/10.1007/978-3-319-16104-4

van Duynhoven, J., Voda, A., Witek, M., & Van As, H. (2010). Time-domain NMR applied to food products. Annual Reports on NMR Spectroscopy (1st ed., Vol. 69). Elsevier Ltd. https://doi.org/10.1016/S0066-4103(10)69003-5

Ziegler, G. R., MacMillan, B., & Balcom, B. J. (2003). Moisture migration in starch molding operations as observed by magnetic resonance imaging. Food Research International, 36(4), 331–340. https://doi.org/10.1016/S0963-9969(02)00224-7

Chapter 2

Exploring *in vitro* gastric digestion of whey protein by time-domain nuclear magnetic resonance and magnetic resonance imaging

This chapter has been published as:

Deng, R., Janssen, A. E. M., Vergeldt, F. J., Van As, H., de Graaf, C., Mars, M., & Smeets, P. A. M. (2020). Exploring *in vitro* gastric digestion of whey protein by time-domain nuclear magnetic resonance and magnetic resonance imaging. *Food Hydrocolloids*, 99, 105348.

Abstract

Gastric digestion is crucial for protein breakdown. Although it has been widely studied with *in vitro* models, verification *in vivo* remains a big challenge. Magnetic resonance imaging (MRI) has the potential to bridge this gap. Our objective was to use the transverse relaxation time (T_2) and rate ($R_2 = T_2^{-1}$) to monitor hydrolysis of protein-rich food during *in vitro* gastric digestion. Whey protein solution and heat-induced hydrogels were digested by means of simulated gastric fluid (SGF). Free amino groups ($-NH_2$ groups) and protein concentration in the supernatant were measured. T_2 and R_2 of the digestion mixture were determined by time-domain nuclear magnetic resonance (TD-NMR) and MRI. Subsequently, relative amplitudes (TD-NMR) for different T_2-values and T_2 distribution (MRI) were determined. For the solution, protein concentration and T_2 did not change during digestion. For the gels, water in supernatant and gel phase could be discriminated on the basis of their T_2-values. During digestion, R_2 of supernatant correlated positively with protein ($-NH_2$ groups) concentration in SGF. Also, the decrease in relative amplitude of gel fraction correlated linearly with the supernatant protein concentration. MRI T_2-mapping showed similar associations between R_2 of supernatant and protein ($-NH_2$ groups) concentration. In conclusion, T_2-measurements by TD-NMR and MRI can be used to monitor *in vitro* gastric digestion of whey protein gels; TD-NMR measurements contributed to interpreting the MRI data. Thus, MRI has high potential for monitoring *in vivo* gastric digestion and this should be further pursued.

2.1 Introduction

Gastric digestion is a crucial step for the breakdown of protein-rich foods (Singh and Gallier, 2014). Both gastric fluid, consisting of acid and pepsin, and the mechanical movement of the stomach are essential for the digestive process (Bornhorst and Singh, 2014). The kinetics of gastric digestion plays a key role in subsequent physiological processes such as gastric emptying and nutrient absorption. *In vitro* digestion models have been developed as useful tools to investigate digestion (Brodkorb et al., 2019; Kong and Singh, 2008; Minekus et al., 2014). The chemical composition of digesta sampled from these model systems can then be analysed, for example with the OPA (o-phthaldialdehyde) method, sodium dodecyl sulfate–polyacrylamide gel electrophoresis (SDS-PAGE), size-exclusion chromatography and mass spectrometry (Luo et al., 2015; MacIerzanka et al., 2012; Nyemb et al., 2016). However, verifying *in vitro* findings *in vivo* (especially in humans) remains a big challenge. Here, we propose that magnetic resonance techniques have the capability to monitor the gastric digestion of protein and can be used to bridge the gap between *in vitro* model systems and *in vivo* digestion.

Time domain nuclear magnetic resonance (TD-NMR) provides information on the state of water proton in foods, and has been widely used as a characterization and process quality control tool in different food systems (van Duynhoven et al., 2010). With TD-NMR, the transverse relaxation time (T_2) of water is determined via the transverse relaxation of ^1H protons. T_2 or the relaxation rate R_2 ($R_2 = T_2^{-1}$) of every water pool provides insight into the degree of exchange of either water protons with protein protons or the exchange of water between water pools such as bulk water with the (internal) water fraction in/around the proteins (Kirtil et al., 2017; Mariette, 2009; Peters et al., 2016). For instance, an earlier study showed a linear positive association between R_2 and casein concentration in solution (Le Dean et al., 2004). Different proton populations (e.g. having different chemical exchange and/or different mobility due to the local environment) arise at different T_2 values, and therefore can be used to discriminate different water fractions in the whole system (Bosmans et al., 2012; Munialo et al., 2016). Thus, the variation in T_2 (or R_2) and the corresponding proton population can be used to indicate the change of macromolecule concentration, water migration, structure in food matrices (Peters et al., 2016). As these above-mentioned changes also take place during digestion, we hypothesize that *in vitro* gastric digestion processes can be monitored by TD-NMR. Bordoni et al. (2014, 2011)

investigated *in vitro* digestion using TD-NMR, and found it can detect accessibility of digestion juice to the food matrix during digestion. Therefore, it is worthwhile to further explore other possibilities of TD-NMR to quantify the hydrolysis of protein during digestion.

Magnetic resonance imaging (MRI) is a non-invasive technique that, among numerous other applications, can be used to examine gastric emptying *in vivo*. MRI can not only provide information on the volume of the gastric content and gastric emptying, but also on intra-gastric air, phase separation and clot formation (Marciani, 2011; Spiller and Marciani, 2019). An earlier study showed that the viscosity of locust bean gum meal is linearly associated with R_2 *in vitro* ($R^2 = 0.99$), and highlighted the possibility to monitor changes in meal viscosity in the gastric lumen *in vivo* by measurement of T_2 (Marciani et al., 1998). However, to our knowledge, the potential of T_2 mapping by MRI for monitoring the hydrolysis of nutrients during gastric digestion has not been further explored. Likewise, MRI has also been applied for visualizing the food state spatially (i.e. water content, fat content, molecular migration, structure change) *in vitro* (Collewet et al., 2013; Lavenson et al., 2011; Li et al., 2018; Nott and Hall, 2005). Because they share similar relaxation principles, T_2 measurements by MRI can be validated with TD-NMR experiments, which can provide extra information on the relaxation parameters (Mariette, 2009). Compared with TD-NMR, T_2-mapping by MRI holds the advantage of visualizing T_2 spatially and the possibility to study digestion *in vivo* in humans. Therefore, we explore if T_2-mapping is a useful method to investigate *in vitro* gastric digestion of protein and bridge the gap between *in vitro* and *in vivo* studies.

The objective of this study was to use T_2 measurements by TD-NMR and MRI to monitor protein hydrolysis during *in vitro* gastric digestion, so as to lay a foundation for further *in vivo* studies. We used whey protein solution and heat-induced whey protein hydrogels since these are widely used as liquid and solid protein-rich model foods (MacIerzanka et al., 2012; Nyemb-Diop et al., 2016; Nyemb et al., 2016; Singh et al., 2015). First, the digestion process was monitored by quantifying free amino groups (-NH_2 groups) and protein concentration in digestion supernatant during *in vitro* gastric digestion; Second, T_2 and R_2 were measured during *in vitro* gastric digestion with the use of TD-NMR and MRI; Third, the associations between R_2 (TD-NMR) and protein hydrolysis was examined; Finally,

MRI T_2 measurements were used to investigate the feasibility of monitoring protein gel digestion.

2.2 Methods and methods

2.2.1 Materials

Pepsin from porcine gastric mucosa (3412 activity units/mg) and all other chemicals were purchased from Sigma Aldrich, Inc. (St. Louis, USA). Whey Protein Isolate (WPI) was purchased from Davisco Food International, Inc. (Le Sueur, USA), with protein content of 97.9 g/100 g dry solid. Milli-Q water (resistivity 18.2 MΩcm at 25 °C, Merck Millipore, Billerica, USA) was used in all experiments.

2.2.2 Preparation of protein solution and gel

WPI solution and gel were prepared as described by Luo et al (2015). WPI was dissolved in water (15 wt% or 20 wt%) and stirred at room temperature for at least 2 h. The protein solutions were used within one day. To prepare the gels, the solutions were centrifuged at 1000 rpm for 10 min to eliminate air bubbles, and were poured into Teflon tubes and then heated in a 90 °C water bath for 30 min. After that, the Teflon tubes were immediately cooled in an ice-water bath. The gels were stored within the Teflon tubes at 4 °C, 1-5 days prior to use. The gels were grinded into 30.0 ± 5.0 mg particles before the digestion.

2.2.3 Preparation of simulated gastric fluid

Phosphate buffer (Na2HPO4-H3PO4-NaCl buffer, pH 2.0, I =154 mM) was used as the simulated gastric fluid (SGF), and pepsin was added to achieve activity at 2000 activity units/mL in the final mixture, as recommended by Minekus et al (2014) and Brodkorb et al (2019). For the control group, no pepsin was added to the SGF.

2.2.4 Time domain NMR

To prepare for the TD-NMR tests, 30 μL WPI solution or 30.0 mg gel was mixed with 120 μL SGF in 7-mm NMR tubes that were afterwards sealed to prevent water loss during the experiment. After mixing, the tubes were kept in an Eppendorf thermomixer (Eppendorf AG, Hamburg, Germany) at 37 °C and with shaking speed at 300 rpm and timing was started. At time 0, 10, 20, 30, 45, 60, 90 and 120 min, the tubes were moved from the thermomixer to a Maran Ultra NMR spectrometer (Resonance Instruments Ltd., Witney,

UK) to perform ^{1}H TD-NMR relaxometry at 0.72 T magnetic field strength (30.7 MHz ^{1}H resonance frequency).

The measurements were controlled by RINMR software (Resonance Instruments Ltd., Witney, UK). The decay of the transverse magnetization, a process characterized by the transverse relaxation time T_2, was measured by the Carr-Purcell-Meiboom-Gill (CPMG) sequence. During the CPMG pulse train, 12288 echoes (five data points per echo) were recorded. 8 transients were recorded with phase cycling, with a repetition time of 8 s. Each echo in the CPMG echo train was phase corrected and each echo was averaged to one data point using the IDL package (ITT Visual Information Solutions, Boulder, CO, USA). The transverse magnetization decay curves were analysed with a numerical inverse Laplace transform by CONTIN, resulting in a distribution of amplitude at different transverse relaxation times (T_2) (Provencher and Vogel, 1983). From the distribution curve, average T_2 and R_2 values of different components were acquired. For the gel samples, amplitude of gel peak was calculated by the sum of amplitude at every specific T_2 value within the gel peak; the relative amplitude of gel ($Rel.Ampl._{Gel}$) was calculated by dividing amplitude of the gel peak by the total amplitude in the whole distribution curve. Change of $Rel.Ampl._{Gel}$ was obtained by dividing the Rel.Ampl.Gel (time t) by Rel.Ampl.Gel (time 0). $\Delta Rel.Ampl._{Gel}$ was calculated by subtracting change of $Rel.Ampl._{Gel}$ in the control condition from that in the digestion condition at the same time point.

2.2.5 MRI scans during in vitro digestion

For the MRI scans, 5 g of WPI gel particles was mixed with 20 mL SGF in a tube (d = 3.5 mm) that was sealed to prevent water loss during the tests. In one batch, there were 12 tubes which contained triplicates of 4-types sample: 20% gel with SGF with/without pepsin and 15% gel with SGF with/without pepsin. After mixing, the batch of tubes was placed in a 3T MRI scanner (Siemens Magnetom Verio, Erlangen, Germany) and T_2 was measured at time 0 min with a 2D multi-echo spin echo (SE) sequence (repetition time (TR) = 400 ms, 10 echo times ranging from 13.2 to 132 ms with an echo-spacing of 13.2 ms, matrix = 192 × 95 mm, FOV = 400 × 283 mm, in-plane resolution = 2.1 mm, 5.0 mm slice thickness, total acquisition time 18.9 s suitable for breath holding) using a body coil enable future validation *in vivo*. After the scan, the tubes were placed in a water bath shaker at 37 °C, 150 rpm and timing were started. At time 10, 30, 45, 60, 90, 115 min, the tubes were transferred into the MRI scanner to repeat the T_2 measurement.

For each time point T_2 maps were calculated from the images of the ten echo times with the MRmap software which uses a Levenberg -Marquard two-parameter curve fitting (Messroghli et al., 2010). Subsequently, for each tube the T_2 maps were segmented manually with MIPAV software (Bazin et al., 2007), and the distribution of T_2 values was visualized in histogram; besides, the SGF and gel phase were segmented separated as illustrated in Fig. 2-S1, and the average T_2 and R_2 of the SGF phase voxels was calculated. The fraction of the gel phase ($Fraction_{Gel}$) was calculated by dividing the number of voxels in the gel phase by the total numbers of voxels in the digestion mixture. The change in $Fraction_{Gel}$ was obtained by dividing $Fraction_{Gel}$ (time t) by $Fraction_{Gel}$ (time 0). The $\Delta Fraction_{Gel}$ was calculated by subtracting the change of $Fraction_{Gel}$ in the control condition from that in the digestion condition.

2.2.6 In vitro gastric digestion

To measure protein hydrolysis, the amount of free amino groups and the protein concentration in supernatant were measured. The *in vitro* gastric digestion was performed under the same conditions as the TD-NMR measurements. At time 0, 10, 20, 30, 45, 60, 90, 120 min, the supernatant was withdrawn and heated by a pre-heated Eppendorf thermomixer at 90 °C, 850 rpm for 5 min to deactivate pepsin.

2.2.6.1 Determination of free amino acid groups

The OPA method as described by Luo et al (2015) was applied. First, 3.81 g Borax and 100 mg SDS were added to 80 mL Milli-Q water. After these reagents were completely dissolved, 80 mg o-Phthaldialdehyde was dissolved in 2 mL ethanol and added to the above-mentioned solution. Next, 88 mg of DL-dithiothreitol was added and further mixed. Finally, the solution was filled up to 100 mL with Milli-Q water and filtered using a 0.45 mm syringe filter. The solution was kept in the dark. A DU 720 spectrophotometer (Beckman Coulter Inc., Pasadena, USA) was set at 340 nm blanked with 1.5 mL OPA reagent and 0.2 mL Milli-Q water.

To make a calibration curve, 200 µL of 50 mg/L, 100 mg/L, 150 mg/L and 200 mg/L L-serine standard solutions were added to 1.5 mL OPA reagent in a cuvette, and mixed by pipetting for 5 s. The mixtures were measured with the spectrophotometer after standing for 3 min. The same procedure was applied to samples from the digestion experiments.

2.2.6.2 Protein concentration in supernatant

The protein concentration (the sum of all protein fractions with different sizes) in supernatant was measured with a Bicinchoninic Acid (BCA) kit (Sigma Aldrich, Inc). For the calibration curve, 100 µL of 200 µg/mL, 400 µg/mL, 600 µg/mL, 800 µg/mL and 1000 µg/mL bovine serum albumin (BSA) standard solutions were added to 2 mL BCA reagent and incubated at 37 °C for 30 min. After cooling down to room temperature, the mixtures were transferred into a cuvette and measured at 562 nm in a spectrophotometer (DU 720). The same procedure was applied to samples from the digestion experiments.

2.2.7 Swelling property of gel

To measure the swelling property of the gels, gel slices with a thickness of 5 mm were soaked in 30 mL SGF without pepsin. At time points 15, 30, 60, 120 min, the gel slices were taken out of the SGF and dried with tissue paper to remove excess liquid, and then weighed. The swelling ratio was calculated as:

$$\textit{S}\text{welling ratio } (\%) = \frac{m_t - m_0}{m_0} \times 100\% \qquad (2.1)$$

where m_t represents the weight of the gel at time t and m_0 is the initial weight of the gel.

2.3 Results and discussion

2.3.1 NMR relaxometry of WPI solution or gel

NMR relaxometry was used to measure the T_2 distribution of the WPI solution or the WPI gel (Fig. 2-1). Due to differences in mobility, local environment and chemical exchange, different proton populations arise at different T_2 values (Peters et al., 2016). This results in the different peaks in the T_2 distribution curve. Thus, the peaks are thought to reflect different components in the digestion mixture. Fig. 2-1a shows that the major population has a T_2 value around 1700 ms. Since protein solution was mixed with SGF, this major peak represents water protons of the whole mixture (including protein solution and SGF). This value is smaller than the T_2 value of free water, which is 2000-3000 ms, because of the fast proton exchange with protein components (Hills et al., 1990). The peak at 7-8 ms might be an fitting error or represent the protein-bound protons, as also observed by Dekkers et al (2016).

Fig. 2-1b shows the T_2 distribution of 15% WPI gel with SGF before digestion. Similar to the WPI solution of Fig. 2-1a, the peak of shortest T_2 at 8 ms represents the protein-bound proton population; the peak of longest T_2 at 2400 ms represents the water proton population in the supernatant phase, labelled with Supernatant. In contrast to Fig. 2-1a, there is one component with an average T_2 of 76 ms. This component represents the water protons located in the protein gel, labelled as Gel. The ratio between the amplitudes of peak Gel and peak Supernatant is around 0.22 which is comparable with the water content ratio (0.21) of protein gel and supernatant. Therefore, further discussion on TD-NMR in this paper will be focused on peak Gel and peak Supernatant to understand the change in both gel phase and supernatant phase during *in vitro* digestion.

We hypothesized that during digestion the average T_2 of supernatant (NMR) would decrease if more protein fraction is released into the digestion mixture. In our digestion system with gels, the relative amplitude of both peak Gel and peak Supernatant would change (e.g., decrease in peak Gel) due to the breakdown of the gels.

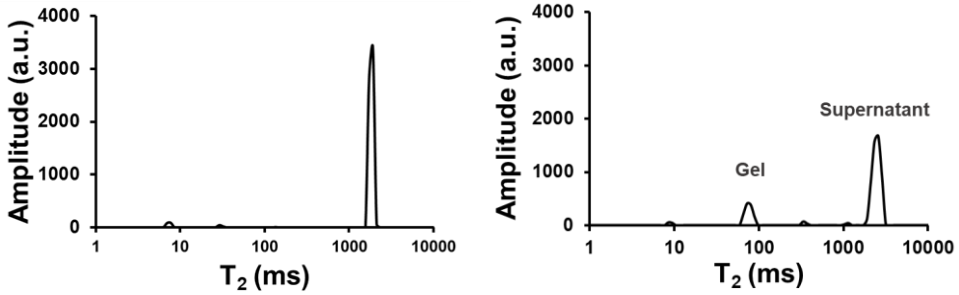

(a) (b)

Fig. 2-1 *The T_2 (TD-NMR) distribution of 20% WPI solution (a) and 15% WPI gel (b) with SGF at digestion time 0 min.*

2.3.2 In vitro digestion of WPI solution by NMR relaxometry

Fig. 2-2a shows the concentration of free amino groups (-NH_2 groups) in the digestion mixture, to quantify the digestion of WPI solution. The concentration of -NH_2 groups increased sharply under digestion conditions, while the concentration in the control condition remained low. This confirms that digestion took place. The protein concentration remained constant over time under both the control and digestion conditions (Fig. 2-2b).

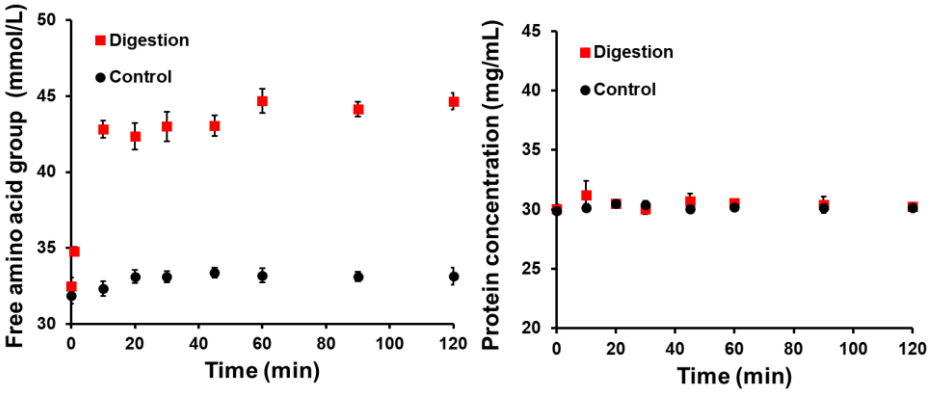

(a) (b)

Fig. 2-2 *Free amino groups (a) and protein concentration (b) during an in vitro gastric digestion experiment using 20% WPI solution. The control group is without pepsin. Error bars are based on the standard deviation of two or three experiments.*

The TD-NMR measurements of the 20% WPI solution are shown in Fig. 2-3. Under digestive conditions there was no statistically significant change ($p = 0.23$, t-test) in the T_2 distribution during *in vitro* digestion (Fig. 2-3a). In contrast, in the control condition there

was a significant decrease ($p < 0.05$, t-test) in average T_2 from 1837 ± 69 ms (Mean ± Standard deviation) at 0 min to 1376 ± 134 ms at 120 min (Fig. 2-3b). The reason for this might be the decrease of the proton mobility which is caused by protein solubility change induced by acidification in the control condition. Acidification and solubility change also take place during digestion, however, due to the action of pepsin, their effects are compensated by the enhanced solubility of proteins and peptides (Dinakar and Kilara, 1996).

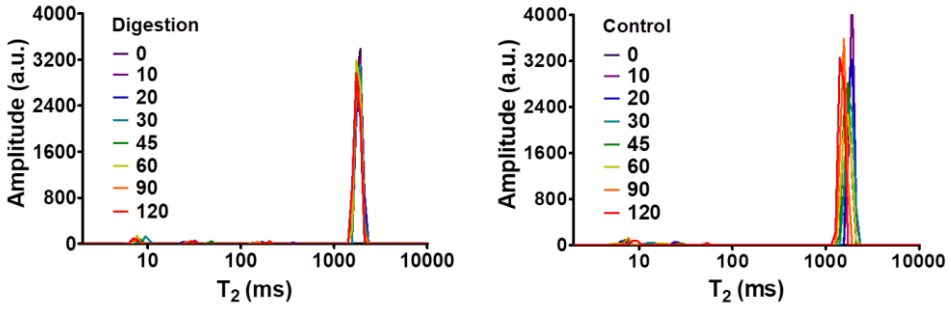

(a) (b)

Fig. 2-3 *The T_2 (TD-NMR) distribution of 20% WPI solution under digestion condition (a) and control condition (without pepsin) (b). Curves with colors from black to red represent time points from 0 to 120 min.*

After 120 min digestion, the degree of hydrolysis (DH) of whey protein solution was around 3.5%. This confirms that native whey protein is the most resistant protein to peptic hydrolysis (Schmidt et al., 1995). Besides, the protein concentration remained the same during digestion. This might be the reason that the T_2 or R_2 ($= T_2^{-1}$) remained unchanged during digestion. Overall, these results indicate that the T_2 values acquired with NMR do not reflect WPI solution hydrolysis during *in vitro* gastric digestion.

2.3.3 In vitro digestion of WPI gel and NMR relaxometry

To study the digestion of structured model foods, 15% WPI gel and 20% WPI gel were used. Protein hydrolysis was quantified by measuring the concentration of $-NH_2$ groups in supernatant over time (Fig. 2-4a). In agreement with previous studies, 15% gel was digested faster than 20% gel, which is due to the summed effect of diffusion limitation, hydrolysis rate and microstructure transformation (Luo et al., 2017).

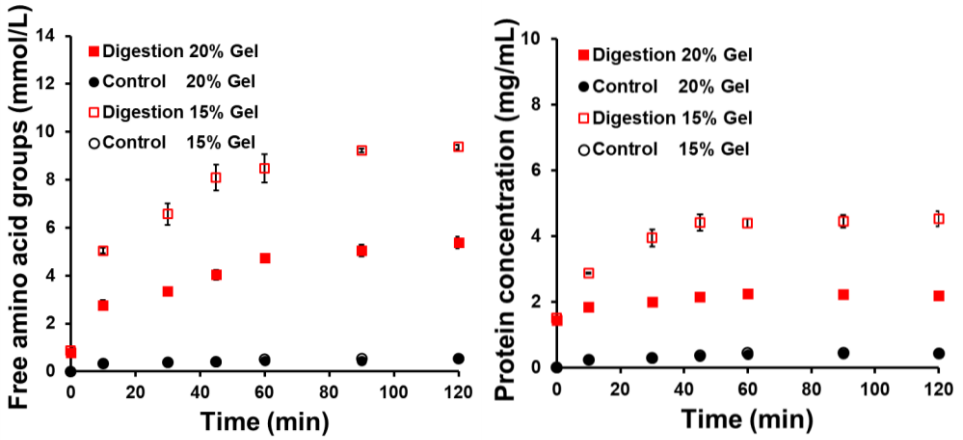

(a) (b)

Fig. 2-4 *Free amino groups (a) and protein concentration (b) in SGF of 20% and 15% WPI gel during in vitro gastric digestion. The control groups are without pepsin. Error bars are based on the standard deviation of two or three experiments.*

The protein concentration in supernatant (Fig. 2-4b) was in line with the concentration of -NH_2 groups during *in vitro* gastric digestion: positive linear correlations (R^2 = 0.97 for 15% WPI gel and R^2 = 0.94 for 20% WPI gel) was found (not shown in the figure). After 120 min of digestion, the DH in the supernatant of 15% and 20% was around 23.5%; this indicates that the protein fraction released in the supernatant was highly hydrolysed.

Fig. 2-5 shows distributed T_2 (TD-NMR) relaxation times of the digestion mixture of 15% gel and 20% gel during *in vitro* digestion. Under digestion conditions, the peak SGF shifted towards shorter T_2 values (Fig. 2-5a), while there was no significant change of the peak Supernatant under control conditions (Fig. 2-5b). Over the course of digestion, more protein fraction (-NH_2 groups) are transported from the gel particle into the supernatant, increasing fast proton exchange which results in decreased T_2 of bulk water (water in supernatant). A larger decrease in T_2-supernatant was observed in 15% compared with 20% gel, which is consistent with the faster digestion of 15% gel. Based on the study by Le Dean et al (2004), a linear relation between R_2 and protein concentration is expected. Since in this case the concentration of -NH_2 groups is in line with the protein concentration in supernatant, R_2 of supernatant is likely to be associated with protein concentration, and even -NH_2 concentration.

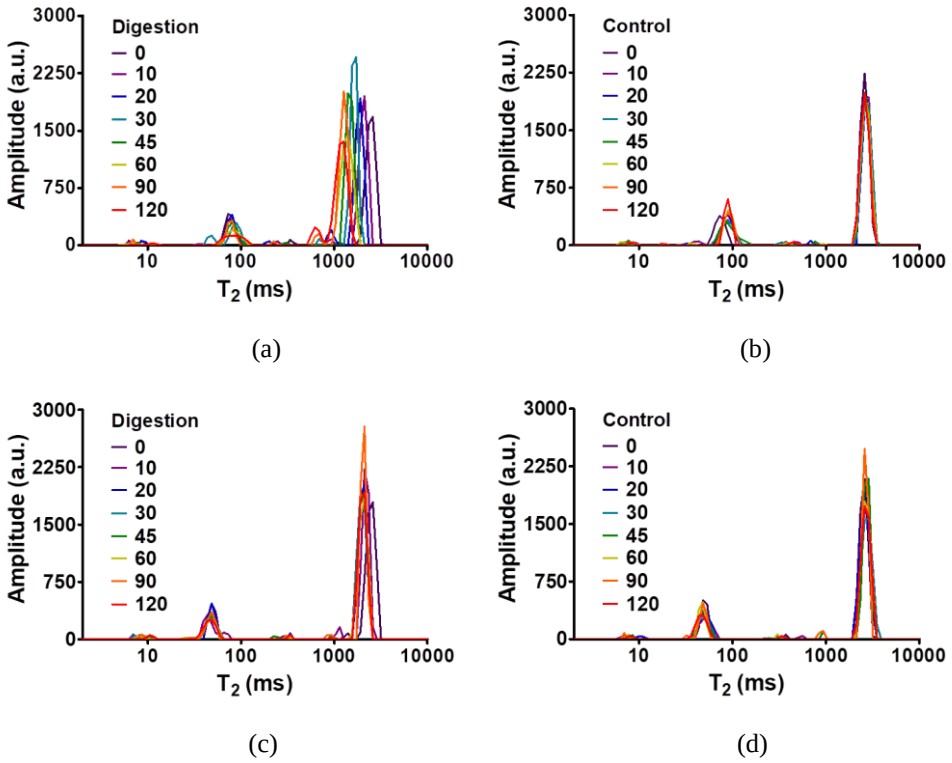

Fig. 2-5 *The T_2 (TD-NMR) distribution of 15% WPI gel under digestion condition (a) and control condition (without pepsin) (b) and that of 20% WPI gel under digestion condition (c) and control condition (d) over time. Curves with colors from black to red represent time points from 0 to 120 min.*

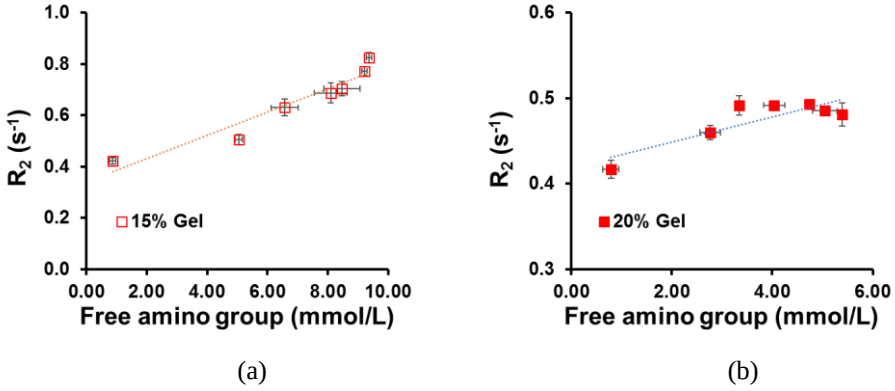

Fig. 2-6 *Correlation between concentration of free amino groups with average R_2 of supernatant of 15% WPI gel (a, R^2 = 0.91) and 20% WPI gel (b, R^2 = 0.71) during in vitro gastric digestion. Error bars are based on the standard deviation of two or three experiments.*

Therefore, associations between the -NH_2 group concentration and the average R_2-supernatant during *in vitro* digestion of both 15% and 20% gel were plotted (with R^2 = 0.91

for 15% gel and R^2 = 0.71 for 20% gel) (Fig. 2-6). Stronger association for 15% gel is probably due to the faster digestion; more peptide released to the supernatant increases the accuracy of detection. The observed linear relationship demonstrates that the digestion of protein gel, as indicated by the increase of -NH_2 group concentration in supernatant, is positively associated with increase of the average R_2 of supernatant. Thus, the average R_2-SGF (TD-NMR) can be used to track the *in vitro* digestion of WPI gel, by indicating the amount of protein fraction (the concentration of -NH_2 groups) in supernatant.

The relative amplitude of gel fraction (Rel.Ampl.$_{Gel}$) during *in vitro* digestion is shown in Fig. 2-7a. Under control conditions, the Rel.Ampl.$_{Gel}$ for the 15% gel increased, and that for the 20% gel it slightly decreased in the beginning but then increased to the initial value. In contrast, under digestion conditions the Rel.Ampl.$_{Gel}$ of both 15% and 20% gel decreased over time. Changes in Rel.Ampl.$_{Gel}$ might be caused by two factors: 1) gel structure breakdown, resulting in transferring of protons from solid gel into liquid supernatant, which mainly happens under digestion conditions; and 2) swelling pressure-induced water migration (Flory and Rehner, 1943; Quesada-Pérez et al., 2011; van der Sman, 2015), which results in either swelling or shrinking of the gels (this can take place under both digestion and control conditions).

Therefore, to further elucidate the mechanism, the swelling/shrinking properties were measured (Fig. 2-7b). The results indicate that with 15% gel there was 5.7% swelling in 120 min, while for 20% gel slight shrinking in the first 30 min and then 1% swelling after 120 min was observed. These different swelling ratios of 15% and 20% gel are thought to be due to the difference in cross-linking density of the gel (de Kruif et al., 2015). This might confirm the pervious hypothesis on the change of Rel.Ampl.$_{Gel}$ under control conditions: the increase in relative amplitude of 15% gel is due to swelling, which causes a growing water proton population in the gel phase over time. In contrast, the 20% gel first shrank in SGF causing a slight decrease of Rel.Ampl.$_{Gel}$ in the beginning and then swelled back to its original state, coherent with the increase of Rel.Ampl.$_{Gel}$ to its original value. Compared with the control condition, for both 15% and 20% gel, larger decreases of Rel.Ampl.$_{Gel}$ under digestion conditions are due to breakdown of the gel phase. Therefore, to eliminate the effect of swelling/shrinking, ΔRel.Ampl.$_{Gel}$ was calculated by subtracting change of Rel.Ampl.$_{Gel}$ under control condition from that under digestion conditions. An negative linear association between ΔRel.Ampl.$_{Gel}$ and protein concentration in supernatant

was observed (Fig. 2-7c). This demonstrates that there were fewer protons in the gel phase with more protein present in the supernatant over time. Thus, the ΔRel.Ampl.$_{Gel}$ can indicate the breakdown of protein gel during *in vitro* digestion. The swelling/shrinking properties of the gels clearly affect the value of Rel.Ampl.$_{Gel}$. This provides an important avenue for further research. In particular, on the effects of swelling and shrinking on digestion.

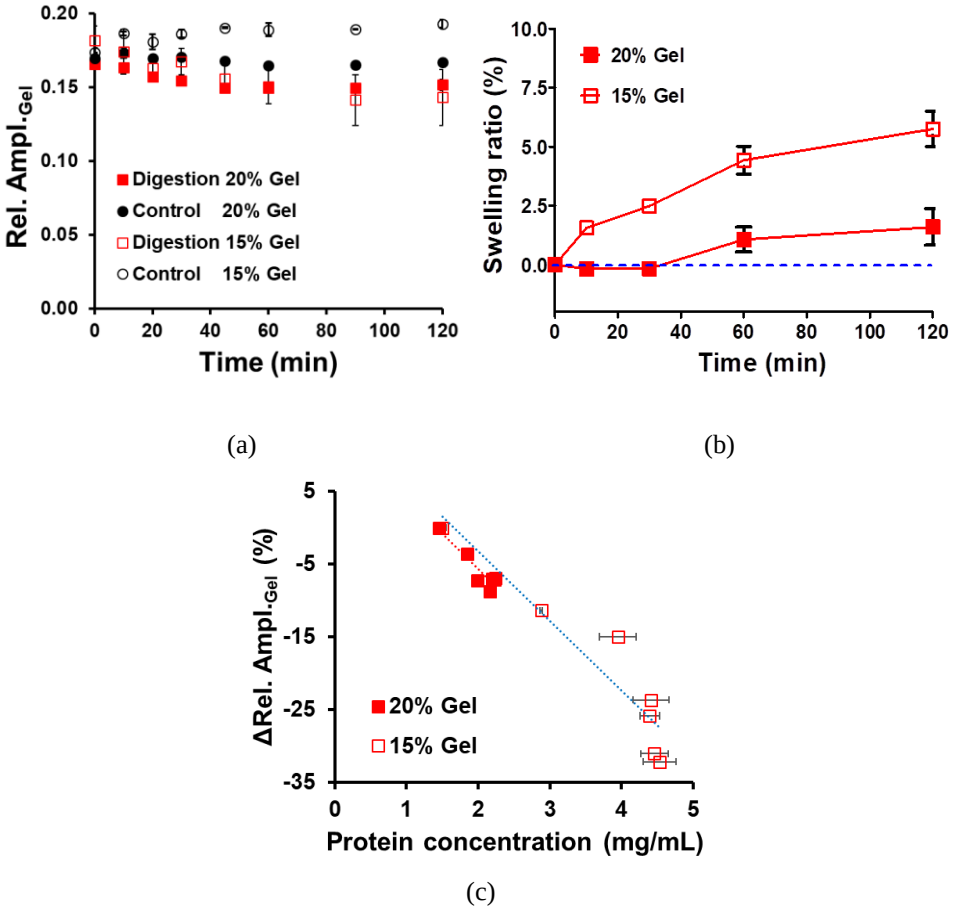

Fig. 2-7 *Relative amplitude of the gel phase (a) and swelling ratio of Gel in SGF (b) over time, and correlation between ΔRel.Ampl.$_{Gel}$ and protein concentration in supernatant of 20% WPI gel (R^2 = 0.85) and 15% WPI gel (R^2 = 0.88) (c) during 120 min of in vitro gastric digestion. Error bars are based on the standard deviation of two or three experiments. The calculation for Rel.Ampl.$_{Gel}$ and ΔRel.Ampl.$_{Gel}$ can be found in Section 2.2.4.*

2.3.4 Monitoring gastric digestion with MRI

Next, we used MRI to monitor *in vitro* gastric digestion of protein gels. Fig. 2-8a shows the color-coded T_2 (MRI) distribution in a cross section of tubes with 15% gel and SGF. Protein gel (lower part of the picture) and supernatant (upper part of the picture) compartments can be distinguished as well as the change in their T_2 spatial distribution over time. Under digestion conditions, the T_2 of supernatant decreased as reflected in the gradual darker color of the supernatant region, with the exception of time points 0-10 min, while under control conditions, there was no change. The decrease of T_2-supernatant during digestion is caused by the increase of protein fraction. The reason that under digestion conditions time points 0-10 min do not follow the above-described trend is because initially the temperature of the SGF with pepsin did not rise up to 37 °C, and this lower temperature induces a shorter T_2 (Mariette, 2009). For 20% gel, under both control and digestion conditions, there was no observable change in the T_2 (MRI) over time (Fig. 2-S2). This is caused by the lower degree of digestion compared with the 15% gel. Therefore, further discussion mainly focuses on the 15% gel results.

To make direct comparison with the result of TD-NMR, whole digestion mixtures were segmented and histogram of T_2 distribution in the digestion mixture against the corresponding number of voxels was obtained. The T_2 distribution of the 15% gel digestion mixture before digestion is shown in Fig. 2-8b. In the T_2 distribution, the two major peaks with average T_2 values of 337 ms and 1676 ms represent the gel and SGF, respectively. This is comparable with the T_2 (TD-NMR) distribution in Fig. 2-1b where the gel peak is at 76 ms and the SGF peak at 2400 ms. The separation of the two peaks based on the T_2 (MRI) histogram was less clear than in the TD-NMR data. We hypothesized this may be due to partial volume effects (Angel et al., 2002); since the diameter of gel particles is smaller than the voxel size, one voxel may contain both SGF and gel. As shown in Fig. 2-S3., phasor analysis (Vergeldt et al., 2017) was employed and confirmed our hypothesis about the partial volume effect.

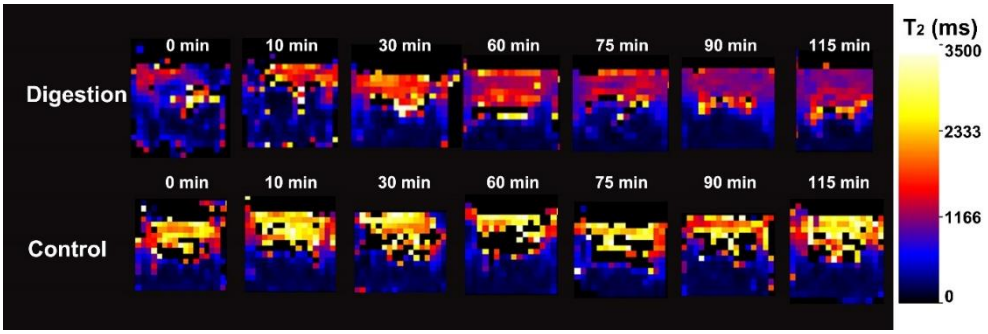

(a)

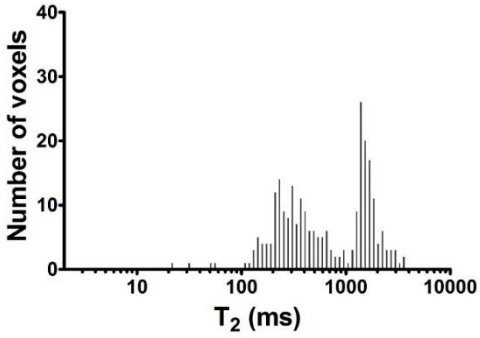

(b)

Fig. 2-8 *Color-coding T_2 (MRI) images (in which each pixel was color-coded according to its T_2 value with light yellow to dark blue representing T_2 value from 3500 ms to 0 ms) of 15% WPI gel under digestion condition (with pepsin) and control condition (without pepsin) from time 0 to 115 min (a) and T_2 (MRI) distribution of 15% gel at digestion time 0 min (b).*

Since the separation of gel and SGF/supernatant in the T_2 histogram was less clear, more accurate phase identification was done by regular approach of MRI image analysis (by directly selecting the region of interest (e.g., supernatant phase) manually as described in Section 2.2.5). Subsequently, the average T_2-supernatant (MRI) and R_2-supernatant (MRI) were calculated from the supernatant region instead of using the supernatant peak from T_2 (MRI) histogram. Guided by the interpretation of TD-NMR results, R_2-supernatant (MRI) was correlated with the concentration of -NH_2 groups in SGF. There was a linear positive correlation, except at time points 0 and 10 min because of the temperature difference (Fig. 2-9a). Furthermore, $\Delta Fraction_{Gel}$, representing the change in gel volume due to digestion, correlated negatively with supernatant protein concentration (Fig. 2-9b). Thus, similar with the results from TD-NMR, not only the average R_2-supernatant (MRI) can be used to monitor hydrolysis of WPI gel by indicating the amount of protein fraction (-NH_2 groups

concentration) in the supernatant during digestion; but also, the volume change of gel can be visualized by T_2-mapping (MRI) to indicate the breakdown of protein gel during digestion.

Future work may focus on further development of the MRI measurement sequence in order to acquire a 3D data set within an acceptable measuring time period (suitable for breath holding). Further, the influence of meal portion, pH, gastric secretion, and gastric emptying on the magnetic resonance parameters should be investigated, so as to lay a solid foundation to link *in vivo* experiments.

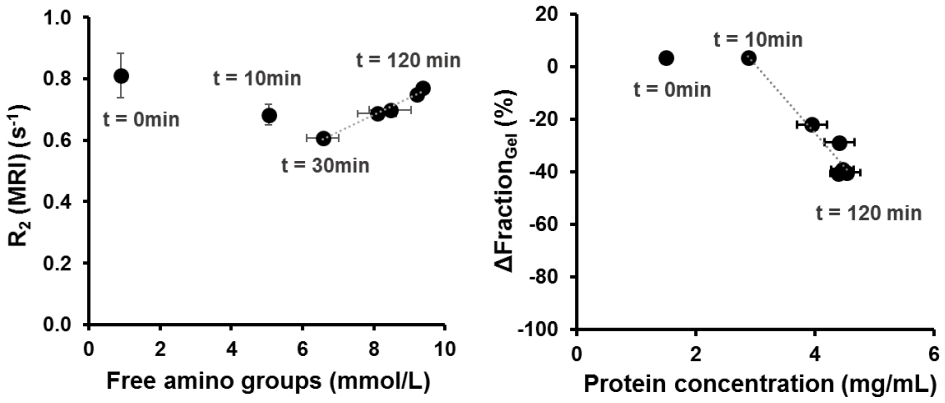

(a) (b)

Fig. 2-9 *Correlation between average R2–SGF (MRI) and free amino groups in the supernatant (R^2 = 0.96) (a) and correlation between $\Delta Fraction_{Gel}$ (MRI) and protein concentration in the supernatant (R^2 = 0.94) (b). Error bars are based on the standard deviation of two or three experiments. The calculation for ΔFractionGel can be found in Section 2.2.5.*

2.4 Conclusion

To verify the *in vitro* findings on gastric digestion of protein rich food in humans, developing a method that is applicable for both contexts is crucial. Here we proposed MRI as the method. To our knowledge, this study is the first to employ TD-NMR T_2 measurements as a method to monitor protein gel hydrolysis during *in vitro* gastric digestion and to subsequently validate it in an MRI setting. We established that *in vitro* gastric digestion of WPI gel can be monitored by TD-NMR T_2 measurement, including: 1) the R_2 value of supernatant, which is linearly correlated with protein ($-NH_2$ groups) concentration (a marker of degree of hydrolysis) in supernatant; 2) the relative amplitude of the gel fraction, which reflects the change in proton population due to water migration and gel breakdown. Digestion of WPI gel can be monitored by MRI T_2-mapping as well, with R_2–supernatant (MRI) and detecting volume change of the gel. Compared to TD-NMR, spatial information in MRI T_2-maps contributed to the phase separation of the fluid and gel fractions. In conclusion, this study shows that MRI has high potential for monitoring *in vivo* gastric digestion and strengthens our ambition of bridging *in vitro* and *in vivo* gastric digestion research with the use of magnetic resonance techniques.

Supplementary material

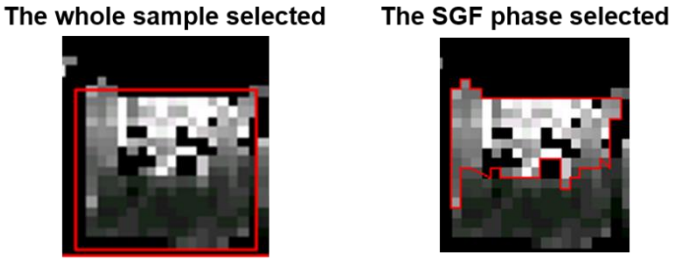

Fig. 2-S1 *Illustration on the segmentation of region of interest, e.g. whole sample and supernatant phase (which is the SGF phase), from MRI T_2 images in MIPAV.*

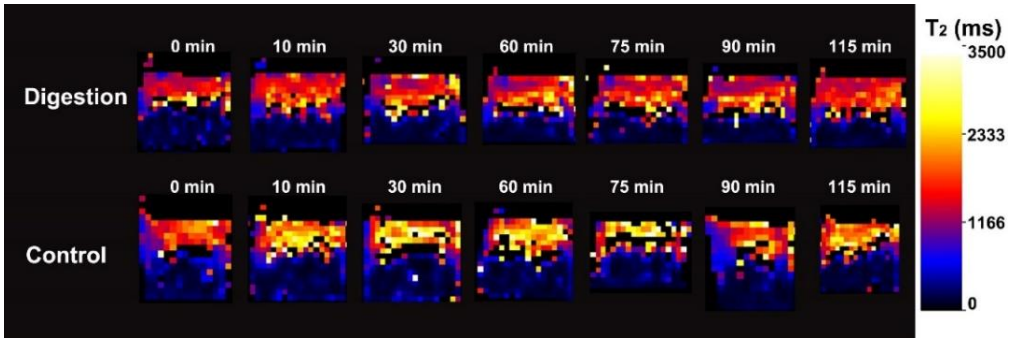

Fig. 2-S2 *Color-coded T_2 (MRI) images (from light yellow to dark blue representing T_2 value from 3500 ms to 0 ms) of 20% WPI gel under digestion condition (with pepsin) and control condition (without pepsin) from time 0 to 115 min.*

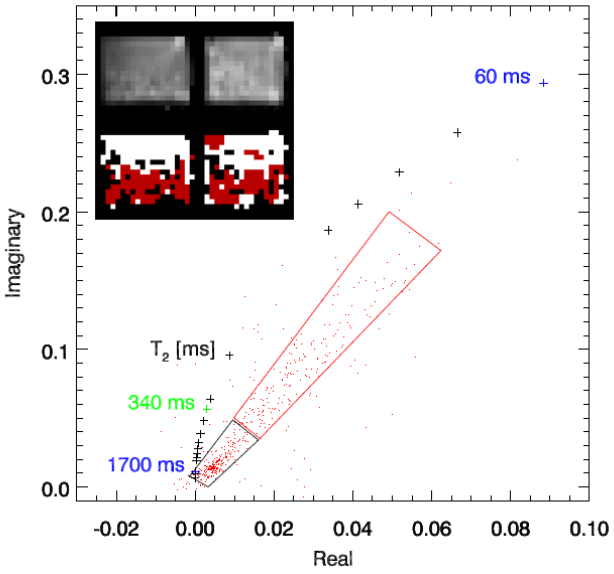

Fig. 2-S3 *Phasor analysis of 15% WPI gel with SGF at time 0 min. The phasor points within the red box are from voxels with red colour, while the points within black box are from voxels with white colour. A mono-exponential decay would result in the phasor points on the semi-circle; while bi-exponential decay would show phasor points on the line connecting T_2 values of the 2 components, and position of the phasor points is determined by the ratio of the 2 components. Current figure showed that the bi-exponential decay took place. This proved that the voxels contained 2 components, protons from both SGF and WPI gel.*

References

Angel, M., Zisserman, A. P., & Brady, M. (2002). Estimation of the partial volume effect in MRI, 6, 389–405.

Bazin, P. L., Cuzzocreo, J. L., Yassa, M. A., Gandler, W., McAuliffe, M. J., Bassett, S. S., & Pham, D. L. (2007). Volumetric neuroimage analysis extensions for the MIPAV software package. Journal of Neuroscience Methods, 165(1), 111–121. https://doi.org/10.1016/j.jneumeth.2007.05.024

Bordoni, A., Laghi, L., Babini, E., Di Nunzio, M., Picone, G., Ciampa, A., … Capozzi, F. (2014). The foodomics approach for the evaluation of protein bioaccessibility in processed meat upon *in vitro* digestion. Electrophoresis, 35(11), 1607–1614. https://doi.org/10.1002/elps.201300579

Bordoni, A., Picone, G., Babini, E., Vignali, M., Danesi, F., Valli, V., … Capozzi, F. (2011). NMR comparison of *in vitro* digestion of Parmigiano Reggiano cheese aged 15 and 30 months. Magnetic Resonance in Chemistry, 49(SUPPL. 1). https://doi.org/10.1002/mrc.2847

Bornhorst, G. M., & Paul Singh, R. (2014). Gastric digestion *in vivo* and *in vitro*: how the structural aspects of food influence the digestion process. Annual Review of Food Science and Technology, 5(1), 111–132. https://doi.org/10.1146/annurev-food-030713-092346

Bosmans, G. M., Lagrain, B., Deleu, L. J., Fierens, E., Hills, B. P., & Delcour, J. A. (2012). Assignments of proton populations in dough and bread using NMR relaxometry of starch, gluten, and flour model systems. Journal of Agricultural and Food Chemistry, 60(21), 5461–5470. https://doi.org/10.1021/jf3008508

Brodkorb, A., Egger, L., Alminger, M., Alvito, P., Assunção, R., Ballance, S., … Recio, I. (2019). INFOGEST static *in vitro* simulation of gastrointestinal food digestion. Nature Protocols, 14(4), 991–1014. https://doi.org/10.1038/s41596-018-0119-1

Collewet, G., Bugeon, J., Idier, J., Quellec, S., Quittet, B., Cambert, M., & Haffray, P. (2013). Rapid quantification of muscle fat content and subcutaneous adipose tissue in fish using MRI. Food Chemistry, 138(2–3), 2008–2015. https://doi.org/10.1016/j.foodchem.2012.09.131

de Kruif, C. G. (Kees)., Anema, S. G., Zhu, C., Havea, P., & Coker, C. (2015). Water holding capacity and swelling of casein hydrogels. Food Hydrocolloids, 44, 372–379. https://doi.org/10.1016/j.foodhyd.2014.10.007

Dekkers, B. L., de Kort, D. W., Grabowska, K. J., Tian, B., Van As, H., & van der Goot, A. J. (2016). A combined rheology and time domain NMR approach for determining water distributions in protein blends. Food Hydrocolloids, 60, 525–532. https://doi.org/10.1016/j.foodhyd.2016.04.020

Dinakar, P., & Kilara, A. (1996). Enhancing the functionality of food proteins by enzymatic modification. Trends in Food Science & Technology, 7(4), 120–125. Retrieved from https://doi.org/10.1016/0924-2244(96)10012-1

Flory, P. J., & Rehner, J. (1943). Statistical mechanics of cross-linked polymer networks II. Swelling. The Journal of Chemical Physics, 11(11), 521–526. https://doi.org/10.1063/1.1723792

Hills, B. P., Takacs, S. F., & Belton, P. S. (1990). A new interpretation of proton NMR relaxation time measurements of water in food. Food Chemistry, 37(2), 95–111. https://doi.org/10.1016/0308-8146(90)90084-H

Kirtil, E., Cikrikci, S., McCarthy, M. J., & Oztop, M. H. (2017). Recent advances in time domain NMR & MRI sensors and their food applications. Current Opinion in Food Science, 17, 9–15. https://doi.org/10.1016/j.cofs.2017.07.005

Kong, F., & Singh, R. P. (2008). A model stomach system to investigate disintegration kinetics of

solid foods during gastric digestion. Journal of Food Science, 73(5), 202–210. https://doi.org/10.1111/j.1750-3841.2008.00745.x

Lavenson, D. M., Tozzi, E. J., McCarthy, M. J., Powell, R. L., & Jeoh, T. (2011). Investigating adsorption of bovine serum albumin on cellulosic substrates using magnetic resonance imaging. Cellulose, 18(6), 1543–1554. https://doi.org/10.1007/s10570-011-9588-x

Le Dean, A., Mariette, F., & Marin, M. (2004). 1H nuclear magnetic resonance relaxometry study of water state in milk protein mixtures. Journal of Agricultural and Food Chemistry, 52(17), 5449–5455. https://doi.org/10.1021/jf030777m

Li, M., Li, B., & Zhang, W. (2018). Rapid and non-invasive detection and imaging of the hydrocolloid-injected prawns with low-field NMR and MRI. Food Chemistry, 242(August 2017), 16–21. https://doi.org/10.1016/j.foodchem.2017.08.086

Luo, Q., Boom, R. M., & Janssen, A. E. M. (2015). Digestion of protein and protein gels in simulated gastric environment. LWT - Food Science and Technology, 63(1), 161–168. https://doi.org/10.1016/j.lwt.2015.03.087

Luo, Q., Borst, J. W., Westphal, A. H., Boom, R. M., & Janssen, A. E. M. (2017). Pepsin diffusivity in whey protein gels and its effect on gastric digestion. Food Hydrocolloids, 66, 318–325. https://doi.org/10.1016/j.foodhyd.2016.11.046

MacIerzanka, A., Böttger, F., Lansonneur, L., Groizard, R., Jean, A. S., Rigby, N. M., … MacKie, A. R. (2012). The effect of gel structure on the kinetics of simulated gastrointestinal digestion of bovine β-lactoglobulin. Food Chemistry, 134(4), 2156–2163. https://doi.org/10.1016/j.foodchem.2012.04.018

Marciani, L. (2011). Assessment of gastrointestinal motor functions by MRI: A comprehensive review. Neurogastroenterology and Motility, 23(5), 399–407. https://doi.org/10.1111/j.1365-2982.2011.01670.x

Marciani, L., Manoj, P., Hills, B. P., Moore, R. J., Young, P., Fillery-Travis, A., … Gowland, P. A. (1998). Echo-planar imaging relaxometry to measure the viscosity of a model meal. Journal of Magnetic Resonance, 135(1), 82–86. https://doi.org/10.1006/jmre.1998.1560

Mariette, F. (2009). Investigations of food colloids by NMR and MRI. Current Opinion in Colloid and Interface Science, 14(3), 203–211. https://doi.org/10.1016/j.cocis.2008.10.006

Messroghli, D. R., Rudolph, A., Abdel-Aty, H., Wassmuth, R., Kuhne, T., Dietz, R., & Schulz-Menger, J. (2010). An open-source software tool for the generation of relaxation time maps in magnetic resonance imaging. BMC Med Imaging, 10, 16. https://doi.org/1471-2342-10-16 [pii]\r10.1186/1471-2342-10-16

Minekus, M., Alminger, M., Alvito, P., Ballance, S., Bohn, T., Bourlieu, C., … Brodkorb, A. (2014). A standardised static *in vitro* digestion method suitable for food-an international consensus. Food and Function, 5(6), 1113–1124. https://doi.org/10.1039/c3fo60702j

Munialo, C. D., van der Linden, E., Ako, K., Nieuwland, M., Van As, H., & de Jongh, H. H. J. (2016). The effect of polysaccharides on the ability of whey protein gels to either store or dissipate energy upon mechanical deformation. Food Hydrocolloids, 52, 707–720. https://doi.org/10.1016/j.foodhyd.2015.08.013

Nott, K. P., & Hall, L. D. (2005). Validation and cross-comparison of MRI temperature mapping against fibre optic thermometry for microwave heating of foods. International Journal of Food Science and Technology, 40(7), 723–730. https://doi.org/10.1111/j.1365-2621.2005.00992.x

Nyemb-Diop, K., Causeur, D., Jardin, J., Briard-Bion, V., Guérin-Dubiard, C., Rutherfurd, S. M., … Nau, F. (2016). Investigating the impact of egg white gel structure on peptide kinetics profile during *in vitro* digestion. Food Research International, 88(Part B), 302–309.

https://doi.org/10.1016/j.foodres.2016.01.004

Nyemb, K., Guérin-Dubiard, C., Pézennec, S., Jardin, J., Briard-Bion, V., Cauty, C., … Nau, F. (2016). The structural properties of egg white gels impact the extent of *in vitro* protein digestion and the nature of peptides generated. Food Hydrocolloids, 54, 315–327. https://doi.org/10.1016/j.foodhyd.2015.10.011

Peters, J. P. C. M., Vergeldt, F. J., Van As, H., Luyten, H., Boom, R. M., & van der Goot, A. J. (2016). Time domain nuclear magnetic resonance as a method to determine and characterize the water-binding capacity of whey protein microparticles. Food Hydrocolloids, 54, 170–178. https://doi.org/10.1016/j.foodhyd.2015.09.031

Provencher, S. W., & Vogel, R. H. (1983). P . Deuflhard et al . (eds .), Numerical Treatment of Inverse Problems in Differential and Integral Equations © Birkhäuser Boston 1983, 304–305.

Quesada-Pérez, M., Maroto-Centeno, J. A., Forcada, J., & Hidalgo-Alvarez, R. (2011). Gel swelling theories: The classical formalism and recent approaches. Soft Matter, 7(22), 10536–10547. https://doi.org/10.1039/c1sm06031g

Schmidt, D. G., Meijer, R. J. G. M., Slangen, C. J., & Van Beresteijn, E. C. H. (1995). Raising the pH of the pepsin-catalysed hydrolysis of bovine whey proteins increases the antigenicity of the hydrolysates. Clinical and Experimental Allergy, 25(10), 1007–1017. https://doi.org/10.1111/j.1365-2222.1995.tb00404.x

Singh, H., & Gallier, S. (2014). Processing of Food Structures in the Gastrointestinal Tract and Physiological Responses. Food Structures, Digestion and Health. https://doi.org/10.1016/B978-0-12-404610-8.00002-5

Singh, H., Ye, A., & Ferrua, M. J. (2015). Aspects of food structures in the digestive tract. Current Opinion in Food Science, 3, 85–93. https://doi.org/10.1016/j.cofs.2015.06.007

Spiller, R., & Marciani, L. (2019). Intraluminal Impact of Food: New Insights from MRI. Nutrients, 11(5), 1147. https://doi.org/10.3390/nu11051147

van der Sman, R. G. M. (2015). Biopolymer gel swelling analysed with scaling laws and Flory-Rehner theory. Food Hydrocolloids, 48, 94–101. https://doi.org/10.1016/j.foodhyd.2015.01.025

van Duynhoven, J., Voda, A., Witek, M., & Van As, H. (2010). Time-domain NMR applied to food products. Annual Reports on NMR Spectroscopy (1st ed., Vol. 69). Elsevier Ltd. https://doi.org/10.1016/S0066-4103(10)69003-5

Vergeldt, F. J., Prusova, A., Fereidouni, F., Van Amerongen, H., Van As, H., Scheenen, T. W. J., & Bader, A. N. (2017). Multi-component quantitative magnetic resonance imaging by phasor representation. Scientific Reports, 7(1), 1–10. https://doi.org/10.1038/s41598-017-00864-8.

Chapter 3

The importance of swelling for *in vitro* gastric digestion of whey protein gels

This chapter has been published as:

Deng, R., Mars, M., Van Der Sman, R. G., Smeets, P. A. M., & Janssen, A. E. M. (2020). The importance of swelling for *in vitro* gastric digestion of whey protein gels. *Food Chemistry*, 330, 127182.

Abstract

In this paper we report the importance of swelling on gastric digestion of protein gels, which is rarely recognized in literature. Whey protein gels with NaCl concentrations 0-0.1M were used as model foods. The Young's modulus, swelling ratio, acid uptake and digestion rate of the gels were measured. Pepsin transport was observed by confocal laser scanning microscopy using green fluorescent protein (GFP). With the increase of NaCl in gels, Young's modulus increased, swelling was reduced and digestion was slower, with a reduction of acid transport and less GFP present both at surface and in the gels. This shows that swelling affects digestion rate by enhancing acid diffusion, but also by modulating the partitioning of pepsin at the food-gastric fluid interface and thereby the total amount of pepsin in the food particle. This perspective on swelling will provide new insight for designing food with specific digestion rate for targeted dietary demands.

3.1 Introduction

Protein is not only an important macro-nutrient for humans, but also a main contributor to food structure, for example in meat, cheese and eggs. The digestion of protein-rich structured food starts in the stomach by mechanical degradation and the chemical action of pepsin and gastric acid. Food structure is a critical factor in food digestion (Bornhorst & Singh, 2014; Singh, Ye, & Ferrua, 2015). For example, the dense structure of a milk clot slows down the casein hydrolysis rate (Ye, Cui, Dalgleish, & Singh, 2016). Another study showed that the structure of whey protein aggregates gels can be manipulated by varying the k-carrageenan concentration, and a denser gel structure delays digestion and thereby the release of curcumin (Alavi et al., 2018). In addition, Hu et al. (2017) found that the gel structure of xanthan-SPI and carrageenan-SPI gels delay the digestion of soybean protein, which was confirmed by scanning electron microscope.

Regarding the effect of food structure on gastric digestion, it is crucial to understand the mechanisms underlying gastric digestion of protein-rich structured food. Currently, the main consensus is that food structure can affect gastric digestion by its impact on mechanical degradation (via the different resistance to physical breakdown), and on chemical degradation (via the different accessibility for gastric acid and pepsin). During gastric digestion, the activity of pepsin is highly dependent on the pH value, with maximum activity between pH 1.5 and 2.5 (Piper & Fenton, 1965). As shown by Bornhorst et al. (2014), pH gradients exist in the stomach, and the activity of pepsin is dependent on the real time local pH. Usually, the pH of a food particle is higher than that of gastric acid, for example cheese pH ~6.7 and fasting gastric pH ~1.5. In the gastric environment, gastric acid would transport into the particle. During uptake of the gastric acid, the pH gradients exist in one food particle and varying among different kinds of food as well. As found by Mennah-Govela et al. (2015), effective diffusivity of gastric acid into the bolus was greater in brown than in white rice due to differences in buffering capacity of proteins in rice. Thus, the uptake of acid into the food particle is crucial for lowering the (internal) local pH to guarantee pepsin activity. In addition, a synergy between acid diffusion and enzymatic reaction was found with the use of time-lapse synchrotron deep-UV fluorescence microscopy to track *in vitro* digestion of protein gels (Floury et al., 2018). Apart from acid uptake, pepsin diffusion is essential for gastric digestion. Pepsin diffusion in protein gels made with whey protein isolate (WPI) or casein is shown to be dependent on crosslinking

density and microstructure and to be one of the important factors on digestion rate (Luo, Borst, Westphal, Boom, & Janssen, 2017; Thévenot, Cauty, Legland, Dupont, & Floury, 2017).

During digestion, erosion by gastric fluid (with acid and enzyme) and dry matter loss take place; in addition to these surface phenomena, transport of acid, enzyme and water occurs. (Somaratne et al., 2020; van der Sman, Houlder, Cornet, & Janssen, 2019). While the transport of acid and enzyme is mostly towards the inside of the food particle, the water migration could be water uptake from the gastric juice towards the food particle or vice versa; either swelling or shrinking could take place. The swelling behaviour of whey protein gels is pH-sensitive, with a minimum swelling ratio close to the isoelectric point of whey proteins (∼5.1) (Betz, Hörmansperger, Fuchs, & Kulozik, 2012). In another study, the swelling of whey protein gels was measured in aqueous solutions with different pH values, e.g., swelling ratio was 24% for pH 2.5 (Oztop, Rosenberg, Rosenberg, McCarthy, & McCarthy, 2010). Thus, during gastric digestion, swelling takes place between gastric fluid and food particles, if swelling pressure differences exist between the food products and the surrounding liquid (van der Sman et al., 2019). Swelling pressure is the summation of elastic pressure, mixing pressure, and ionic pressure (Flory & Rehner, 1943; Quesada-Pérez, Maroto-Centeno, Forcada, & Hidalgo-Alvarez, 2011; van der Sman, 2015). As illustrated in Fig. 3-S1, when swelling takes place, it is likely that together with the water flow acid and enzyme are transported from gastric fluid to food. Mass transport of acid and enzyme is not only taking place via diffusion, due to a gradient in the concentration, but also via convection, due to the bulk water motion (van der Sman et al., 2019). We hypothesize that water migration is an important factor in gastric digestion. Most digestion studies have focused on the change of dry matter or nutrients, and the effect of swelling on food digestion has not yet been examined specifically.

Therefore, this study was conducted to better understand the role of swelling during gastric digestion of solid food. We prepared whey protein gels with different NaCl concentrations at gelation as model systems for protein-rich structured foods and measured their swelling ratio and digestion rate. Finally, we proposed how swelling might affect digestion.

3.2 Methods and methods

3.2.1 Materials

Pepsin from porcine gastric mucosa (561 activity units/mg) and other chemicals were purchased from Sigma Aldrich, Inc. (St. Louis, USA). Whey Protein Isolate (WPI) was purchased from Davisco Food International, Inc. (Le Sueur, USA), with protein content of 97.9 g/100 g dry solid and ash 1.9 g/100 g dry solid. Green fluorescent protein (GFP, MV = 26.9 kDa) was produced in-house at Wageningen University & Research, with the method as described by Nolles et al. (2015). Milli-Q water (resistivity 18.2 MΩcm at 25 °C, Merck Millipore, Billerica, USA) was used in all experiments.

3.2.2 Preparation of protein gel and simulated gastric fluid

WPI solution and gel were prepared as described previously (**Chapter 2**). WPI was dissolved in water (15 wt%), or in NaCl solution (15 wt%) with concentrations of 0, 0.01 M, 0.05 M and 0.1 M at neutral pH. Due to the ash content in whey protein isolate powder, there is approximately 0.03 M salt present in WPI gels before adding extra salt. The protein solutions were stirred at room temperature for at least 2 h. To prepare the gels, the solutions were centrifuged at 1000 rpm for 10 min to eliminate air bubbles and were poured into Teflon tubes with a diameter of 20 mm and then heated in a 90 °C water bath for 30 min with rotating. After that, the Teflon tubes were immediately cooled in an ice-water bath. The gels were stored within the sealed Teflon tubes at 4 °C, 1-5 days prior to use.

Simulated gastric fluid (SGF) was prepared with HCl and NaCl (pH 2.0, I = 154 mM) (Kong & Singh, 2008). Pepsin was added to achieve activity at 2000 activity units/mL, as recommended by Minekus et al (2014) and Brodkorb et al (2019). For the control group, no pepsin was added to the SGF.

3.2.3 Young's Modulus

Gels were sliced with a gel slicer into cylinders of 5 mm in height and 20 mm in diameter. Compression tests were performed with a Texture Analyzer (Instron Corp. 5564, USA) using a static load cell of 2000 N. Gel samples were compressed to 80% of their initial height between two parallel plates at a constant deformation rate of 1 mm/s. Measurements were performed at 20 °C in triplicate. As described in Urbonaite et al (2014), the Hencky's strain (ε_h) and true stress ($\sigma(t)$, Pa) are defined as:

$$\varepsilon_h = | \, ln\frac{h(t)}{h_0} \, | \tag{3.1}$$

$$A(t) = \frac{h_0}{h(t)} \cdot A_0 \tag{3.2}$$

$$\sigma(t) = \frac{F(t)}{A(t)} \tag{3.3}$$

$$E = \frac{d\sigma}{d\varepsilon_h} \tag{3.4}$$

Where h_0 is the initial height of the gel slice and $h(t)$ is the height of gel after being compressed for time t. With an assumption that volume of gel remained the same during deformation, the contact surface area (A(t), m2) at time t can be calculated with Equation (3.2), where A_0 is the initial contact surface area of the gel slice. F(t) is the measured force (with unit N). Young's modulus (E, Pa) is defined as the slope from the linear part of stress over strain curve within region 0.05 and 0.15 as Equation (3.4).

3.2.4 In vitro gastric digestion

The *in vitro* gastric digestion was initiated by putting a slice of gel into 30 mL SGF in a tube with a diameter of 35 mm. The gel slices were in the same shape as described in Section 3.2.3. The digestion was performed at 37 °C in a water-jacket compartment stirring at 100 rpm.

3.2.5 Determination of free amino acid groups

At different time points during *in vitro* digestion, the supernatant was withdrawn and heated by a pre-heated Eppendorf thermomixer at 90 °C, 850 rpm for 5 min to deactivate pepsin. To track the extent of digestion, the free amino groups in the supernatant were measured by the o-phthaldialdehyde (OPA) method, as described previously (**Chapter 2**). Briefly, the OPA reagent was prepared and kept in the dark. A DU 720 spectrophotometer (Beckman Coulter Inc., Pasadena, USA) was set at 340 nm blanked with 1.5 mL OPA reagent and 0.2 mL Milli-Q water. To make the calibration curve, 0.2 mL L-serine standard solutions (0~200 mg/L) were added to 1.5 mL OPA reagent in a cuvette, and mixed by pipetting for 5 s. The mixtures were measured with the spectrophotometer after standing for 3 min. The same procedure was applied to samples from the digestion experiments.

3.2.6 Mass change

After 120 min digestion as described in Section 3.2.3, the remaining gel was removed from the system and dried with tissue paper to remove excess liquid, and then weighed. The mass change of gels was calculated as:

$$Mass\ change\ (\%) = \frac{m_{120} - m_0}{m_0} \times 100\% \quad (3.5)$$

where m_{120} represents the weight of the gel after t = 120 min digestion and m0 is the initial weight of the gel.

3.2.7 Swelling property

To measure the swelling property of the gels, we performed same procedure as described in 3.2.3 but using SGF without pepsin. During 120 min incubation, the gel slices were taken out of the SGF and dried with tissue paper to remove excess liquid, and then weighed. The swelling ratio was calculated using Equation (3.6).

$$Swelling\ ratio\ (\%) = \frac{m_t - m_0}{m_0} \times 100\% \quad (3.6)$$

Where m_t represents the weight of the gel after t min incubation and m_0 is the initial weight of the gel.

3.2.8 Acid uptake

Under the same conditions as described in Section 3.2.3, by using SGF both with and without pepsin, pH of the supernatant was recorded during 120 min incubation. The pH change of SGF can reflect acid uptake by the gels. We calculated the amount of $[H^+]$ uptake by gel during incubation and the acid uptake by protein after 120 min incubation with Equation (3.7) and (3.8):

$$\Delta[H^+]/_{gram\ Gel} = \frac{10^{-pH_0} - 10^{-pH_{120}}}{m_{Gel}} \quad (3.7)$$

$$Acid\ uptake\ (mol/kg\ protein) = \frac{10^{-pH_0} - 10^{-pH_{120}}}{m_{Gel} \times c(protein)} \times V_{SGF} \quad (3.8)$$

pH_{120} and pH_0 represent pH of the supernatant at 120 min and time 0; m_{Gel} (g) represents the initial weight of the gel slice; c(protein) is the protein concentration in the gels (0.15 g protein per g gel); V_{SGF} is the volume of incubating SGF (30 mL).

3.2.9 Green fluorescent protein transport

The diffusivity of green fluorescent protein (GFP) in the gels was shown to be comparable to that of pepsin (Luo et al., 2017). In our study GFP was used to represent pepsin. GFP solution was prepared with 0.32 µmol/L GFP and 154 mM NaCl at neutral pH (because of the pH-dependency of the used fluorophore). A slice of the gel was soaked in 10 mL of the GFP solution, with a shaking speed of 50 rpm at room temperature. The gel slices were in the same shape as described in Section 3.2.3. After 1.5 h, the gel slices were taken out of the solutions and were cut. A narrow slice was obtained by cutting from middle of the original gel slice as illustrated in Fig. 3-S2. Firstly, a narrow slice (~2 mm) was obtained by cutting from middle of the original gel slice. After that, the middle narrow slice was laid down on a glass slide. Then the region (2×2 mm^2) as drawn in green in Fig. 3-S2 was measured by a confocal laser scanning microscopy (CLSM) to obtain the fluorescent intensity. The excitation wavelength was 488 nm. Fluorescence intensity was recorded through a 177 µm pinhole using a 515 nm filter. The acquired images were loaded into Image J and the green fluorescent intensity at every pixel was extracted. The same measurement was done to measure the gels under control condition using a 154 mM NaCl solution without GFP. Because of the pH dependency of the swelling properties, we measured the swelling behaviours of gels in the GFP solution (0.32 µmol/L GFP and 154 mM at neutral pH) under the set-up of GFP experiment by the same way as described in Section 3.2.6.

3.2.10 Statistical analysis

Independent-samples t-tests and analysis of variance (ANOVA) tests followed by a post hoc LSD test were performed with SPSS statistics software (IBM SPSS Statistics for Windows, Version 25, IBM Corp). Effects were considered statistically significant at $p < 0.05$. The expressions 'value ± value' represent 'mean ± standard deviation'.

3.3 Results

3.3.1 Characterization of the protein gels

The Young's modulus of the gels reflects their hardness and is shown in Fig. 3-1. With increasing of NaCl concentration from 0 to 0.05 M, Young's modulus of gels increased significantly ($p < 0.05$, t-test) from 68.15 ± 16.05 kPa to 249.3 ± 38.34 kPa, indicating the hardness of the gels was enhanced. No significant difference was found between the gel with NaCl 0.05 M and 0.1 M (p = 0.47, t-test). The observation that Young's modulus stops increasing at a certain salt concentration is in accordance with the results from another study (Urbonaite et al., 2016). The presence of NaCl can create coarse gels with dense protein aggregation and capillary water in between aggregations, this is because the electrostatic repulsion is reduced, and protein aggregation is facilitated. As a result, the protein aggregation yields thicker strands, and thereby an increase in hardness. On the other hand, the protein aggregation in strands could reduce the availability of protein, and therefore enlarge the pore size of the protein gel, resulting in decreased hardness of the gel. This increase of pore size is reported in the SEM images of Urbonaite et al. (2016). This explains that the gel with 0.1M NaCl (likely with larger pore size) did not show higher Young's modulus than the gel with 0.05M NaCl. Moreover, we would expect a decrease of Young's modulus in gels with higher NaCl concentration.

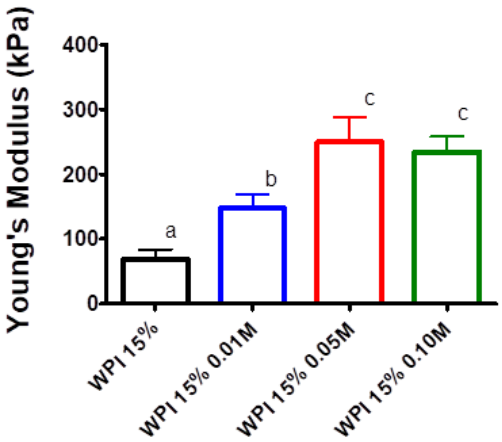

Fig. 3-1 *Young's Modulus of 15% WPI gels with NaCl varying from 0~0.1M; the error bars represent standard deviation, and columns with the same letter did not differ significantly.*

The swelling properties of the gels were measured by the wet mass change during 2 h incubation in the SGF without pepsin. During the incubation, it needs to be noted that there was hardly no solid loss of the gels, which has also been shown in previous studies (Luo, Boom, & Janssen, 2015). The swelling behaviour of WPI gels with NaCl 0~0.1M in SGF without pepsin is shown in Fig. 3-2. All the gels swelled during the 120 min incubation, and less swelling took place with the increase of NaCl concentration (0-0.1M) in the gel. The difference in swelling ratio among the gels is likely driven by the difference in swelling pressure between the gels and SGF. In the current study, even though the protein concentration in all the gels and SGF was the same, addition of NaCl increased the hardness (Young's modulus). This is likely the reason for the observed decrease of the swelling ratio. Moreover, this observation can also be explained by Flory–Rehner theory; among all the gels with an increase of Young's modulus, elastic pressure increased and mixing pressure increased, which in total resulted in the decrease of swelling ratio (van der Sman, 2015).

Although the swelling of the gels in SGF is a dynamic and complex process, our results show that the swelling properties of gels can be manipulated through varying structure, for example by using different amounts of NaCl at gelation.

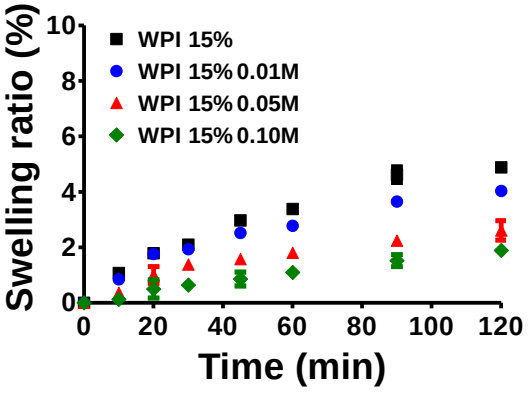

Fig. 3-2 *Swelling ratio of 15% WPI gels with NaCl varying from 0~0.1M in SGF without pepsin; the error bars represent standard deviation.*

3.3.2 Protein gel digestion

To evaluate the digestion rate of the WPI gels with 0~0.1M NaCl, we measured the free amino groups in the supernatant. With an increase of NaCl concentrations in the gel, the free amino groups released slower from the gel slice to the SGF (Fig 3-3a). The mass loss after 120 min digestion (Fig. 3-3b) was comparable with Fig. 3-3a, showing the order of degree of digestion rate: 0 M > 0.01M > 0.05M ≈ 0.1M. Combining this information with Young's modulus of the gels, it suggests that the increase of hardness was approximately in line with the decrease in the rate of digestion. Thus, the food with higher hardness is more resistant to be digested, and this has been shown from many other studies. (Guo, Ye, Lad, Dalgleish, & Singh, 2014; Hu et al., 2017).

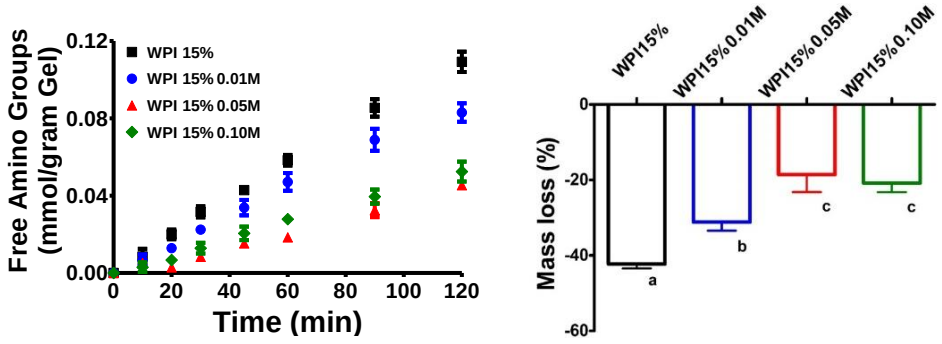

(a) (b)

Fig. 3-3 *Free amino groups in the SGF during 120 min digestion (a) and mass loss after 120 min digestion (b) of 15% WPI gels with NaCl varying from 0~0.1M; the error bars represent standard deviation, and columns with the same letter did not differ significantly.*

These results combined with the swelling results from Section 3.3.1 show that faster digestion (faster release of peptides) took place under higher swelling conditions. The gel with 0.1 M NaCl is an exception: compared with the gel with 0.05M NaCl, there tended to be less swelling (t120min, p = 0.051, t-test), but a similar amount of free amino groups was released (t120min, p = 0.312, t-test). This might be due to the presence of larger pore sizes in the coarse gel with 0.1M NaCl as discussed in section Section 3.3.1; the larger pore sizes might improve the accessibility of acid and/or pepsin, so as to partly compensate the effect of less swelling. Overall, we observed that digestion of gels was faster when more swelling took place. The potential mechanism could be that the swelling behaviour of gels subsequently affected the accessibility of acid and pepsin during the digestion. This is further discussed in Section 3.3.3 and Section 3.3.4.

3.3.3 Acid uptake

To track the acid uptake of the WPI gels, the pH in the supernatant was recorded, and the concentration change of H^+ (in the supernatant) per gram of gel was calculated under control (without pepsin, Fig. 3-4a) and digestion conditions (with pepsin, Fig. 3-4b). Under the control condition, the pH change indicates the H^+ transport from the supernatant to gel slice, since the solid loss of the gels was negligible. The pH of supernatant and acid uptake increased over time in all samples (Fig. 3-4a). The highest acid uptake was found with 0 M NaCl; with the addition of NaCl in the gels, smaller acid uptake was found in the supernatant. After 120 min, $[H^+]$ uptake was significantly decreased from 5.7 ± 0.1 mM/g gel without NaCl to 4.7 ± 0.1 mM/g gel with 0.1M NaCl ($p<0.05$, t-test). Thus, the acid moved slower with decreased swelling ratio, with the increase of Young's modulus of the gels. Moisture uptake was found to be positively related with acid uptake as well in sweet potatoes (Somaratne et al., 2019). Acid and water uptake were not always consistent in some studies (Mennah-Govela & Bornhorst, 2016; Mennah-Govela et al., 2015). This is because there are factors driving acid uptake but not water uptake, for example buffering capacity of food particles.

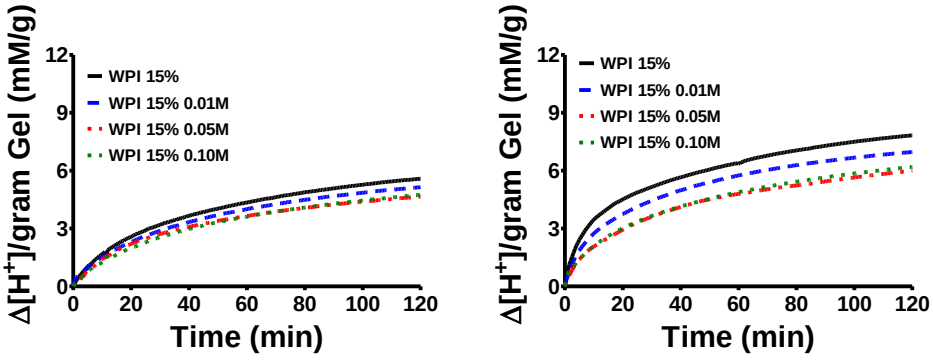

Fig. 3-4 *Acid uptake of per gram of protein gels during 120 min incubation under control conditions (a) and digestion condition (b).*

In our study, after 2h the acid uptake measured by pH change of the SGF was 0.95 ± 0.01 ~ 1.14 ± 0.02 mol/kg protein in the gels. The actual acid uptake is lower than the demanded amount to reach pH 2. This amount is 1.67 ± 0.1 mol/kg protein as reported previously (Luo, Zhan, Boom, & Janssen, 2018). This shows that in our study all the gels need more acid uptake to reach equilibrium due to the buffering capacity of the protein gels.

Therefore, the difference in acid uptake among the gels is likely due to the difference in acid diffusion or convection instead of a difference in buffering capacity.

To further figure out the reason of different acid uptake among gels, we calculated acid convection, which is the amount of acid transporting together with water flow, using Equation (3.9).

$$Acid\ convection\ (mol/kg\ protein) = \frac{Swelling\ ratio_{120} \times \rho_{SGF} \times 10^{-pH_{SGF}}}{c(protein)} \quad (3.9)$$

where $swelling\ ratio_{120}$ represents the swelling ratio of the gels after 120 min incubation; ρ_{SGF} is the mass density of SGF (1 kg/L); pH_{SGF} is the pH value of SGF (2); c(protein) is the protein concentration in the gels (0.15 g protein per g gel).

The amount of acid convection is from 0.001-0.003 mol/kg protein in gels with 0.1 M NaCl to without NaCl; higher convection of acid took place in the gels with more swelling. The convection is hundreds of times lower than the actual measured acid uptake. This indicates that the amount of acid convection is too small to differentiate acid uptake among the gels. Thus, it suggests that the difference of acid uptakes among the gels is because of the different amount of acid diffusion. With the fact that more acid uptake took place in the gels with more swelling, it is likely that swelling could increase the diffusion of acid so as to increase the acid uptake. The acid diffusion coefficient (De) has been shown to be larger in foods with more loosen structure, for example De 1.2×10^{-9} m^2/s in canned red beets and 1.1×10^{-10} m^2/s in raw red beets (Mennah-Govela et al., 2020). Therefore, the potential mechanism might be that swelling increases free space which could enhance the acid diffusion in the gels.

Under digestion conditions, the pH of supernatant increased with time and there was more acid uptake compared to the control condition in all the samples (Fig. 3-4b). The highest increase took place in gel without NaCl ($[H^+]$ uptake of 8.1 ± 0.2 mM/g gel), while the smallest increase was in gel with 0.05M NaCl ($[H^+]$ uptake of 6.1 ± 0.1 mM/g gel) and 0.1M ($[H^+]$ uptake of 6.3 ± 0.1 mM/g gel). The acid uptake under digestion conditions is due to the sum effect of the acid uptake by the gels and the cleavage of peptide bonds due to digestion. During protein hydrolysis, when a peptide bond is cleaved, a carboxyl and an amino group are released; in the gastric (acidic) environment, these groups undergo ionization which results in an increase of pH. As shown by Luo et al. (2018), the pH change

(or $[H^+]$ uptake) due to hydrolysis is proportional to the degree of hydrolysis of protein gels. Thus, it is to be expected that among all the gels under digestion conditions, the difference in $[H^+]$ uptake is in accordance with digestion results (Fig. 3-3a). The results show that acid uptake increases when the swelling ratio increases and that gels with more acid uptake show a larger degree of digestion. This confirms our hypothesis that swelling can increase the transport of gastric acid into protein gel particle. It is interesting to know whether there is more enzyme present inside the gel if the swelling is stronger.

3.3.4 Green fluorescent protein transport

Since the diffusivity of green fluorescent protein (GFP) was shown to be similar to that of pepsin in WPI gels by Luo et al. (2017), we used GFP to represent pepsin to explore how swelling would affect pepsin transport. GFP experiment cannot be conducted at the exact same condition (pH, temperature) as gastric digestion due to the limitation of GFP stability. To understand how the swelling properties affect GFP transport, we measured the swelling/shrinking properties of gels under the set-up of GFP experiments (Fig. 3-5a). With increase of NaCl in the gels, less swelling took place and even turned to shrinking with 0.05M and 0.1M NaCl. The trend among the different gels was similar to the swelling results of the gels in SGF (Fig. 3-2), although the swelling ratio of each gel under these two conditions was not the same. This may be due to pH differences (pH 7.0 for Fig. 3-5a and pH 2.0 for Fig. 3-2), in agreement with the finding that swelling behaviour of whey protein gels is pH-sensitive (Betz et al., 2012). The relation between swelling property and GFP transport would be discussed based on the swelling results in Fig. 3-5a.

The gels were observed with CLSM (Fig. 3-5b) after soaking in solution with or without GFP (control condition). For the control condition, the homogenous fluorescent signal was visible in the area of the gel, while with GFP a gradient of the green fluorescent signal present from the edge to the middle. The fluorescent intensity was plotted against the distance from the surface of gels (Fig. 3-5c). Under control conditions the intensity was very low and consistent in the gel region, while with GFP, fluorescent intensity gradually decreased from the surface till 1 mm depth. This indicates that at this specific excitation wavelength the signal from GFP was dominant, even though whey protein had a small contribution to the fluorescent signal. Besides, the GFP concentration differed depending on the distance from edge of the gel.

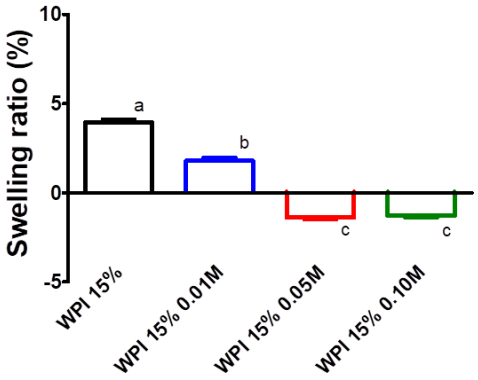

(a)

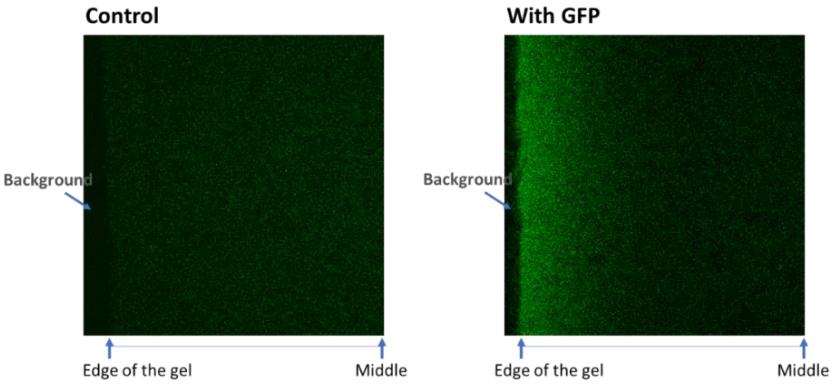

(b)

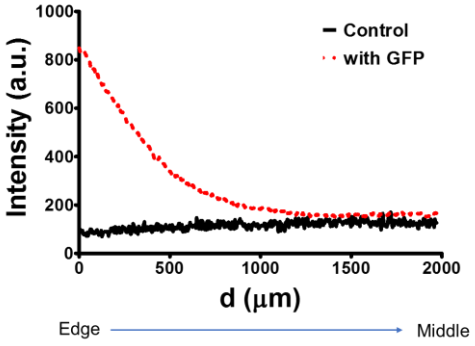

(c)

Fig. 3-5 *Swelling ratio of 15% WPI gels with NaCl from 0~0.1M in the GFP solutions (a, the error bars represent standard deviation, and columns with the same letter did not differ significantly), fluorescent images (b) and fluorescent intensity distribution (c) of 15% WPI gels after incubation under control conditions (without GFP) and conditions with GFP.*

To focus on the fluorescent signal from GFP specifically, the fluorescent signal of the gels under control conditions was subtracted from that under conditions with GFP (Fig. 3-6a). In all the gels, the concentration of GFP was higher near the surface and decreased towards the middle. With increase of Young's Modulus in the gels (with less swelling), the GFP intensity decreased not only in the gels and but obviously also at their boundary.

To compare the transport of GFP in the gels, we corrected the surface intensity as 1, and calculated relative fluorescent intensity from the surface to the middle of gels (Fig. 3-6b). The decrease curves of GFP intensity from surface to middle of different gels are similar and overlap. This shows that the movement rate of GFP did not change regardless of the different swelling properties of the gels. This is consistent with the finding from a previous study in which the GFP diffusion coefficient does not differ between gel without and with 0.05M NaCl (Luo et al., 2019). In fact, the higher amount of GFP at the surface and in the gel was observed in gels with higher swelling ratio and digestion rate. The difference in GFP intensity on the surface of gels might be explained by different partitioning of GFP between the protein gel and the gastric fluid. In mass transfer from one phase to the other, the overall mass transfer coefficient is also dependent on the partition coefficient (Wesselingh & Krishna, 2000). Partition coefficients of protein between hydrogel and liquid have been shown to be dependent on pH and ionic strength (Sassi, Shaw, Han, Blanch, & Prausnitz, 1996). As described by Van der Sman (2018), a difference in ionic strength induces a difference in the elastic pressure of the swelling pressure. The partitioning coefficient of a solute, defined as the concentration in the gel divided by the concentration in the liquid, decreases with an increase of elastic pressure of the gel.

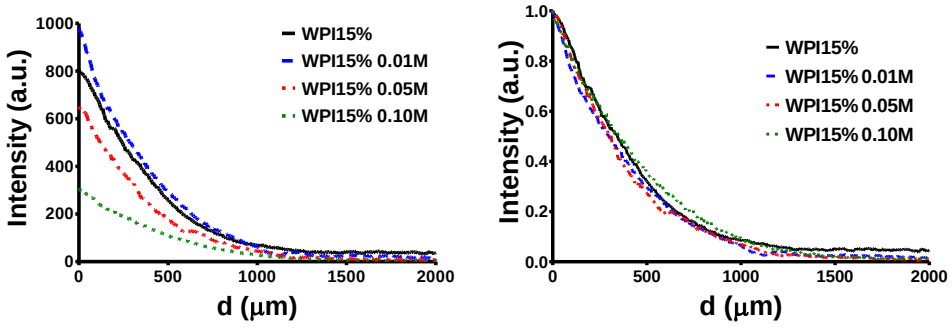

(a) (b)

Fig. 3-6 *Fluorescent intensity distribution (a) and relative fluorescent intensity distribution (b) in 15% WPI gels with NaCl from 0~0.1M.*

The results show that more swelling leads to a higher partition coefficient. It is this phenomenon that happens at the interface between the gastric juice and the gel particle that seems to be responsible for the higher GFP concentration inside the gel. If we relate this to pepsin transport towards the gel or food particle, the properties of the gel (or food) might define the partition coefficient of pepsin between the gel (or food) and the gastric fluid.

The results suggest that with more swelling even though the convection/diffusion of pepsin might not be enhanced, more pepsin positioning inside of gel at the surface could increase the pepsin concentration in the gel and thereby the digestion rate. As mentioned above, the GFP experiment that we conducted was not under the same conditions as the digestion experiment (e.g., pH, enzyme concentration), but it does show that the partitioning property of pepsin is crucial for digestion. The factors affecting the partition coefficient of pepsin on food surface are worthwhile to be further explored to better understand gastric digestion.

3.4 Conclusion

This study pointed out the important role of swelling during digestion. During *in vitro* gastric digestion of WPI gels with different Young' modulus (as a result of gelation with different NaCl concentration 0-0.1 M), the digestion rate, acid uptake and GFP intensity on the surface and inside of the gels were increased with the increase of swelling ratio. This suggests that swelling can increase the acid diffusion to lower the local pH in food particle for gastric digestion. Different swelling properties could modulate the partitioning of pepsin on the food-gastric fluid interface and are crucial for the total amount of pepsin in the food and therefore the digestion rate of food particles. The swelling effect on *in vivo* gastric digestion and on the subsequent digestion phases need to be further explored. Therefore, swelling properties of food particles should be taken into consideration when studying food digestion, and the factors affecting the partitioning property of pepsin need to be further investigated. This will yield better knowledge on the mechanisms of food particle digestion which can provide novel perspectives on designing food with different rates of digestion and nutrient release to satisfy specific target groups.

Supplementary material

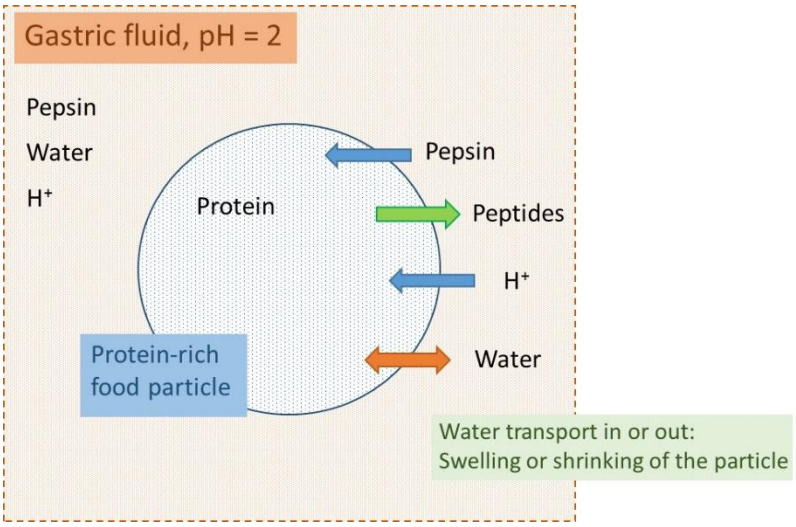

Fig. 3-S1 *Schematic illustration of factors on chemical degradation during gastric digestion.*

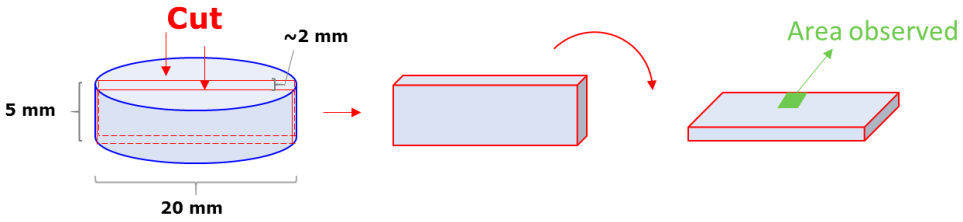

Fig. 3-S2*. Illustration on the sample preparation for confocal laser scanning microscopy measurement*

References

Alavi, F., Emam-Djomeh, Z., Yarmand, M. S., Salami, M., Momen, S., & Moosavi-Movahedi, A. A. (2018). Cold gelation of curcumin loaded whey protein aggregates mixed with k-carrageenan: impact of gel microstructure on the gastrointestinal fate of curcumin. Food Hydrocolloids, 85(March), 267–280. https://doi.org/10.1016/j.foodhyd.2018.07.012

Betz, M., Hörmansperger, J., Fuchs, T., & Kulozik, U. (2012). Swelling behaviour, charge and mesh size of thermal protein hydrogels as influenced by pH during gelation. Soft Matter, 8(8), 2477–2485. https://doi.org/10.1039/c2sm06976h

Bornhorst, G. M., Rutherfurd, S. M., Roman, M. J., Burri, B. J., Moughan, P. J., & Singh, R. P. (2014). Gastric pH distribution and mixing of soft and rigid food particles in the stomach using a dual-marker technique. Food Biophysics, 9(3), 292–300. https://doi.org/10.1007/s11483-014-9354-3

Bornhorst, G. M., & Singh, R. P. (2014). Gastric digestion *in vivo* and *in vitro*: how the structural aspects of food influence the digestion process. Annual Review of Food Science and Technology, 5(1), 111–132. https://doi.org/10.1146/annurev-food-030713-092346

Brodkorb, A., Egger, L., Alminger, M., Alvito, P., Assunção, R., Ballance, S., … Recio, I. (2019). INFOGEST static *in vitro* simulation of gastrointestinal food digestion. Nature Protocols, 14(4), 991–1014. https://doi.org/10.1038/s41596-018-0119-1

Deng, R., Janssen, A. E. M., Vergeldt, F. J., Van As, H., de Graaf, C., Mars, M., & Smeets, P. A. M. (2020). Exploring *in vitro* gastric digestion of whey protein by time-domain nuclear magnetic resonance and magnetic resonance imaging. Food Hydrocolloids, 99. https://doi.org/10.1016/j.foodhyd.2019.105348 (*Chapter 2 in this thesis*)

Flory, P. J., & Rehner, J. (1943). Statistical mechanics of cross-linked polymer networks II. Swelling. The Journal of Chemical Physics, 11(11), 521–526. https://doi.org/10.1063/1.1723792

Floury, J., Bianchi, T., Thévenot, J., Dupont, D., Jamme, F., Lutton, E., … Le Feunteun, S. (2018). Exploring the breakdown of dairy protein gels during *in vitro* gastric digestion using time-lapse synchrotron deep-UV fluorescence microscopy. Food Chemistry, 239, 898–910. https://doi.org/10.1016/j.foodchem.2017.07.023

Guo, Q., Ye, A., Lad, M., Dalgleish, D., & Singh, H. (2014). Effect of gel structure on the gastric digestion of whey protein emulsion gels. Soft Matter, 10(8), 1214–1223. https://doi.org/10.1039/c3sm52758a

Hu, B., Chen, Q., Cai, Q., Fan, Y., Wilde, P. J., Rong, Z., & Zeng, X. (2017). Gelation of soybean protein and polysaccharides delays digestion. Food Chemistry, 221, 1598–1605. https://doi.org/10.1016/j.foodchem.2016.10.132

Kong, F., & Singh, R. P. (2008). A model stomach system to investigate disintegration kinetics of solid foods during gastric digestion. Journal of Food Science, 73(5), 202–210. https://doi.org/10.1111/j.1750-3841.2008.00745.x

Luo, Q., Boom, R. M., & Janssen, A. E. M. (2015). Digestion of protein and protein gels in simulated gastric environment. LWT - Food Science and Technology, 63(1), 161–168. https://doi.org/10.1016/j.lwt.2015.03.087

Luo, Q., Borst, J. W., Westphal, A. H., Boom, R. M., & Janssen, A. E. M. (2017). Pepsin diffusivity in whey protein gels and its effect on gastric digestion. Food Hydrocolloids, 66, 318–325. https://doi.org/10.1016/j.foodhyd.2016.11.046

Luo, Q., Sewalt, E., Borst, J. W., Westphal, A. H., Boom, R. M., & Janssen, A. E. M. (2019). Analysis and modeling of enhanced green fluorescent protein diffusivity in whey protein gels.

Food Research International, 120, 449–455. https://doi.org/10.1016/j.foodres.2018.10.087

Luo, Q., Zhan, W., Boom, R. M., & Janssen, A. E. M. (2018). Interactions between acid and proteins under *in vitro* gastric condition-a theoretical and experimental quantification. Food and Function, 9(10), 5283–5289. https://doi.org/10.1039/c8fo01033a

Mennah-Govela, Y. A., & Bornhorst, G. M. (2016). Acid and moisture uptake in steamed and boiled sweet potatoes and associated structural changes during *in vitro* gastric digestion. Food Research International, 88(Part B), 247–255. https://doi.org/10.1016/j.foodres.2015.12.012

Mennah-Govela, Y. A., Bornhorst, G. M., & Singh, R. P. (2015). Acid diffusion into rice boluses is influenced by rice type, variety, and presence of α-amylase. Journal of Food Science, 80(2), E316–E325. https://doi.org/10.1111/1750-3841.12750

Mennah-Govela, Y. A., Keppler, S., Januzzi-Guerreiro, F., Follador-Lemos, C., Vilpont, K., & Bornhorst, G. M. (2020). Acid and moisture uptake into red beets during *in vitro* gastric digestion as influenced by gastric pH. Food Biophysics. https://doi.org/10.1007/s11483-019-09623-w

Minekus, M., Alminger, M., Alvito, P., Ballance, S., Bohn, T., Bourlieu, C., … Brodkorb, A. (2014). A standardised static *in vitro* digestion method suitable for food-an international consensus. Food and Function, 5(6), 1113–1124. https://doi.org/10.1039/c3fo60702j

Nolles, A., Westphal, A. H., De Hoop, J. A., Fokkink, R. G., Kleijn, J. M., Van Berkel, W. J. H., & Borst, J. W. (2015). Encapsulation of GFP in complex coacervate core micelles. Biomacromolecules, 16(5), 1542–1549. https://doi.org/10.1021/acs.biomac.5b00092

Oztop, M. H., Rosenberg, M., Rosenberg, Y., McCarthy, K. L., & McCarthy, M. J. (2010). Magnetic resonance imaging (MRI) and relaxation spectrum analysis as methods to investigate swelling in whey protein gels. Journal of Food Science, 75(8). https://doi.org/10.1111/j.1750-3841.2010.01788.x

Piper, D. W., & Fenton, B. H. (1965). pH stability and activity curves of pepsin with special reference to their clinical importance. Gut, 6(5), 506–508. https://doi.org/10.1136/gut.6.5.506

Quesada-Pérez, M., Maroto-Centeno, J. A., Forcada, J., & Hidalgo-Alvarez, R. (2011). Gel swelling theories: The classical formalism and recent approaches. Soft Matter, 7(22), 10536–10547. https://doi.org/10.1039/c1sm06031g

Sassi, A. P., Shaw, A. J., Han, S. M., Blanch, H. W., & Prausnitz, J. M. (1996). Partitioning of proteins and small biomolecules in temperature- and pH-sensitive hydrogels. Polymer, 37(11), 2151–2164. https://doi.org/-10.1016/0032-3861(96)85860-5

Singh, H., Ye, A., & Ferrua, M. J. (2015). Aspects of food structures in the digestive tract. Current Opinion in Food Science, 3, 85–93. https://doi.org/10.1016/j.cofs.2015.06.007

Somaratne, G., Ferrua, M. J., Ye, A., Nau, F., Floury, J., Dupont, D., & Singh, J. (2020). Food material properties as determining factors in nutrient release during human gastric digestion: a review. Critical Reviews in Food Science and Nutrition, 0(0), 1–17. https://doi.org/10.1080/10408398.2019.1707770

Somaratne, G., Reis, M. M., Ferrua, M. J., Ye, A., Nau, F., Floury, J., … Singh, J. (2019). Mapping the Spatiotemporal Distribution of Acid and Moisture in Food Structures during Gastric Juice Diffusion Using Hyperspectral Imaging. Journal of Agricultural and Food Chemistry, 67(33), 9399–9410. https://doi.org/10.1021/acs.jafc.9b02430

Thévenot, J., Cauty, C., Legland, D., Dupont, D., & Floury, J. (2017). Pepsin diffusion in dairy gels depends on casein concentration and microstructure. Food Chemistry, 223, 54–61. https://doi.org/10.1016/-j.foodchem.2016.12.014

Urbonaite, V., de Jongh, H. H. J., van der Linden, E., & Pouvreau, L. (2014). Origin of Water Loss

from Soy Protein Gels. Journal of Agricultural and Food Chemistry, 62(30), 7550–7558. https://doi.org/10.1021-/jf501728t

Urbonaite, V., van der Kaaij, S., de Jongh, H. H. J., Scholten, E., Ako, K., van der Linden, E., & Pouvreau, L. (2016). Relation between gel stiffness and water holding for coarse and fine-stranded protein gels. Food Hydrocolloids, 56, 334–343. https://doi.org/10.1016/j.foodhyd.2015.12.011

van der Sman, R. G. M. (2015). Biopolymer gel swelling analysed with scaling laws and Flory-Rehner theory. Food Hydrocolloids, 48, 94–101. https://doi.org/10.1016/j.foodhyd.2015.01.025

van der Sman, R. G. M. (2018). Theoretical investigation of the swelling of polysaccharide microgels in sugar solutions. Food and Function, 9(5), 2716–2724. https://doi.org/10.1039/c8fo00452h

van der Sman, R. G. M., Houlder, S., Cornet, S., & Janssen, A. (2019). Physical chemistry of gastric digestion of proteins gels. Current Research in Food Science, 1–26. https://doi.org/10.1016/j.crfs.2019.11.003

Wesselingh, J. A., & Krishna, R. (2000). Mass transfer in multicomponent mixtures. Delft: Delft University Press.

Ye, A., Cui, J., Dalgleish, D., & Singh, H. (2016). Formation of a structured clot during the gastric digestion of milk: Impact on the rate of protein hydrolysis. Food Hydrocolloids, 52, 478–486. https://doi.org/-10.1016/j.foodhyd.2015.07.023

Chapter 4

Monitoring pH and whey protein digestion by TD-NMR and MRI in a novel semi-dynamic *in vitro* gastric simulator (MR-GAS)

This chapter has been published as:

Deng, R., Seimys, A., Mars, M., Janssen, A. E. M., & Smeets, P. A. M. (2022). Monitoring pH and whey protein digestion by TD-NMR and MRI in a novel semi-dynamic *in vitro* gastric simulator (MR-GAS). *Food Hydrocolloids*, 125, 107393.

Abstract

Gastric digestion is crucial for protein breakdown. Magnetic resonance techniques have a great deal of potential but remain underexplored with regard to their application in the study of food digestion via MRI-markers, such as transverse (R_2) and longitudinal (R_1) relaxation rates. R_2 has been used to monitor gastric digestion of whey protein gels, but only in a static *in vitro* model. It is essential to investigate whether relaxation rates can be valid measures of digestion under dynamic circumstances. We developed a novel MRI-compatible semi-dynamic gastric simulator (MR-GAS) that includes controlled gastric secretion, emptying and mixing at body temperature. Protein hydrolysis and pH were measured during protein gel digestion in the MR-GAS. R_2 and R_1 of the supernatant were measured by time-domain nuclear magnetic resonance (TD-NMR). The stomach chamber of the MR-GAS was also scanned with MRI to measure R_2 and R_1. For TD-NMR, 99% of the variance in R_2 and 96% of variance in R_1 could be explained as a function of protein concentration and $[H^+]$. For MRI, the explained variances were 99% for R_2 and 60% for R_1. From these analysis, the obtained equations enabled the prediction of protein concentration and pH by R_2 and R_1. The normalised root mean squared deviation of the predictions for protein concentration were 0.15 (NMR) and 0.18 (MRI), and for pH were 0.12 (NMR) and 0.29 (MRI). In conclusion, the MR-GAS model may be used in a clinical MRI to monitor gastric digestion under *in vitro* dynamic circumstances, by measuring R_2 and R_1. These results underscore the potential of MRI to monitor nutrients hydrolysis and pH changes in future *in vivo* studies.

4.1 Introduction

Gastric digestion is a complex dynamic process. It is essential for the breakdown of food matrices, especially those found in protein-rich solid foods. Ingestion of food stimulates the secretion of gastric fluid, which contains pepsin and gastric acid (Singh and Gallier, 2014). Food particles are broken down by mechanical and enzymatic digestion, and the resulting chyme is emptied through the pylorus into the small intestine (Bornhorst, 2017). For dietary proteins, the enzymatic digestion in the stomach by pepsin is especially important since it affects their subsequent digestion and absorption (Bordoni et al., 2011).

In recent years, researchers have developed multiple *in vitro* digestion models and approaches to study gastric digestion (Gouseti et al., 2019). These models are useful for studying the molecular mechanisms behind protein breakdown, and have the advantage of well-controlled and reproducible conditions and easy sampling (Brodkorb et al., 2019; Kong and Singh, 2008; Minekus et al., 2014). However, an *in vitro* model cannot entirely simulate realistic gastrointestinal conditions since *in vivo* digestion comprises a diverse and interconnected set of processes and feedback mechanisms. Moreover, many *in vitro* measurements and conditions cannot be applied *in vivo* due to practical limitations and ethical concerns (Bordoni et al., 2011). This creates a challenge for the verification of *in vitro* results with *in vivo* studies. Therefore, it is important to explore non-invasive approaches feasible for monitoring both *in vitro* and *in vivo* digestion.

Magnetic resonance imaging (MRI) has great potential as a non-invasive approach for examining gastric digestion *in vivo*, not only because it can be used to assess gastric process at a macroscopic level (e.g. gastric emptying), but also because it can be used to study intraluminal processes on a molecular level (Marciani, 2011; Smeets,et al, 2020; Spiller & Marciani, 2019). Additionally, time-domain nuclear magnetic resonance (TD-NMR), which has the same underlying principles as MRI, can provide extra information and aid the interpretation of *in vitro* and *in vivo* measurements with MRI, even though NMR is limited to *in vitro* measurements (**Chapter 2**) (Deng, et al., 2020a).

Transverse relaxation time (T_2) or rate ($R_2 = T_2^{-1}$) and longitudinal relaxation time (T_1) or rate ($R_1 = T_1^{-1}$) can be measured with both NMR and MRI. R_2 and R_1 reflect how protons in a magnetic field relax back to their equilibrium position after excitation by a radiofrequency pulse. R_2 refers to the spin-spin relaxation in the x-y plane, and R_1 refers to the relaxation of

the net magnetisation to realign itself with the direction of the external magnetic field; it is usually lower than R_2 (Hashemi et al., 2012). The main applications of R_2 and R_1 are based on the relaxation behaviour of water protons (Mariette, 2009). Variations in R_2 and R_1 reflect changes in macromolecule concentration, water migration and structure in food matrices, but also environmental parameters, such as pH and temperature (Mariette, 2009; Peters et al., 2016). While this indicates the potential of R_2 and R_1 for monitoring digestive processes, many factors in play require careful validation of the meaning of R_2 and R_1 changes in different digestion contexts. As a first step, our recent study provided evidence that changes in R_2 can reflect protein hydrolysis of whey protein gels in a static *in vitro* digestion model (**Chapter 2**). It is, however, unclear if relaxation rates can also be used to monitor protein digestion under dynamic circumstances, such as changing pH and protein concentration. To monitor these two variables during digestion, we hypothesised that it would be useful to include R_1 as an additional parameter. As such, we aimed to investigate the extent to which the combination of R_2 and R_1 measurements could be used to monitor digestion in a dynamic *in vitro* model, using whey protein gels as the model food.

To this end, we developed a novel MRI-compatible semi-dynamic Gastric Simulator (MR-GAS). In this model, we performed *in vitro* gastric digestion of whey protein gels in the laboratory and in a clinical MRI scanner. We quantified the degree of digestion and pH in the supernatant and measured its R_2 and R_1 with TD-NMR and MRI. Finally, the feasibility of R_2 and R_1 measurements to monitor pH and protein concentration under semi-dynamic gastric digestion conditions was evaluated by comparing the measured values and predictions.

4.2 Materials and methods

4.2.1 Materials

Pierce™ BCA Protein Assay Kit was purchased from Thermo Fisher Scientific, Inc. (Waltham, Massachusetts, USA). Pepsin from porcine gastric mucosa (541-623 activity units/mg), gastric mucin from porcine stomach and all other chemicals were purchased from Sigma Aldrich, Inc. (St. Louis, USA). Whey Protein Isolated (WPI) was purchased from Davisco Food International, Inc. (Le Sueur, USA). WPI has a protein content of 97.9 wt%, fat ≤ 1 wt%, ash ≤ 0.5 wt%, and lactose ≤ 0.5 wt% (percentages on dry matter basis). Milli-Q water (resistivity 18.2 MΩ.cm at 25 °C, Merck Millipore, Billerica, USA) was used in all experiments.

4.2.2 Preparation of WPI gels

WPI gels were prepared as described previously (**Chapter 2**). WPI was dissolved in water (15 wt% or 20 wt%) and stirred at room temperature for 2-3 h. No pH adjustments were done. The solutions were centrifuged at 1,000 rpm for 10 min to eliminate air bubbles. Then the solutions were transferred to Teflon tubes and heated in a 90 °C water bath for 30 min. After that, the Teflon tubes were immediately cooled in an ice-water bath and then stored at 4 °C, 1-5 days prior to use. Before digestion experiments, the gels were cut into 5 mm diameter square particles with a gel cutter.

4.2.3 Preparation of simulated gastric fluid

Simulated gastric fluid (SGF) was prepared by dissolving NaCl (8.775 g/L), gastric mucin (1.5 g/L), pepsin (2,000 activity units/mL) (Brodkorb et al., 2019; Kong and Singh, 2008). The initial pH of the SGF was adjusted to 1.5 using 2M HCl (Guo et al., 2015).

4.2.4 MR-GAS set-up

The MRI-compatible semi-dynamic gastric simulator (MR-GAS) set-up is shown in Fig. 4-1. It consisted of a gastric secretion unit, a gastric empty unit, a stomach chamber, a water bath and tubing to deliver different flows. It is referred to as 'semi-dynamic' because it lacked stomach muscle contraction and the constant rates of gastric secretion and emptying that are *in vivo*, which are regulated by the nutrients density, digestion rate etc. The stomach chamber is a water-jacketed compartment of 500 mL heated to 37 ˚C by a

circulating heater (Julabo GmbH, Germany). One of the main challenges for an MRI compatible digestion system is avoiding the use of metal. For gastric mixing, instead of magnetic stirrers, an airflow with a pressure of 0.2 bar was introduced to the bottom of the stomach chamber with a custom-built circular tubing with equally distributed holes. This was used to create air bubbles that mixed the food particles and SGF. To mimic gastric secretion, SGF, preheated to 37 ˚C in a container with water, was delivered to the stomach chamber via a syringe pump (NE-500 Programmable OEM Syringe Pump, New Era Pump Systems, Inc., USA) through a 5 mm (inner-diameter) PVC tube. Gastric content was emptied by a peristaltic pump (Watson Marlow, USA) through a 4 mm (inner-diameter) PVC tube. A sealed vessel with water was placed between the stomach chamber and the peristaltic pump to prevent emptied digesta from blocking the peristaltic pump tube.

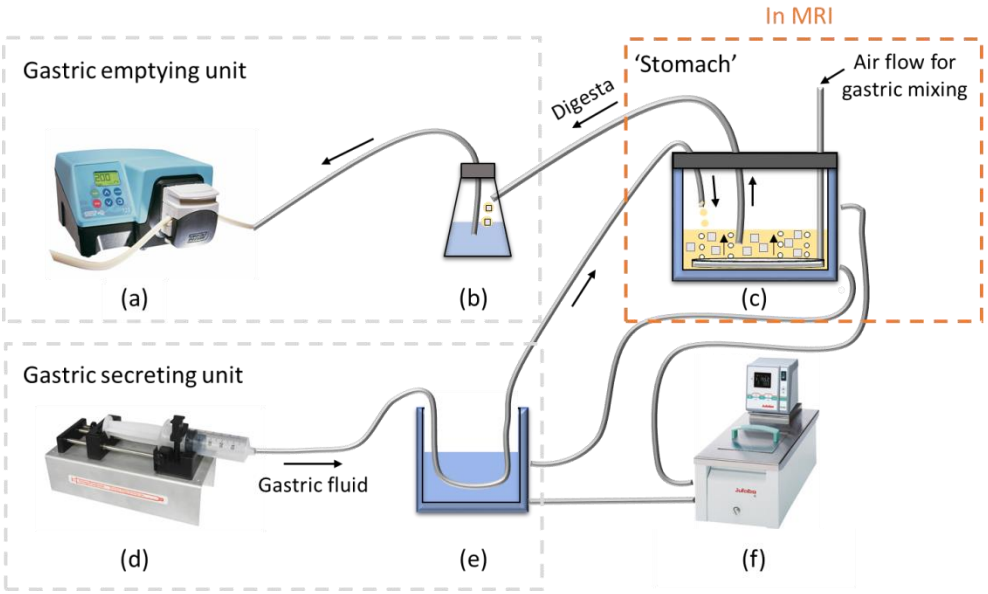

Fig. 4-1 *MRI semi-dynamic compatible gastric simulator (MR-GAS), consisting of a peristaltic pump (a), a sealed vessel with water (b), a water-jacketed 'stomach' chamber (c), a syringe pump (d), a container with water to preheat SGF (e), a circulating heater (f).*

4.2.5 In vitro gastric digestion in the MR-GAS

To initiate digestion, 50 g of the WPI gel particles were placed in the stomach chamber containing 150 mL of pre-heated SGF at 37 ºC. Gastric secretion was immediately started at a rate of 2.5 mL/min and maintained throughout digestion. Gastric emptying was started

30 min after the start of digestion at a rate of 3.33 mL/min. The rates of gastric secretion and emptying were based on a digestion model reflecting normal adults (Guo et al., 2015).

4.2.6 Protein digestion measurements

To examine the extent of protein hydrolysis during digestion, we measured the free amino groups and protein concentration in the supernatant in the MR-GAS stomach chamber. At t = 0, 5, 10, 15, 20, 30, 60, 90 and 120 min after starting digestion, 1 mL supernatant samples were withdrawn from the stomach chamber. Each sample was placed in an Eppendorf tube containing sodium bicarbonate (0.015 g) and vortexed for 5 s to elevate pH to 8 and stop pepsin activity as recommended by Brodkorb et al. (2019). After that, the concentration of released amino groups (-NH_2 groups) was measured with the OPA (o-phthaldialdehyde) method, as described previously (**Chapter 2**). The protein concentration was measured by the BCA (Bicinchoninic Acid) method with the use of Pierce™ BCA Protein Assay Kit. The degree of hydrolysis (DH) was calculated with Equations (4.S1-4.S5) in the Supplementary material.

During digestion, the pH of the supernatant was monitored with a pH meter (Metrohm Titrino 877, Switzerland). The H^+ balance was calculated with Equations (4.S6-4.S11) in the Supplementary material.

4.2.7 TD-NMR measurements

At t = 0, 15, 30, 60, 90 and 120 min after starting digestion, 150 μL supernatant samples were collected from the stomach chamber and immediately (within 30 s) measured with TD-NMR as follows: Each sample was pipetted in a 7 mm NMR tube, and the tube was sealed to prevent water loss during the measurements. It was then placed in a Maran Ultra NMR spectrophotometer (Resonance Instruments Ltd., Witney, UK) to perform ^1H TD-NMR relaxometry at 0.72 T with the use of RINMR software (Resonance Instruments Ltd., Witney, UK).

T_2 was measured by the Carr-Purcell-Meiboom-Gill (CPMG) sequence (P. McIntosh, 2013). During the CPMG pulse train, 12,288 echoes (five data points per echo) were recorded with an echo time of 0.8 ms. Four transients were recorded with phase cycling, with a repetition time of 15 s. Each echo in the CPMG echo train was phase-corrected and averaged to one data point by using an in-house routine programmed in IDL (ITT Visual

Information Solutions, Boulder, CO, USA). The transverse magnetisation decay curves were analysed with a numerical inverse Laplace transform by CONTIN, and the distribution of amplitude at different T_2 values was established (Provencher & Vogel, 1983). From the distribution curve, average T_2 was acquired, and R_2 (= T_2^{-1}) values were calculated.

T_1 was measured by Continuous Wave Free Precession (CWFP-T_1) pulses with low flip angles (Moraes et al., 2016). The first pulse was a 180° pulse, followed by a pause ($T_p/2$ = 125 µs) and a flip angle of ≈22° separated by T_p (250 µs). During the CWFP-T1 pulse train, 32,768 echoes (two data points per echo) were recorded with an echo time of 0.5 ms. Four transients were recorded with phase cycling and a relaxation delay of 40 s. Each echo in the CWFP-T_1 echo train was phase-corrected, and each echo was averaged to one data point using an in-house IDL routine. Average T_1 was acquired and used to calculate average R_1 (= T_1^{-1}).

4.2.8 MRI measurements

For the MRI scans, the MR-GAS stomach chamber was placed in a 3T MRI scanner (Philips Ingenia Elition X, Philips Medical Systems, the Netherlands). A 16-channel small extremity coil was wrapped around the stomach chamber. MRI scans were conducted at baseline before adding protein gels and after digestion for 5, 15, 30, 45, 60 and 90 min. During each scan, the gastric secretion, gastric emptying, air mixing and the recirculating heater were switched off to reduce artefacts caused by motion/influx. For T_2 mapping, a 2D multi-echo spin-echo sequence was used (repetition time = 3,000 ms, 32 echo times ranging from 60 to 2520 ms with an echo-spacing of 80 ms, matrix = 64 × 64, field of view (FOV) = 120 × 120 mm, in-plane resolution = 1.87 × 1.87 mm, 3.0 mm slice thickness, total acquisition time = 1 min 20 s).

For the image processing, the first echo time of 60 ms was removed to reduce systematic error and to achieve a better fit (Bonny et al., 1996; Milford et al., 2015). T_2-maps were calculated based on the acquired images at 31 echo times using a Levenberg-Marquard two-parameter curve fitting in MATLAB R2018b (MathWorks, Natick, USA) with Equation (4.1).

$$M_t = M_0 \cdot e^{-\frac{t}{T_2}} + offset \tag{4.1}$$

With t (echo time) and M_t, which is the voxel intensity at echo time t, we calculated the T_2 of each voxel, offset and M_0 (voxel equilibrium magnetic intensity).

For T_1 mapping, a 2D multi-echo GR/IR sequence was used (8 inversion times (TI) of 150, 570, 985, 1400, 1900, 2700, 4000 and 5000 ms, matrix = 64 × 64, FOV = 120 × 120 mm, in-plane resolution = 1.87 × 1.87 mm, 3.0 mm slice thickness, acquisition time 1-4 s per TI).

T_1-maps were calculated based on the acquired images at 8 inversion times using a Levenberg-Marquard two-parameter curve fitting in MATLAB R2018b (MathWorks, Natick, USA) using Equation (4.2).

$$M_t = 1 - M_0 \cdot \left(1 - e^{-\frac{TI}{T_1}}\right) \tag{4.2}$$

With the inversion time (TI) and M_t, which is the voxel intensity at TI, we calculated M_0 (voxel equilibrium magnetic intensity) and T_1 for each voxel.

For each time point, the supernatant was segmented manually on both the T_1 and T_2 map with the use of the MIPAV software (Bazin et al., 2007) (Fig. 4-S1 in Supplementary material). The mean T_1, R_1 (=T_1^{-1}), T_2 and R_2 (=T_2^{-1}) of the supernatant were calculated.

4.2.9 Statistical analysis

The means and standard deviations were calculated based on duplicates. In this paper, the expressions 'value ± value' represent 'mean ± standard deviation'. In the figures, the error bars represent standard deviations. The regression analyses for R_2 and R_1 with protein concentration and [H^+] were performed with the Curve Fitting Tool in Matlab R2018b (MathWorks, Natick, USA). To evaluate the goodness of prediction compared to the measured value, the normalised root mean squared deviation (NRMSD) was calculated with Equation (4.3).

$$NRMSD = \frac{1}{\overline{y^m}} \cdot \sqrt{\frac{\sum_{i=1}^{n}\left(y^m{}_i - y^e{}_i\right)^2}{n}} \tag{4.3}$$

Where $\overline{y^m}$ is the mean of the measured values at all data points; $y^m{}_i$ and $y^e{}_i$ are the measured value and predicted value respectively at data point i; n is the total amount of data points.

4.3 Results and discussion

4.3.1 Digestion of protein gels in MR-GAS

The MR-GAS was set up and tested for the digestion of WPI gels under lab conditions. The concentration of free amino groups (-NH_2 groups, Fig. 4-2a) and protein concentration (Fig. 4-2b) in the supernatant showed the extent of protein digestion over time.

During the first 30 min of digestion, the concentration of -NH_2 groups increased by 5.57 ± 0.23 mM for the 15% WPI gel and by 3.28 ± 0.20 mM for the 20% gel. Throughout the rest of gastric digestion, the concentration of -NH_2 groups increased slower for both gels. As expected, the change in protein concentration was similar to that in -NH_2 groups: in the first 30 min, protein concentration of the 15% gel increased by 3.67 ± 0.13 and that of the 20% gel by 2.05 ± 0.04 mg/mL. The finding that protein gels were digested at a rapid rate in the first 30 min during the gastric phase is in line with previous studies (**Chapter 2**; Luo et al., 2015). To mimic gastric emptying, the supernatant was removed from the stomach chamber after digestion for 30 min till the end. Therefore, the real-time peptide concentration in the supernatant (in Fig. 4-2a) does not represent the total amount of peptide produced. The total amount of peptide produced was calculated to obtain the degree of hydrolysis, which is discussed later. In line with other studies, the 15% gel was digested faster and to a larger extent than the 20% gel (**Chapter 2**; Luo et al., 2015). This is because the higher crosslinking density in 20% gel slows down the digestion via limiting pepsin diffusion, hydrolysis rate and microstructure transformation (Luo et al., 2017).

When protein concentration was plotted against the free amino acid group concentration in the supernatant, linear associations were observed for both gels (Fig. 4-2c). The slope of the 15% gel was higher than that of the 20% gel. This indicates that the average size of released peptides from both gels remains constant during digestion, and the average size of released peptides from the 20% gel was smaller compared to that from the 15% gel.

Compared to the results with a static model from **Chapter 2**, the degree of hydrolysis (DH) of protein gels in the MR-GAS was much higher (Fig. 4-2d); after 2 h of digestion, DH of the 15% gel was 2.6% in the static model, whereas it was 7.3% in the MR-GAS. For the 20% gel, DH was 1.0% in the static model and 3.1% in the MR-GAS. A higher digestion rate in dynamic models is comparable with results from other studies (Egger et al., 2018; Mennah-Govela and Bornhorst, 2021; Miralles et al., 2018). Interestingly, for both gels, the

slope of the DH curves in the static model decreased after one hour and the curves appear to nearly reach plateaus, while DH curves in the MR-GAS retained a rapid increase over two hours. Digestion in another dynamic digestion model showed a similar trend of increased DH to our results with MR-GAS (Mennah-Govela & Bornhorst, 2021). The reason for the difference between static and (semi-)dynamic digestion in DH changes is that with a (semi-)dynamic model, there is a continuous supply of pepsin and acid. This (1) increases the enzyme to substrate ratio and (2) lowers the pH. Both accelerate the enzymatic hydrolysis. Compared to a static model, the higher digestion rate in the MR-GAS confirmed the importance of performing *in vitro* digestion experiments under (semi-)dynamic conditions.

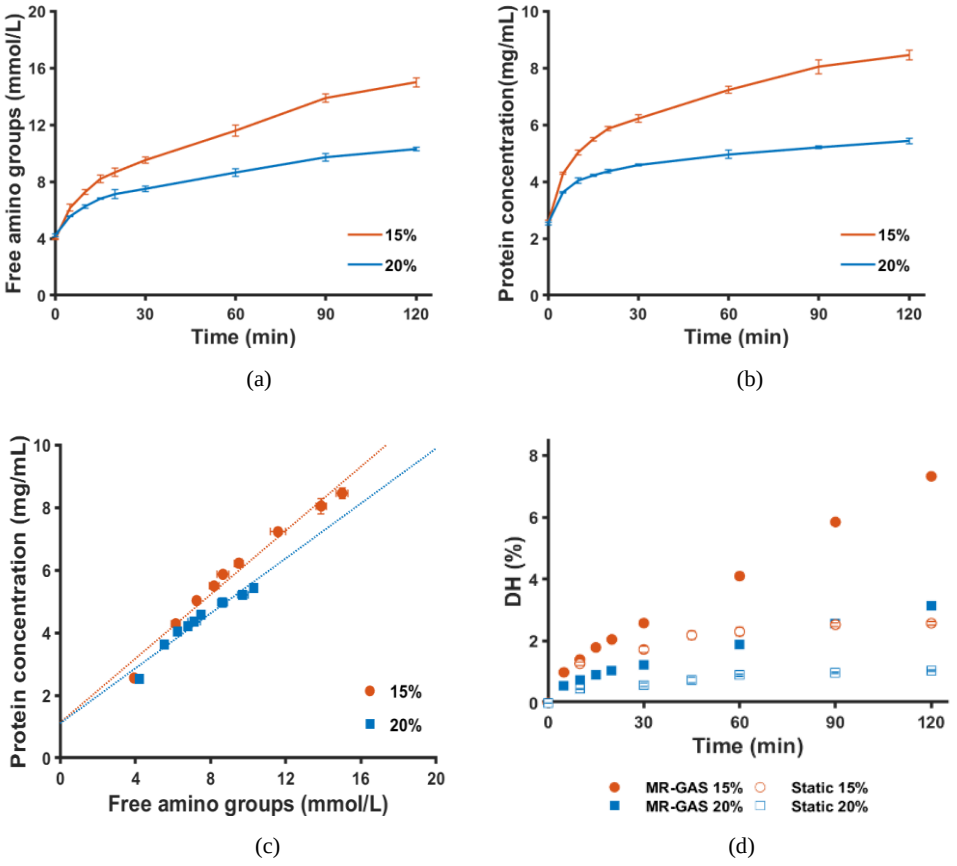

Fig. 4-2 *Free amino groups (a), protein concentration (b), the linear correlation (with explained variance of 0.96 and 0.96) between protein concentration and free amino groups (c) in the supernatant during gastric digestion of 15% gel and 20% gel, and DH (d) of 15% gel and 20% gel in MR-GAS and a static digestion model (data from* ***Chaper 2****)*

The pH of the supernatant was measured during the digestion of the 15% and 20% gels (Fig. 4-3a). The initial pH was 1.5. Within the first 15-30 min, the pH increased as a result of the buffering capacity of the gels and the released protein fraction from the gels to the supernatant (**Chapter 3**). After around 30 min, the pH of the supernatant decreased for both gels. It should be noted that SGF was continuously secreted throughout digestion, which decreased the pH, even though H^+ was taken up due to the buffering capacity and protein hydrolysis. Although the peptide concentration in the supernatant during digestion of the 20% gel was lower than that of the 15% gel, the pH in the supernatant of the 20% gel was higher than that of the 15% gel. This is likely due to the higher buffering capacity of the 20% gel. This is in accordance with another study in which protein gels with higher protein concentrations showed higher buffering capacity and a higher pH increase during gastric digestion (Luo et al., 2018).

A mass balance of H^+ was set up, which included the gastric juice secretion, uptake of H^+ due to buffering capacity and protein hydrolysis, gastric emptying, and the net H^+ in the supernatant (Fig. 4-S2). As shown in Fig. 4-3b, the majority of H^+ was taken up during digestion, as a sum result of buffering capacity and protein hydrolysis. The entire H^+ uptake of the 20% gel was higher than that of the 15% gel. After 2 h of digestion, acid uptake of the 15% gel was 1.9 mol/kg protein. This value is higher than that of the same gel in a static digestion model (1.6 mol/kg protein, **Chapter 3**), because of faster protein hydrolysis in the MR-GAS. Although we did not measure the amount of acid uptake without pepsin during the buffering reaction of our gel till pH 1.5, Mennah-Govela et al. (2019) reported that it was 1.2 mol/kg protein for a 16% WPI gel. The curve also shows that after 2 h of digestion, equilibrium was not yet reached, which implies that the pH of protein gels may still be higher than that of the SGF and that digestion could still be progressing. This is in line with the increasing trend of the DH curve in Fig. 4-2d.

To summarise, similar to previous studies, the 15% gel digested faster than the 20% gel, and both gels digested faster in the MR-GAS than in a static digestion model. The MR-GAS model has proven to be an adequate semi-dynamic digestion model. Remarkably, mixing of the gastric contents with the use of airflow was apparently effective and allowed the use of the stomach chamber within an MRI scanner.

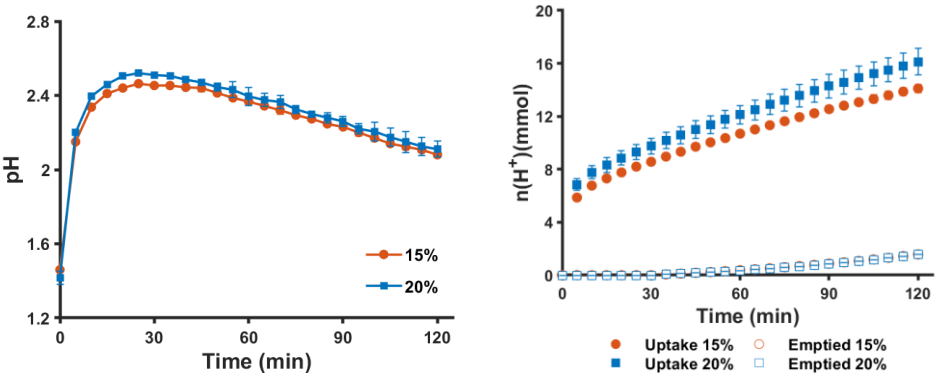

(a) (b)

Fig. 4-3 *pH of the supernatant during gastric digestion of 15% gel and 20% gel (a) and the amount of acid uptake by the system and acid emptied of 15% gel and 20% gel during digestion (b).*

4.3.2 R_2 and R_1 during digestion in MR-GAS

During the digestion of the 15% and the 20% gels in the MR-GAS, the supernatant was sampled, and transverse (R_2) and longitudinal (R_1) relaxation rates were measured by TD-NMR (Fig. 4-4). For both gels, R_2 increased over time and the fastest in the first 15 min (Fig. 4-4a). A faster and larger increase in R_2 was observed for the 15% gel compared to the 20% gel. It has been reported that R_2 can be linearly positively associated with protein concentration in solutions at the same pH (Le Dean et al., 2004). It has also been shown that a higher H^+ concentration (i.e. lower pH) and smaller molecular size decrease R_2 (Ozel et al., 2018). In the current work, the effect of molecular size on R_2 may be ignored since the average size of the released protein fraction remained consistent during digestion (see Section 4.3.1). Therefore, the increased R_2 over time is presumably due to the release of protein into the supernatant. Moreover, the rapid increase of pH (decrease of $[H^+]$) in the first 15 min likely contributes to the increased R_2 as well. The significantly slower increase in R_2 after 15 min may be due to the slower increase in protein concentration and the increase in $[H^+]$. In line with our previous findings (**Chapter 2**), a faster and larger increase in R_2 was observed for the 15% compared to the 20% gel, due to the faster digestion of the 15% gel.

Compared to R_2, R_1 increased less during digestion (Fig. 4-4b). Similar to R_2, higher protein concentration, lower $[H^+]$ and larger molecular size increase R_1 (Mariette, 2009; Oztop et al., 2010). Therefore, in the current study, the increase in R_1 could be attributed not only to

the increase in protein concentration but also to the steep decrease in $[H^+]$. Similar to R_2, a faster and larger increase in R_1 was observed for the 15% compared to the 20% gel, because of a higher protein concentration in the supernatant. Compared to R_2, R_1 showed less sensitivity to the changes in the protein concentration in the supernatant. In summary, both R_2 and R_1 increase during digestion and can therefore potentially serve as markers to track digestion.

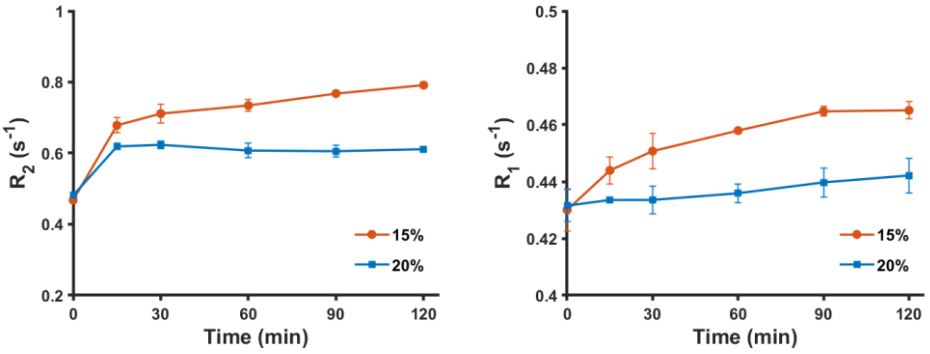

(a) (b)

Fig. 4-4 *R_2 (a) and R_1 (b) of supernatant during digestion of 15% gel and 20% gel, measured via TD-NMR.*

4.3.3 Estimating protein concentration and pH with the use of R_2 and R_1

To check the feasibility of using R_2 and R_1 for monitoring digestion, we investigated the relationships between R_2 and R_1 with protein concentration and $[H^+]$ using data of the 15% gel and applied the obtained equations to predict the digestion of the 20% gel. Linear regression (Fig. 4-S3 in Supplementary material) resulted in the following empirical equations and explained variance (R^2):

$$R_2 = 0.46 + 0.05 \cdot c_{protein} - 1.31 \cdot c_{protein} \cdot [H^+] \quad (R^2 = 0.99) \qquad (4.4)$$

$$R_1 = 0.41 + 0.006 \cdot c_{protein} - 0.02 \cdot c_{protein} \cdot [H^+] \quad (R^2 = 0.96) \qquad (4.5)$$

Using Equations (4.4) and (4.5), we predicted the concentration of protein and H^+ in the supernatant during digestion of 20% gel and calculated the pH ($= -\log[H^+]$) and compared these predictions with the measured values as shown in Fig. 4-5. The normalised root mean squared deviation (NRMSD) was used to examine the goodness of prediction. An NRMSD of 0 indicates a perfect prediction. The NRMSD was 0.15 and 0.12 for the protein concentration and pH respectively. Thus, predicted protein concentration and pH were

similar to the measured values. However, there was a small difference between the prediction and the measured values. This may be explained by the size of the released peptide from the 20% gel, which was slightly smaller than that from the 15% gel (see Section 4.3.1). This smaller molecular size results in a smaller relaxation rate. In summary, the results show that R_2 and R_1 can be effectively used as markers of changes in protein concentration and pH during *in vitro* gastric digestion of protein gels.

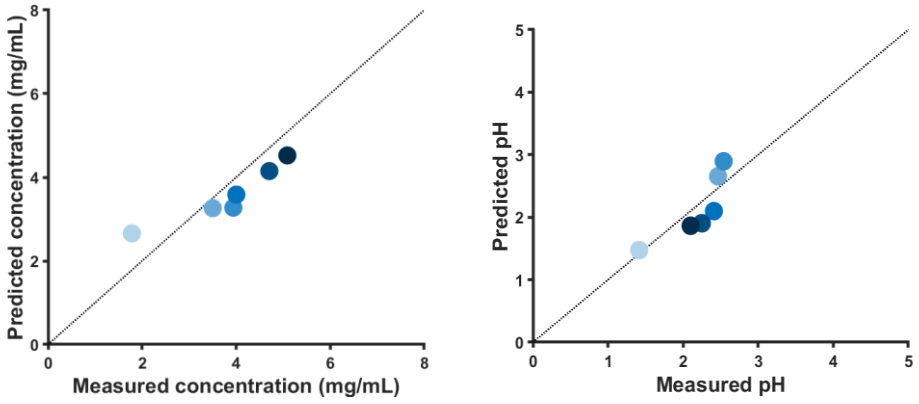

(a) (b)

Fig. 4-5 *Predicted against measured protein concentration (a) and predicted against measured pH (b) in the supernatant during digestion of 20% gel (Scatters with light to darker blue represent individual time points from 0 to 120 min). Predictions based on TD-NMR data.*

4.3.4 Monitoring digestion in the MR-GAS with MRI

To further assess their potential for *in vivo* applications, R_2 and R_1 were measured by MRI during gastric digestion of 15% and 20% gels in the MR-GAS. While we only sampled supernatant in the TD-NMR measurements, with the MRI measurements, we measured both the gel and supernatant since the entire stomach chamber of the MR-GAS was placed in the MRI. Fig. 4-6 shows the colour-coded T_2 distribution and T_1 distribution in the stomach chamber during digestion of the 15% gel over time. In the baseline scan, there is only SGF present because that represents the fasting state. From t = 5 min onwards, two phases can be distinguished in the T_2 and T_1 maps, with protein gel particles visible in the lower part and the supernatant in the upper part. Fig. 4-7 shows the average R_2 and R_1 of the supernatant plotted against digestion time. The R_2 of the supernatant increased from 0.48 ± 0.001 to 0.77 ± 0.02 s^{-1} during 90 min of digestion (Fig. 4-7a), as was reflected in the change of colour from red to a darker blue in the T_2 map (Fig. 4-6a). This increase in R_2

was mainly caused by an increased protein concentration in the digesta. A smaller increase in R_2 was observed for the 20% gel because this gel was digested to a less extent. R_2 changes show a similar trend as that measured with TD-NMR (Fig. 4-4a), so we refer to the discussion in Section 4.3.2.

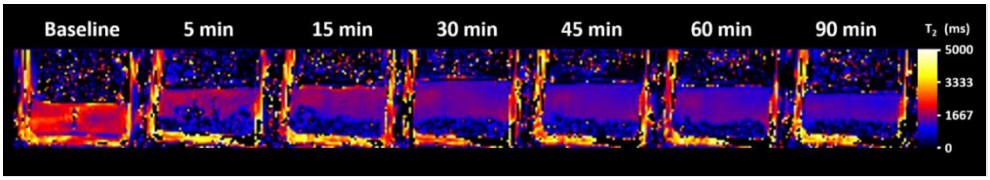

(a)

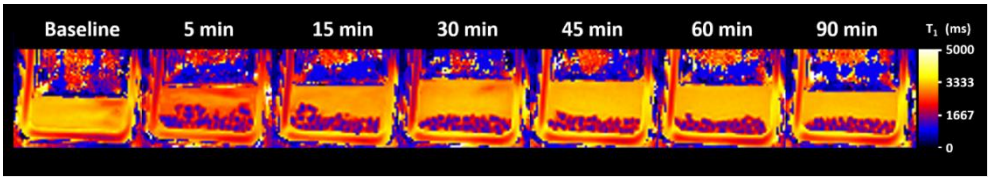

(b)

Fig. 4-6 *T_2 maps (a) and T_1 maps (b) of the gastric content in MR-GAS during digestion of WPI 15% from baseline to 90 min ($T_2 = R_2^{-1}$ and $T_1 = R_1^{-1}$).*

The R_1 of both the 15% and the 20% gels did not change much during digestion, except for an increase at t = 5 min for the 15% gel (Fig. 4-7b). The reason for this may be that R_1 is highly dependent on the magnetic field strength (Korb and Bryant, 2002). Since the MRI has a higher field strength (3T), it results in a smaller R_1 compared to that measured with TD-NMR (0.72 T). This could make the change in R_1 even smaller and harder to detect than with TD-NMR. The increase of R_1 at 5 min for the 15% gel was unexpected. Nelson & Tung (1987) showed that a lower temperature increases R_1, and a stronger temperature effect was shown in the liquids with higher protein concentrations. Since, in our experiment, the SGF was heated to 37 ˚C while the gel was at room temperature. The addition of the gel into the SGF resulted in a transient temperature decrease of approximately 5 ˚C at t = 5 min. This could have caused the observed increase in R_1. The higher protein concentration in the supernatant of the 15% gel may have reinforced this temperature effect compared to the 20% gel. However, more systematic research about how temperature affects the relaxation rates of acidic samples need to be conducted to support this explanation.

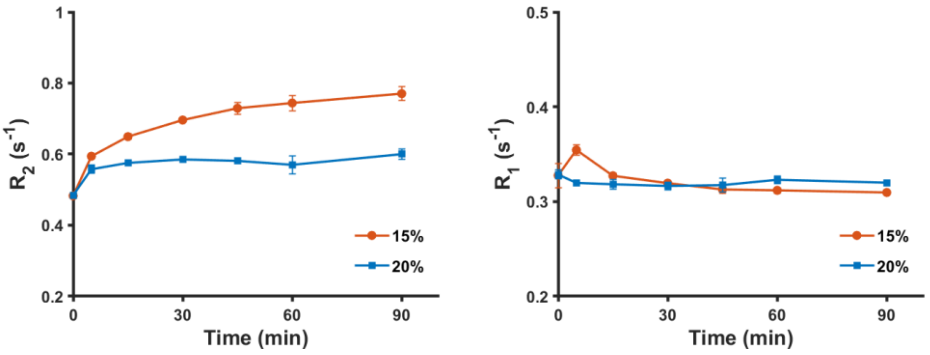

(a) (b)

Fig. 4-7 *R_2 (a) and R_1 (b) values of supernatant during 90 min digestion, measured via MRI.*

We determined the relationships between R_1 and R_2 with protein concentration and $[H^+]$ using data of the 15% gel and applied the obtained equation to predict the digestion of the 20% gel. Linear regression (Fig. 4-S4 in Supplementary material) resulted in the following empirical equations and explained variance (R^2):

$$R_2 = 0.39 + 0.05 \cdot c_{protein} - 0.29 \cdot c_{protein} \cdot [H^+] \quad (R^2 = 0.99) \tag{4.6}$$

$$R_1 = 0.38 - 0.008 \cdot c_{protein} - 0.38 \cdot c_{protein} \cdot [H^+] \quad (R^2 = 0.60) \tag{4.7}$$

The lower explained variance in Equation (4.7) was caused by the increase in R_1 at t = 5 min; omitting this data point increased the explained variance from 0.60 to 0.85. This is shown in Fig. 4-S5 in Supplementary material. Using original Equations (4.6) and (4.7) (without omitting t = 5 min), we predicted the protein concentration and $[H^+]$ in the supernatant during digestion of the 20% gel and calculated the pH ($= -\log[H^+]$). We compared the predictions with the measured values (Fig. 4-8). The NRMSD values were 0.18 and 0.29 for the protein concentration and pH respectively, and the values did not decrease, even when using the obtained equations that omitted t = 5 min (shown in Fig. 4-S6 in Supplementary material). These NRMSD values were higher than those in the TD-NMR analysis. These less good predictions may be due to the fact that the R_1 (MRI) did not change much during digestion, so contributed less to the prediction. Thus, in this context, other magnetic resonance markers may be better suited as proxy measures for nutrient hydrolysis and pH change during digestion; however, they are currently underexplored (Smeets et al., 2020). The current results indicate that R_2 and R_1 are potential markers of protein concentration and acidic pH and may be used to monitor the semi-dynamic gastric

digestion of protein gels in a clinical MRI. Such *in vitro* results can contribute to the interpretation of similar measures done *in vivo*.

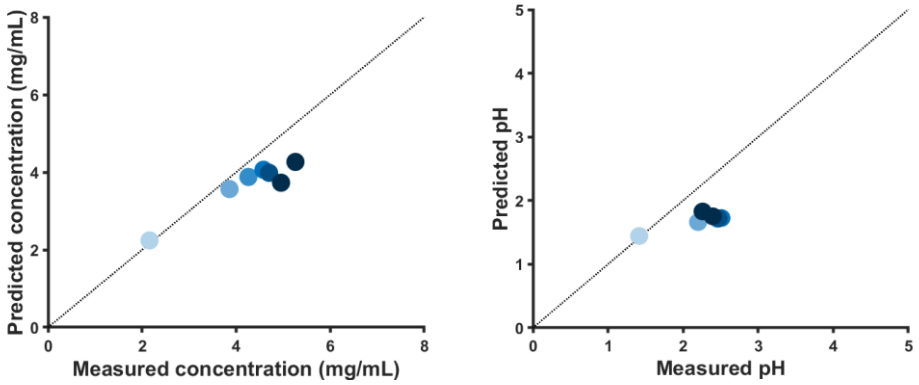

(a) (b)

Fig. 4-8 *Predicted against measured protein concentration (a) and predicted against measured pH (b) in the supernatant during digestion of 20% gel (Scatters with light to darker blue represent individual time points from 0 to 120 min). Predictions based on MRI data.*

Based on the current study, the applications of MR-GAS can be further extended, including altering the rate of gastric secretion and emptying to mimic different gastric responses to different stages of gastric digestion, to different types of food or to represent different populations. Furthermore, it would be worthwhile exploring the application of the MR parameters to study digestion of other more complex food matrices and using a naturalistic pH trajectory.

4.4 Conclusion

In this study, we developed the MR-GAS: the first semi-dynamic MRI compatible *in vitro* gastric digestion model. The results demonstrate its capability to incorporate gastric secretion, emptying and mixing not only in a lab set-up, but also in a clinical MRI scanner. The protein digestion rate in the MR-GAS is comparable with that reported for other semi-dynamic models. Furthermore, we show that R_2 and R_1, as measured with NMR and MRI, can be used to monitor digestion under dynamic circumstances: protein concentration and pH were the two main parameters that changed in the supernatant during digestion and the relationships between them with R_2 and R_1 were analysed with linear regression. Therefore, using the empirical equations obtained from the linear regression analysis, we were able to predict the protein concentration and pH with the input of measured R_2 and R_1. Prediction with the use of R_2 and R_1 from TD-NMR was more accurate than that from MRI. Further research on MRI derived R_2 and R_1 measurements will be essential to bring *in vitro* results and *in vivo* data together, and the MR-GAS model can contribute to this translation. In conclusion, the MR-GAS is a useful tool for *in vitro* digestion MRI research and R_2 and R_1 could serve as markers of changes in protein concentration and pH during digestion. These findings set the stage for monitoring gastric protein digestion *in vivo* using MRI in the future.

Supplementary material

1. The calculation equations for Section 4.2.6.

a) The degree of hydrolysis (DH) was calculated by Equation (4.S1-S5).

$$DH = \frac{n(-NH_{2_{t_i}})}{n(-NH_{2_{total}})} \cdot 100\% \quad (4.S1)$$

$$n(-NH_{2_{total}}) = h_{tot} \cdot m_{Gel} \cdot c(protein) \quad (4.S2)$$

$$n(-NH_{2_{t_i}}) = n(-NH_{2_{t_{i-1}}}) + \sum_{t_{i-1}}^{t_i} n(-NH_{2_{emptied}}) - \sum_{t_0}^{t_i} n(-NH_{2_{SGF}}) \quad (4.S3)$$

$$\sum_{t_{i-1}}^{t_i} n(-NH_{2_{emptied}}) = \frac{c(-NH_{2_{t_i}}) + c(-NH_{2_{t_i}})}{2} \cdot r_e \cdot (t_i - t_{i-1}) \quad (4.S4)$$

$$\sum_{t_0}^{t_i} n(-NH_{2_{SGF}}) = c(-NH_{2_{SGF}}) \cdot V_0 + c(-NH_{2_{SGF}}) \cdot r_s \cdot (t_i - t_{i-1}) \quad (4.S5)$$

Where $n(-NH_{2_{t_i}})$ is the -NH_2 groups released from WPI gels between t_0 to t_i, $n(-NH_{2_{total}})$ is the total -NH_2 groups in the WPI gels. In Equation (4.S2), h_{tot} is the number of peptide bonds per gram protein (8.8 meq/g for WPI); m_{Gel} is the initial weight of the gels (50 g) and c(protein) is the protein concentration in the gels (0.15 g or 0.2 g protein per g gel). In Equation (4.S3), $\sum_{t_{i-1}}^{t_i} n(-NH_{2_{emptied}})$ is the amount of -NH_2 groups removed from the stomach chamber from t_{i-1} to t_i because of gastric emptying; $\sum_{t_0}^{t_i} n(-NH_{2_{SGF}})$ is the amount of -NH_2 groups originally from in SGF from t_0 to t_i. In Equation (4.S4), $c(-NH_{2_{t_i}})$ is the concentration of -NH_2 group at time point t_i (measured by OPA), and r_e is the rate of gastric emptying (3.33 ml/min). In equation 5, $c(-NH_{2_{SGF}})$ is the concentration of -NH_2 group in SGF (measured by OPA), V_0 is the volume of SGF at baseline (150 mL), and r_s is the gastric secretion rate (2.5 mL/min).

b) The H^+ balance was calculated with Equations (4.S6-S11).

$$n(H^+)_{supernatant_{t_i}} = 10^{-pH_{t_i}} \cdot V_{t_i} \quad (4.S6)$$

$$n(H^+)_{emptied_{t_i}} = n(H^+)_{emptied_{t_{i-1}}} + \sum_{t_{i-1}}^{t_i} n(H^+)_{emptied} \quad (4.S7)$$

$$\sum_{t_{i-1}}^{t_i} n(H^+)_{emptied} = \frac{10^{-pH_{t_i}} + 10^{-pH_{t_{i-1}}}}{2} \cdot r_e \cdot (t_i - t_{i-1}) \quad (4.S8)$$

$$n(H^+)_{uptake_{t_i}} = \sum_{t_0}^{t_i} n(H^+)_{SGF} - n(H^+)_{emptied_{t_i}} - n(H^+)_{supernatant_{t_i}} \quad (4.S9)$$

$$\sum_{t_0}^{t_i} n(H^+)_{SGF} = n(H^+)_{net_{t_0}} + 10^{-pH_{t_0}} \cdot r_s \cdot (t_i - t_0) \quad (4.S10)$$

$$n(H^+)_{uptake_{t_i}}/kg\ protein = \frac{n(H^+)_{uptake_{t_i}}}{m_{Gel} \cdot c(protein)} \quad (4.S11)$$

In Equation (4.S6), $n(H^+)_{supernatant_{t_i}}$ is the amount of net H^+ in the supernatant in MR-GAS at the time point t_i; pH_{t_i} is the pH valued at t_i, and V_{t_i} is the volume of the supernatant at t_i; In Equation (4.S7), $n(H^+)_{emptied_{t_i}}$ is the amount of H^+ removed from the stomach chamber from t_0 to t_i because of gastric emptying; $\sum_{t_{i-1}}^{t_i} n(H^+)_{emptied}$ is the amount of H^+ removed from the stomach chamber from t_{i-1} to t_i because of gastric emptying. In Equation (4.S9), $n(H^+)_{uptake_{t_i}}$ represents the amount of H^+ uptake by the system; $\sum_{t_0}^{t_i} n(H^+)_{SGF}$ is the amount of H^+ provided by SGF from t_0 to t_i.

2. Illustration of segmentation on the MRI image

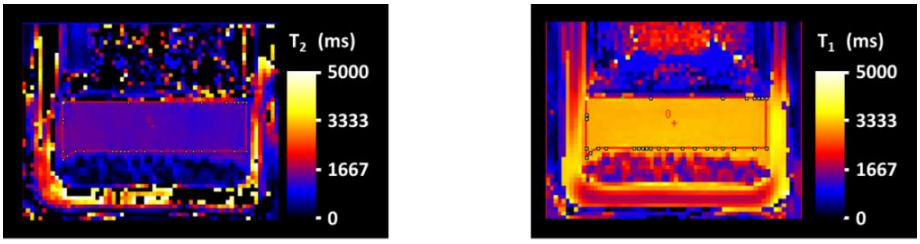

(a) (b)

Fig.4-S1 *Region of interest selection on a T_2 map (a) and a T_1 map (b). The region inside of the red line is considered the supernatant phase.*

3. Illustration of H^+ balance

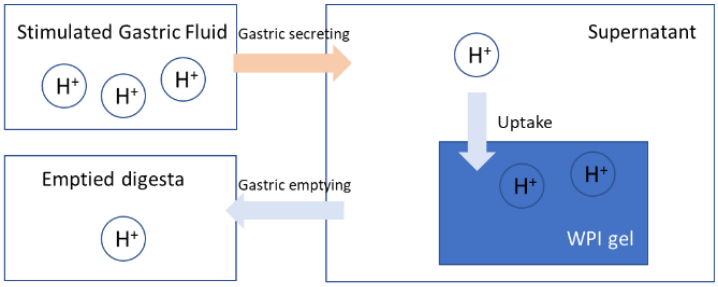

$$n(H^+)_{supernatant} = n(H^+)_{SGF} - n(H^+)_{uptake} - n(H^+)_{emptied}$$

Fig. 4-S2 *The illustration of the mass balance of H^+ in MR-GAS. The H^+ is provided by simulated gastric fluid (SGF) and is either still present in the supernatant in the stomach chamber, or taken up by the system due to the buffering capacity or protein hydrolysis of the WPI gels, or removed from the stomach chamber because of gastric emptying.*

4. The relationships between R_2 and R_1 with protein concentration and $[H^+]$

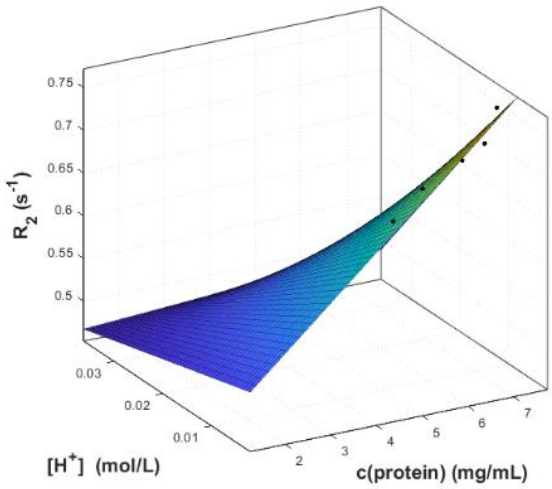

(a)

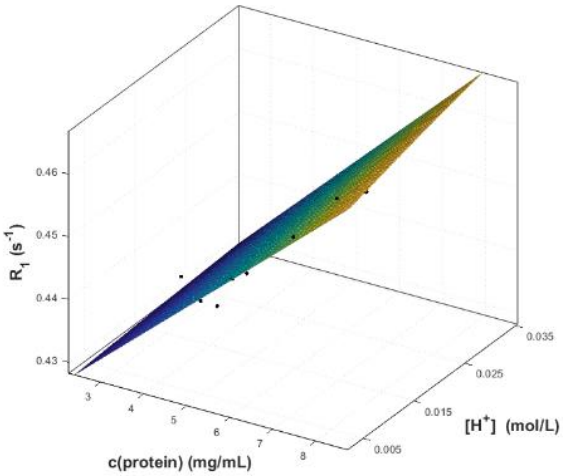

(b)

Fig.4-S3 *The relationships between R2 (a) and R1 (b) with protein concentration and H+ concentration, measured via TD-NMR.*

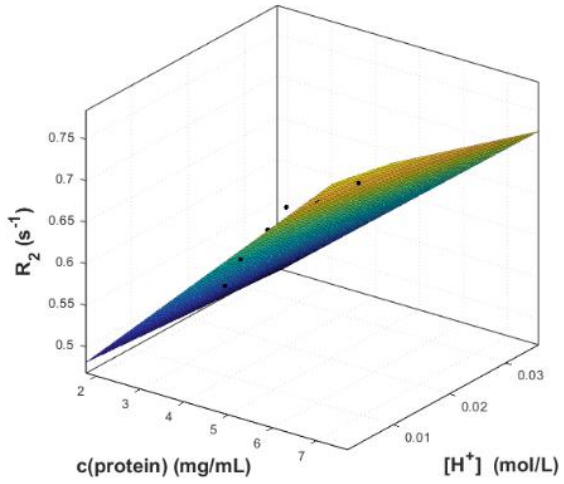

(a)

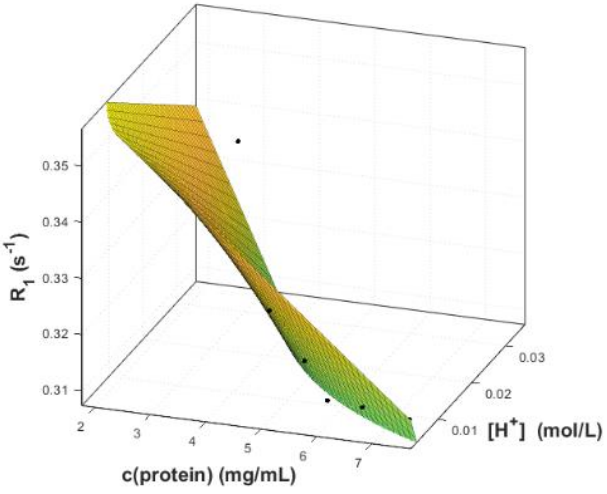

(b)

Fig.4-S4 *The relationships between R_2 (a) and R_1 (b) with protein concentration and H^+ concentration, measured via MRI.*

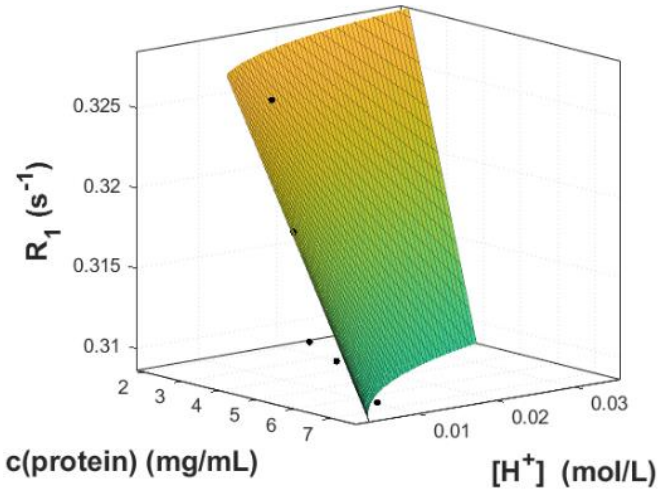

Fig.4-S5 *The relationships between R_1 with protein concentration and H^+ concentration, measured via MRI (Similar as Fig 4b but omitting the data point at t = 5min)*

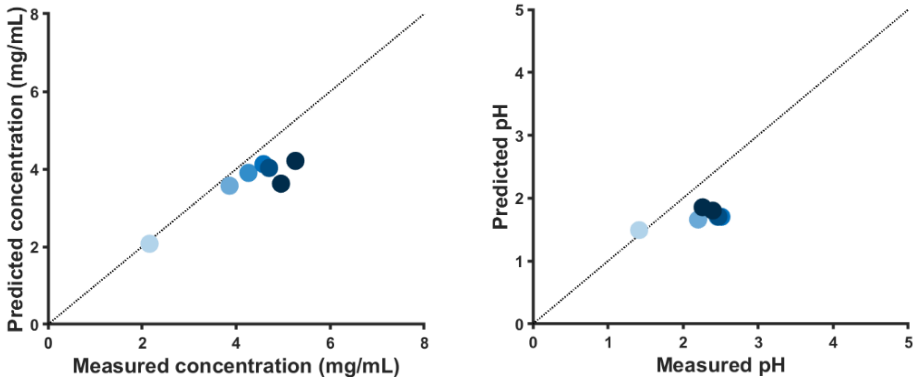

(a) (b)

Fig.4-S6 *Predicted against measured protein concentration (a) and predicted against measured pH (b) in the supernatant during digestion of 20% gel (Scatters with light to darker blue represent individual time points from 0 to 120 min). Similar as Fig.4-8 in the manuscript, but predictions here are based on MRI data using equations omitting data point at t = 5 min. The NRMSD is 0.19 and 0.29 for protein concentration and pH respectively.*

References

Bazin, P. L., Cuzzocreo, J. L., Yassa, M. A., Gandler, W., McAuliffe, M. J., Bassett, S. S., & Pham, D. L. (2007). Volumetric neuroimage analysis extensions for the MIPAV software package. Journal of Neuroscience Methods, 165(1), 111–121. https://doi.org/10.1016/j.jneumeth.2007.05.024

Bonny, J. M., Zanca, M., Boire, J. Y., & Veyre, A. (1996). T2 maximum likelihood estimation from multiple spin-echo magnitude images. Magnetic Resonance in Medicine. https://doi.org/10.1002/mrm.1910360216

Bordoni, A., Picone, G., Babini, E., Vignali, M., Danesi, F., Valli, V., … Capozzi, F. (2011). NMR comparison of *in vitro* digestion of Parmigiano Reggiano cheese aged 15 and 30 months. Magnetic Resonance in Chemistry, 49(SUPPL. 1). https://doi.org/10.1002/mrc.2847

Bornhorst, G. M. (2017). Gastric mixing during food digestion: mechanisms and applications. Annual Review of Food Science and Technology, 8(1), 523–542. https://doi.org/10.1146/annurev-food-030216-025802

Brodkorb, A., Egger, L., Alminger, M., Alvito, P., Assunção, R., Ballance, S., … Recio, I. (2019). INFOGEST static *in vitro* simulation of gastrointestinal food digestion. Nature Protocols, 14(4), 991–1014. https://doi.org/10.1038/s41596-018-0119-1

Deng, R., Janssen, A. E. M., Vergeldt, F. J., Van As, H., de Graaf, C., Mars, M., & Smeets, P. A. M. (2020). Exploring *in vitro* gastric digestion of whey protein by time-domain nuclear magnetic resonance and magnetic resonance imaging. Food Hydrocolloids, 99, 105348. https://doi.org/10.1016/j.foodhyd-.2019.105348 (Chapter 2 in this thesis)

Deng, R., Mars, M., Van Der Sman, R. G. M., Smeets, P. A. M., & Janssen, A. E. M. (2020). The importance of swelling for *in vitro* gastric digestion of whey protein gels. Food Chemistry, 330, 127182. https://doi.org/10.1016/j.foodchem.2020.127182 (Chapter 3 in this thesis)

Egger, L., Ménard, O., Baumann, C., Duerr, D., Schlegel, P., Stoll, P., … Portmann, R. (2018). Digestion of milk proteins: Comparing static and dynamic *in vitro* digestion systems with *in vivo* data. Food Research International, (October), 0–1. https://doi.org/10.1016/j.foodres.2017.12.049

Gouseti, O., Bornhorst, G. M., Bakalis, S., & Mackie, A. (2019). Interdisciplinary Approaches to Food Digestion. (O. Gouseti, G. M. Bornhorst, S. Bakalis, & A. Mackie, Eds.), Interdisciplinary Approaches to Food Digestion. Cham: Springer International Publishing. https://doi.org/10.1007/978-3-030-03901-1

Guo, Q., Ye, A., Lad, M., Ferrua, M., Dalgleish, D., & Singh, H. (2015). Disintegration kinetics of food gels during gastric digestion and its role on gastric emptying: An *in vitro* analysis. Food and Function, 6(3), 756–764. https://doi.org/10.1039/c4fo00700j

Hashemi, R. H., Bradley, W. G., & Lisanti, C. J. (2012). MRI: The Basics: The Basics. Lippincott Williams & Wilkins.

Kong, F., & Singh, R. P. (2008). A model stomach system to investigate disintegration kinetics of solid foods during gastric digestion. Journal of Food Science, 73(5), 202–210. https://doi.org/10.1111/j.1750-3841.2008.00745.x

Korb, J. P., & Bryant, R. G. (2002). Magnetic field dependence of proton spin-lattice relaxation times. Magnetic Resonance in Medicine. https://doi.org/10.1002/mrm.10185

Le Dean, A., Mariette, F., & Marin, M. (2004). 1H nuclear magnetic resonance relaxometry study of water state in milk protein mixtures. Journal of Agricultural and Food Chemistry, 52(17), 5449–5455. https://doi.org/10.1021/jf030777m

Luo, Q., Boom, R. M., & Janssen, A. E. M. (2015). Digestion of protein and protein gels in simulated gastric environment. LWT - Food Science and Technology, 63(1), 161–168. https://doi.org/10.1016/j.lwt.-2015.03.087

Luo, Q., Borst, J. W., Westphal, A. H., Boom, R. M., & Janssen, A. E. M. (2017). Pepsin diffusivity in whey protein gels and its effect on gastric digestion. Food Hydrocolloids, 66, 318–325. https://doi.org-/10.1016/j.foodhyd.2016.11.046

Luo, Q., Zhan, W., Boom, R. M., & Janssen, A. E. M. (2018). Interactions between acid and proteins under *in vitro* gastric condition-a theoretical and experimental quantification. Food and Function, 9(10), 5283–5289. https://doi.org/10.1039/c8fo01033a

Marciani, L. (2011). Assessment of gastrointestinal motor functions by MRI: A comprehensive review. Neurogastroenterology and Motility, 23(5), 399–407. https://doi.org/10.1111/j.1365-2982.2011.01670.x

Mariette, F. (2009). Investigations of food colloids by NMR and MRI. Current Opinion in Colloid and Interface Science, 14(3), 203–211. https://doi.org/10.1016/j.cocis.2008.10.006

Mennah-Govela, Y. A., & Bornhorst, G. M. (2021). Breakdown mechanisms of whey protein gels during dynamic *in vitro* gastric digestion. Food and Function. https://doi.org/10.1039/d0fo03325a

Mennah-Govela, Y. A., Singh, R. P., & Bornhorst, G. M. (2019). Buffering capacity of protein-based model food systems in the context of gastric digestion. Food & Function, 10(9), 6074–6087. https://doi.org/10.1039/C9FO01160A

Milford, D., Rosbach, N., Bendszus, M., & Heiland, S. (2015). Mono-exponential fitting in T2-relaxometry: Relevance of offset and first echo. PLoS ONE. https://doi.org/10.1371/journal.pone.0145255

Minekus, M., Alminger, M., Alvito, P., Ballance, S., Bohn, T., Bourlieu, C., … Brodkorb, A. (2014). A standardised static *in vitro* digestion method suitable for food-an international consensus. Food and Function, 5(6), 1113–1124. https://doi.org/10.1039/c3fo60702j

Miralles, B., del Barrio, R., Cueva, C., Recio, I., & Amigo, L. (2018). Dynamic gastric digestion of a commercial whey protein concentrate†. Journal of the Science of Food and Agriculture, 98(5), 1873–1879. https://doi.org/10.1002/jsfa.8668

Moraes, T. B., Monaretto, T., & Colnago, L. A. (2016). Rapid and simple determination of T1 relaxation times in time-domain NMR by Continuous Wave Free Precession sequence. Journal of Magnetic Resonance, 270, 1–6. https://doi.org/10.1016/j.jmr.2016.06.019

Nelson, T. R., & Tung, S. M. (1987). Temperature dependence of proton relaxation times *in vitro*. Magnetic Resonance Imaging, 5(3), 189–199. https://doi.org/10.1016/0730-725X(87)90020-8

Ozel, B., Aydin, O., Grunin, L., & Oztop, M. H. (2018). Physico-Chemical Changes of Composite Whey Protein Hydrogels in Simulated Gastric Fluid Conditions. Journal of Agricultural and Food Chemistry, 66(36), 9542–9555. research-article. https://doi.org/10.1021/acs.jafc.8b02829

Oztop, M. H., Rosenberg, M., Rosenberg, Y., McCarthy, K. L., & McCarthy, M. J. (2010). Magnetic resonance imaging (MRI) and relaxation spectrum analysis as methods to investigate swelling in whey protein gels. Journal of Food Science, 75(8). https://doi.org/10.1111/j.1750-3841.2010.01788.x

P. McIntosh, L. (2013). CPMG. In G. C. K. Roberts (Ed.), Encyclopedia of Biophysics (p. 386). Berlin, Heidelberg: Springer Berlin Heidelberg. https://doi.org/10.1007/978-3-642-16712-6_320

Peters, J. P. C. M., Vergeldt, F. J., Van As, H., Luyten, H., Boom, R. M., & van der Goot, A. J.

(2016). Time domain nuclear magnetic resonance as a method to determine and characterize the water-binding capacity of whey protein microparticles. Food Hydrocolloids, 54, 170–178. https://doi.org/10.1016/j.foodhyd-.2015.09.031

Singh, H., & Gallier, S. (2014). Processing of food structures in the gastrointestinal tract and physiological responses. Food Structures, Digestion and Health. https://doi.org/10.1016/B978-0-12-404610-8.00002-5

Smeets, P. A. M., Deng, R., van Eijnatten, E. J. M., & Mayar, M. (2020). Monitoring food digestion with magnetic resonance techniques. Proceedings of the Nutrition Society, 1–11. https://doi.org/10.1017/S0029665-120007867

Spiller, R., & Marciani, L. (2019). Intraluminal impact of food: new insights from MRI. Nutrients, 11(5), 1147. https://doi.org/10.3390/nu11051147

Chapter 5

Gastric digestion of whey protein gels: an MRI human trial

This chapter will be submitted as:

Deng, R., Mars, M., Janssen, A. E. M., & Smeets, P. A. M. Gastric digestion of whey protein gels: an MRI human trial.

Abstract

Food structure affects the breakdown kinetics of food. This has been extensively studied via *in vitro* digestion models. However, *in vitro* findings need to be verified *in vivo* as human digestive physiology is inherently complex. Previously, we found that MRI parameters (T_1 and T_2 relaxation times) can serve as markers of protein digestion. Here, we assessed the effect of food hardness and protein content on gastric emptying, and additionally investigated the application of the MRI parameters to monitor *in vivo* gastric digestion. A randomized cross-over trial was conducted with 18 healthy males (age: 27 ± 5; BMI 23 ± 1 kg/m^2). They ingested three gels differing in hardness and protein content: a soft gel with low protein content (Soft-LP), a hard gel with low protein content (Hard-LP), and a hard gel with high protein content (Hard-HP) . Before and after ingestion, abdominal MRI scans and appetite and well-being ratings were obtained. At the end participants ate an ad libitum lunch. Gastric content volume and T_1 and T_2 of the gastric content were determined from the MRI scans. Gastric content volume was different among treatments: High-HP < Soft-HP < Soft-LP, although some time points are not statistically significantly different. With all treatments, mean T_1 and T_2 of the measured stomach content decreased after ingestion from baseline and then gradually increase since 15 min. The treatments showed different T_1 and T_2 values: Hard-HP < Soft-HP < Soft-LP, although not all the time points were statistically significantly different. High protein content is the main factor in delaying gastric emptying and high hardness is an additional factor. T_1 and T_2 measurements can provide extra information on the dilution and digestion taking place in the stomach. This study suggests the potential of these MRI parameters and provides insights on *in vivo* digestion that can be used to link *in vitro* and *in vivo* digestion research.

5.1 Introduction

The prevalence of overweight and obesity in societies has increased dramatically worldwide. Different approaches have been investigated to tackle the increase in obesity, including attempts to modify eating behavior and to promote physical activity. Delayed gastric emptying may contribute to earlier satiation and a prolonged feeling of satiety, which would limit the amount of food consumed (Norton et al., 2015; Sah et al., 2016). This may work through the release of GI hormones to modulate food intake when the nutrients are sensed in the small intestine. A better understanding of the interaction of different food properties with gastric digestion and related physiological processes can help the food industry in designing innovative foods that alter GI transit time and control the rate of release of micronutrients (Bornhorst & Singh, 2014; Norton, Moore, & Fryer, 2007).

The significant influence of food structure on the disintegration kinetics of food matrix has been well established by various *in vitro* studies (Bornhorst & Singh, 2014; Singh et al., 2015). Food with higher hardness or crosslinking density showed a slower rate of gastric digestion. The mechanism involves the different rates of erosion and rates of pepsin, gastric acid and water transportation. Based on the *in vitro* studies, it is expected that the difference in disintegration kinetics caused by different food structures would result in different gastric digestion and emptying rates in humans. Moreover, with an *in vitro* dynamic digestion model, faster gastric emptying was observed with softer whey protein gels compared to the harder variations (Guo et al. 2015). This needs to be verified in humans where the physiological effects can be demonstrated.

Limited knowledge about the effect of food structure on *in vivo* gastric emptying has been acquired with human trials, although some studies investigated the gastric emptying of solid meals. Early studies focused more on the nutrient composition and density and physical properties of the meal, for example liquid/solid composition and particle size of the solid; from these studies, the nutrient density of the meal was found as the most important factor for gastric emptying (Fisher et al., 1982; Houghton et al., 1988; Hunt and Stubbs, 1975; Urbain et al., 1989; Weiner et al., 1981). More recently, researchers started to investigate the impact of different food structures on gastric emptying. For example, Marciani et al. (2001b) showed that harder gel beads resulted in a slower gastric emptying compared to the softer variation, however, the gel beads were made with agar which is non-caloric.

Moreover, Marciani et al. (2013) compared gastric emptying of two equicaloric meals with a different structure (bread and rice pudding) and found that bread meal resulted in a slower gastric emptying compared to rice pudding meal. Another studied showed that changing the food microstructure of a mixed solid/liquid meal by blending it to a soup slowed gastric emptying and enhanced intestinal response to the meal, and this combination of effects resulted in prolonged satiety (Marciani et al., 2012). A better understanding of the relationship between the structure of the solid food, *in vivo* gastric digestion and changes in satiety remains to be developed.

Previous research showed that magnetic resonance techniques are potential methods not only for observing intragastric processes and gastric emptying, but also the molecular changes accompanying digestive processes (Smeets et al., 2020; Spiller and Marciani, 2019). As non-invasive techniques, they can be applied on both to *in vitro* samples and *in vivo*. Thus, they can be used to bridge the gap between *in vitro* and *in vivo* digestion studies and aid in their validation. However, the application of magnetic resonance imaging (MRI) markers in studying digestion is as yet underexplored.

Therefore, food with structure differences need to be well-designed and further examined to better understand how the structure of solid food affects gastric emptying. Whey protein gels, which are easy-prepared and structure-alterable systems, have been widely used as solid-model foods to study the mechanism of gastric digestion of solid food (Deng et al., 2020; Luo et al., 2017; Remondetto, Beyssac, & Subirade, 2004; Sarkar et al., 2016). In this study, we aim to investigate how food structure and nutrient density of different protein gels affect human gastric emptying and satiety. Our previous work showed the potential of the MRI parameters, transverse relaxation time (T_2) and longitudinal relaxation time (T_1), as markers to monitor pH and protein digestion in a semi-dynamic *in vitro* digestion model (as shown in **Chapters 2** and **4**). Therefore, a secondary aim of this chapter is to examine to which extent the relaxation times can inform *in vivo* gastric digestion.

5.2 Materials and methods

5.2.1 Participants

The participants were 18 males (age: 27 ± 5 y; BMI 23 ± 1 kg/m^2). They were recruited via flyers/posters and the internet in the Wageningen area. Inclusion criteria were aged between 18 and 45 years; BMI between 18.5 and 25 kg/m^2; self–reported good general health. Exclusion criteria were vegan; allergic or intolerant to any of the ingredients of the food used in the study; use of any medication that may alter normal stomach function; having a gastric disorder or regular gastric complaints; not being able to undergo MRI scanning.

The potential participants were informed about the details of this study via online information meetings and were asked to fill out an inclusion questionnaire to be screened for eligibility. Subsequently, they were invited for a screening session including measurements of weight and height and tasting the test meals.

Study procedures were approved by the Medical Ethical Committee of Wageningen University and Research (WUR) and in accordance with the Declaration of Helsinki. The trial NL74166.081.20 was registered with the Dutch Trial Registry (www.trialregister.nl, NL8822). Written informed consent was signed by all the participants before their participation.

5.2.2 Treatments: whey protein gels and water

The three whey protein gels were differed in protein content and hardness. They were prepared with whey protein isolate (WPI, Davisco Food International, Inc., USA), tap water, tabletop sweetener (Zoetjes, Albert Hein, the Netherlands), table salt (NaCl) and vanilla aroma (Aroma Vanilla, Dr. Oetker, the Netherlands). Table 5-1 shows the energy content, hardness, and the recipe of the three gels.

WPI was first dissolved in tap water in a shaker and then stirred at room temperature for 2 h. After that, vanilla aroma, sweetener and table salt (added only to one variation of the gels) were dissolved into the protein solution. Subsequently, the protein solution was transferred to ceramic containers covered with a perforated plastic foil and then placed into a steam oven (Rational, Germany) at 90 °C for 30 min. The gels were stored in the refrigerator at 4 °C for 24 h. After 24 h, the gels were cut into particles of 5 mm diameter and again stored at 4 °C in a sealed plastic container before providing to participants. All

gels were prepared 24 – 48 h before the session. The hardness of the gels were measured by an Texture Analyzer (Instron Corp. 5564, USA) with the method described previously in **Chapter 3**.

Table 5-1 *Characteristics and recipe of the gels per portion (200 g).*

Treatments	Soft-LP	Hard-LP	Hard-HP
Energy (kcal)	102	102	135
Hardness (kPa)	67.0 ± 18.9	213.7 ± 43.2	264.9 ± 37.5
WPI (g)	25.94	25.90	33.93
Vanilla aroma (g)	0.20	0.20	0.20
Sweetener (g)	0.24	0.24	0.24
Salt (NaCl) (g)	0	0.40	0
Water (g)	173.6	173.3	165.6

The name of the three gels represents their characteristic: Soft-LP represents the gel with low protein content and low hardness; Hard-LP represents the gel with low protein content and high hardness; Hard-HP represents the gel with high protein content and high hardness. Energy content was estimated by means of the Atwater factor of 4 kcal per g protein.

5.2.3 Study procedures

Participants were asked to attend three sessions with a washout period of minimum 7 days in between sessions. Each participant always attended the session at the same time in the morning. Participants were asked to fast overnight from 22.00 h onwards (no food, only water), and to no longer drink water from 1.5 hours before the visit. An overview of the session is shown in Fig. 5-1. After arrival, participants provided verbally baseline appetite (including hunger, fullness and thirst) and wellbeing (including nauseous and general wellbeing) ratings on a 100-point scale and a baseline abdominal MRI scan was performed. After that, participants were asked to exit the scanner and to consume 200 g of protein meal and 100 g of water at room temperature within 10 min. The consumption was video-recorded by a webcam. After ingestion, participants were placed in an MRI scanner where abdominal scans and appetite and wellbeing ratings were obtained every 10 min from 15-85 min after ingestion. During this period, participants were lying in the scanner, listening to a radio station of their choice. At the end of the session, participants were provided with an ad libitum pasta meal (whole grain pasta, red pesto sauce, carrots, broccoli, tomatoes and chickpeas; 100 kcal/100 g) and water. Approximately 1 kg of pasta (1000 kcal) was

provided on a large serving plate with cutlery. Participants were instructed to eat until feeling comfortably full. Intake of water and food was determined by weighing before and after consumption.

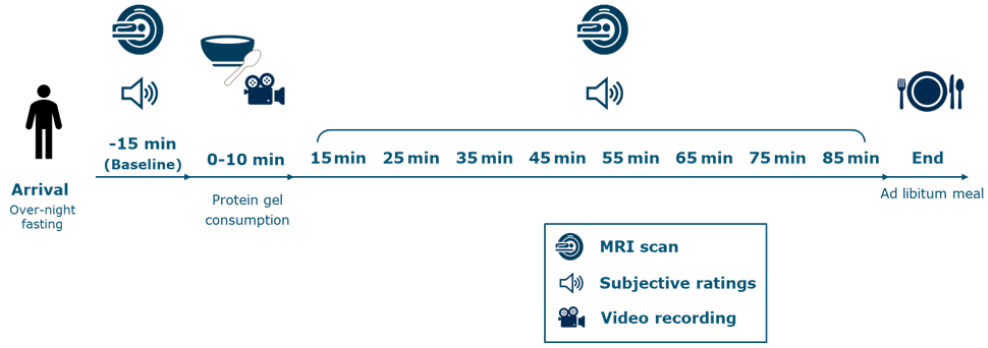

Fig. 5-1 *Schematic overview of one treatment session for one participant*

5.2.4 MRI measurements

Participants were scanned with a 1.5 T MRI scanner (Ingenia, Philips Medical Systems, Best, the Netherlands). A body coil was placed on the participant. During each scan, participants were asked to hold their breath on expiration to fixate the position of the diaphragm and the stomach and to minimize motion artefacts. Four different scan sequences were used.

To assess gastric emptying, a T_2-weighted spin echo sequence was used (repetition time (TR) = 400 ms, echo time (TE) = 90 ms, 33 axial slices with FOV = 400 × 400 mm, in-plane resolution = 0.78 × 0.78 mm, slice thickness = 6.0 mm, total acquisition time = 16 s).

For T_2 mapping, a 2D GraSe sequence was used (TR = 392 ms, 5 echo times ranging from 20 to 100 ms with an echo-spacing of 20 ms, FOV = 400 × 400 mm, in-plane resolution = 1.56 × 1.56 mm, 5 sagittal slices with slice thickness = 5.0 mm, total acquisition time = 10 s).

For T_1 mapping, a 2D inversion recovery (IR) sequences were used (TR = 5 ms, TE =2.5 ms and 9 inversion times (TI) of 150, 570, 985, 1400, 1900, 2300, 2700, 3100 and 4000 ms; FOV = 400 × 400 mm, in-plane resolution = 1.56 × 1.56 mm, single sagittal slice corresponding to the middle slice of the T_2-mapping scan, thickness = 5.0 mm, acquisition time 1-4 s per TI).

A roadmap for the T_1 and T_2 images was acquired using T_2-weighted spin echo sequence mentioned above but in the sagittal direction (TR = 1500 ms, TE =120 ms, 5 sagittal slices with FOV = 400 × 400 mm, in-plane resolution = 1.56 × 1.56 mm, 5 slices with slice thickness = 5.0 mm, total acquisition time = 5 s).

5.2.5 MRI image analysis

The transverse anatomical abdominal MRI scans were used to calculate the gastric content volume over time. At each time point, the scan consisted of 33 slices across the abdomen area. In each slice, the gastric content was manually delineated (Illustrated in Fig. 5-S1) with the MIPAV software (Bazin et al., 2007). For each time point, the total gastric content volume was calculated by multiplying the area of gastric content with the slice thickness and then summing over the results from all slices. Gastric emptying was defined as the decrease in gastric content volume over time. The area under the curve of gastric content volume over time was calculated.

T_2 maps were calculated by the scanner software. This calculation was based on the images acquired at different echo times with the GraSE sequence (Bonny et al., 1996; Milford et al., 2015).

For obtaining T_1 maps, several steps of analysis were performed. Firstly, image registration of acquired images at different TI was performed to correct the possible de-phase among scans at different breath-holds. The registration was performed in Matlab 2021a using the roadmap at the same time point as a reference. After that, T_1 maps were calculated based on the registered images at different TI using a Levenberg-Marquard two-parameter curve fitting in Matlab 2021a using Equation (5.1).

$$M_t = 1 - M_0 \cdot (1 - e^{-\frac{TI}{T_1}}) \tag{5.1}$$

With the inversion time (TI) and M_t which is the voxel intensity at TI, we calculated M_0 (voxel equilibrium magnetic intensity) and T_1 for each voxel.

The stomach content region in the roadmap was segmented with the use of the MIPAV software (Bazin et al., 2007) and stored as a binary mask. For each time point, this mask was multiplied with the T_1 or T_2 maps to subtract the stomach content. Subsequently, mean T_1 and T_2 values of the stomach content were calculated.

5.2.6 Statistical analysis

The means and standard errors were calculated for all the measured outcomes. Analysis of variance (ANOVA) tests followed by Post-hoc HSD Turkey test were performed to examine the difference among treatments in eating time, eating rate and area under the curve of gastric content volume. A linear mixed model was used to analyse the change in gastric content volume over time and compare treatment effects; gastric content volume was added as a dependent variable; fixed factors were time, treatment and their interaction; participants were added as a random effect. The same analysis was applied for mean T_1 and T_2 of the stomach content. Effects were considered statistically significant at $p < 0.05$.

5.3 Results

5.3.1 Oral processing behavior of the gels

Table 5-2 also shows the mean consumption time and rate for the three gels. Ingestion times for Soft-LP were the shortest, followed by Hard-LP and Hard-HP. Gel type affected eating rate: For Soft-LP, it was significantly shorter than for Hard-LP and Hard-HP ($p < 0.01$), while the Hard-LP and Hard -HP gels had similar eating rates ($p = 0.89$).

Table 5-2 *Mean ± SE eating time and rate of the three protein gels (n = 17)*

	Soft-LP	Hard-LP	Hard-HP	p-value
Eating time of the treatment (s)	356 ± 42^{a}	553 ± 41^{b}	625 ± 47^{b}	<0.01
Eating rate of the gels (g/s)	0.77 ± 0.12^{a}	0.42 ± 0.052^{b}	0.37 ± 0.039^{b}	<0.01
Eating rate of the entire treatment (g/s)	1.16 ± 0.18^{a}	0.63 ± 0.076^{b}	0.55 ± 0.057^{b}	<0.01

Comparison among treatments was test with ANOVA followed by Post-hoc HSD Turkey test. Columns with different letters indicates statistically significant differences (p<0.05).

5.3.2 Gastric emptying and satiety

The gastric volume over time for the three treatments is shown in Fig. 5-2. Overall, for all treatments, gastric volume content increased from baseline (-15 min) to the first measured time point after the protein gel consumption (15 min) and then decreased till the end of the scan session. Furthermore, the type of treatment affected the gastric content volume. The emptying of Soft-LP was systematically faster than Hard-LP, while the Hard-LP was systematically faster than the Hard-HP. It should be noted that not all the time points were statistically significant different. Different area under curve (AUC) of the gastric content was observed: compared to the AUC of Soft-LP, the AUC of Hard-LP is 13% higher, and the AUC of Hard-HP is 26% higher.

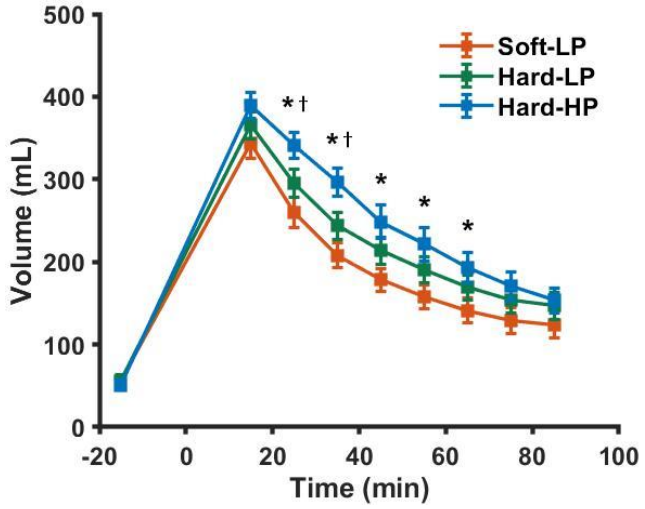

(a)

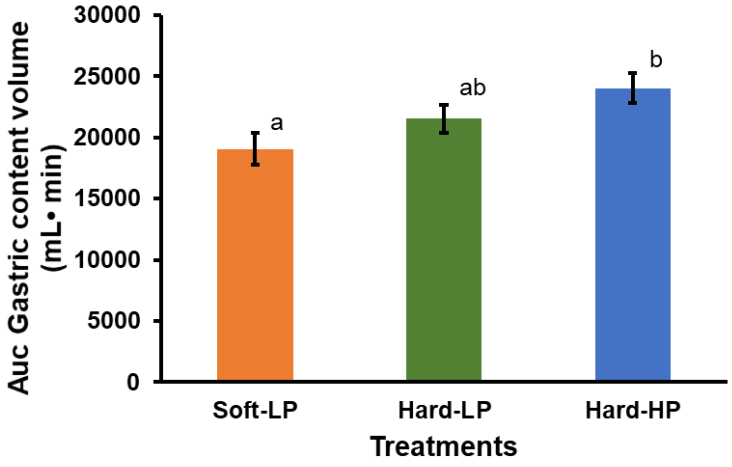

(b)

Fig. 5-2 *Total gastric content volume over time (a) and area under curve (b) for the three treatments (n = 18, mean ± SE). a: The signs '*' and '†' indicate significant differences between Soft-LP and Hard-HP, and between Hard-LP and Hard-HP, respectively (p < 0.05). b: differet letters indicate significant differences (p < 0.05). For total gastric content volume, hard-HP was significantly higher (p < 0.05) than Soft-LP between until 65 min and than Hard-LP at 25 and 35 min, while during the entire period Soft-LP was not different from Hard-LP (p > 0.17). The effect of gel-type on AUC was significant (p < 0.05), with a significant difference between Soft-LP and Hard-HP (p < 0.05). The difference between Hard-LP and Soft-LP or Hard-HP was not statistically significant (p = 0.35).*

No significant difference in appetite ratings and ad libitum intake between the three treatments was found (all p-values > 0.05) (Fig. 5-S2).

5.3.3 T_1 and T_2 of the gastric content

Fig. 5-3a shows an example of T_2 maps where the T_2 distribution in the stomach was colour-coded during digestion over time. The baseline scan shows the fasting state where only gastric fluid was present. From t = 15 min onwards, the food bolus showed up in the stomach area as well. The mean T_2 of the measured stomach content is shown in Fig. 5-3b. For all treatments, T_2 was around 1s at baseline, decreased at t =15 min, and gradually increased during digestion. The treatments show an effect on the T_2 values: Soft-LP > Hard-LP > Hard-HP, although not all the time points are statistically significant different.

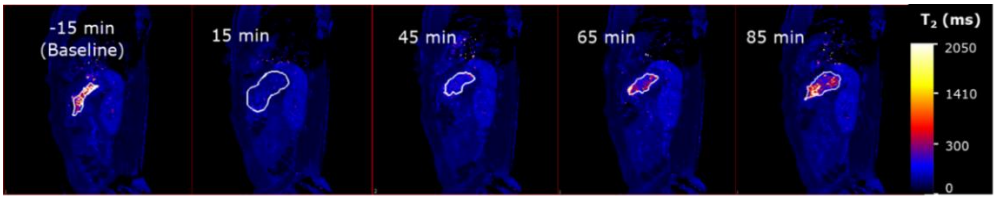

(a)

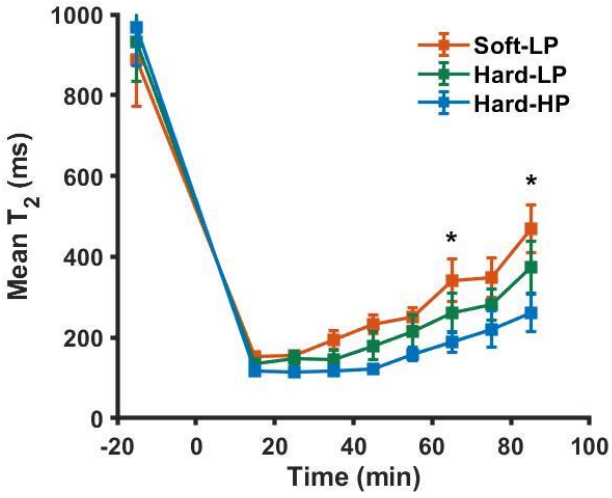

(b)

Fig. 5-3 *(a) Color-coded T_2 maps from one participant and (b) mean ± SE T_2 values of the measured gastric content during digestion (n = 18). The signs '*' indicate significant differences between Soft-LP and Hard-HP ($p < 0.05$). Among the treatments, T_2 for Hard-HP was significantly lower than for Soft-LP at 65 min and 85 min ($p < 0.05$), while during the entire period T_2 for Hard-LP was not different from that for Soft-LP ($p > 0.25$) or Hard-HP ($p > 0.14$).*

Fig. 5-4a. shows an example of T_1 maps where the T_1 distribution in the stomach was color-coded during digestion over time. Similar to T_2, the mean T_1 of the measured stomach content was highest (around 2.2 s) at baseline, decreased at t = 15 min, and gradually increased during digestion (Fig. 5-4b). Here the treatments also show an effect on the T_1 values: Hard-HP was all the time with the lowest T_1. Initially, Soft-HP was lower than Soft-LP, at later time points they became more similar. As before not all the time points differed significantly.

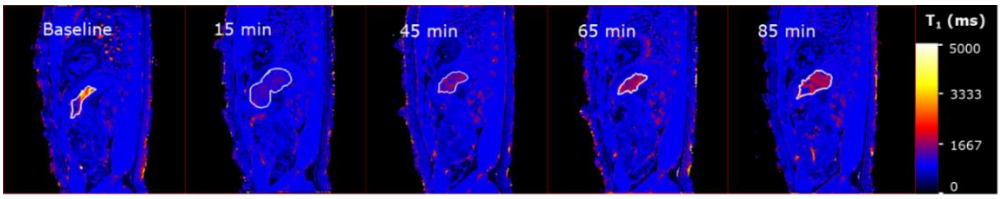

(a)

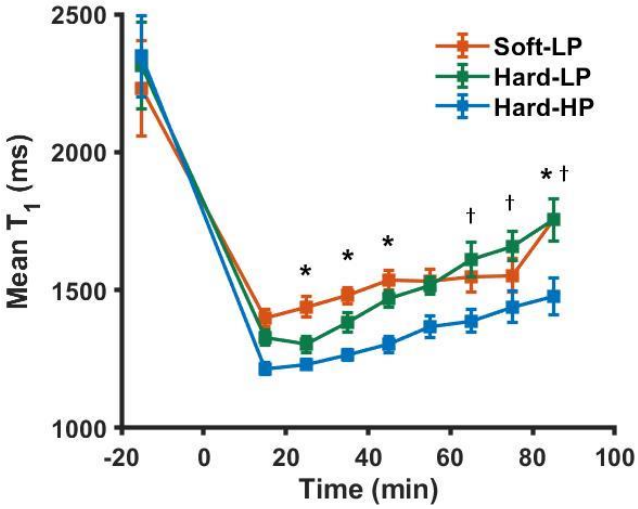

(b)

Fig. 5-4 *(a) Color-coded T_1 maps from one participant and (b) Mean ± SE T_1 of the measured gastric content during digestion (n = 18). The signs '*' and '†' indicate significant differences between Soft-LP and Hard-HP, and between Hard-LP and Hard-HP, respectively ($p < 0.05$). Among the treatments, Hard-HP was significantly lower than Soft-LP from 25 till 45 min and 85 min ($p < 0.05$), and lower than Hard-LP from 65 min till 85 min ($p < 0.05$), while during the entire period Hard-LP was not different from Soft-LP ($p > 0.33$).*

5.4 Discussion

5.4.1 The effect of eating rate on gastric digestion

As expected, higher hardness induced a slower eating rate, while the difference only in the protein content did not affect the eating rate. The observed impact of the hardness on eating rate is in line with other studies studying oral processing: Lasschuijt et al. (2017) reported a higher number of chews and a slower eating rate for the harder gels compared to the softer gels; Guo et al. (2013) showed that during oral processing gels' fragmentation degree increased linearly with gel hardness and softer gel had a faster eating rate and a larger threshold particle size for swallowing.

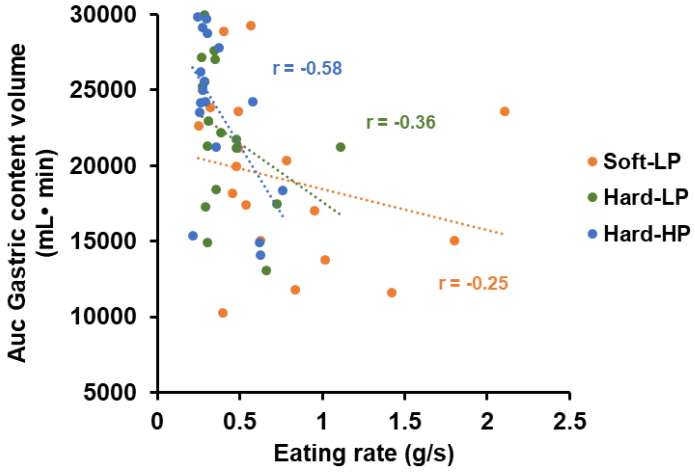

***Fig. 5-5**. Association between gastric content AUC and eating rate. Each point represents one participant under one treatment.*

The difference in eating rate is expected to have an impact on gastric digestion, since, with a slower eating rate, the particle size of the gels is reduced (Devezeaux de Lavergne et al., 2015), which would result in a larger relative surface area for erosion and enzymatic digestion. For example, a longer chewing time resulted in a higher degree of protein hydrolysis in the chicken products (Chen et al. 2020). Moreover, the protein availability of meat was impaired in people with a reduced chewing capacity (Rémond et al., 2007). The result of this study shows that the lower eating rate links probably with longer gastric retention time. As shown in Fig. 5-5, the gastric content AUC shows a negative association with the eating rate, especially with the Hard-HP gel. It suggests that the duration of food

particles in the stomach is longer with a decrease in the eating rate. Therefore, a slow eating rate might be a good strategy to enhance gastric digestion.

5.4.2 The impact of food properties on gastric emptying

The gastric content volume results show that food properties (in this case: protein content and hardness) are important factors in modulating gastric emptying. Here, the term gastric emptying refers to the decrease of whole stomach content volume instead of the meal volume. The biggest difference in gastric emptying dynamics was observed between Soft-LP and Hard-HP, which also differed the most in terms of hardness and protein content among the treatments. However, surprisingly the clear difference in hardness between Soft-LP and Hard-LP did not result in a significant difference in gastric emptying, although the gastric content volume of Hard-LP is higher than that of Soft-HP. Some *in vivo* studies showed that hardness has a significant impact on gastric emptying: Marciani et al. (2001b) reported that softer agar gel beads emptied faster than harder ones, suggesting that softer food is disintegrated faster than harder food. However, their gels were non-caloric and indigestible by pepsin, and thus it might be that hardness became the main driver in their case.

A further comparison could be made with *in vitro* studies. Our previous work showed that harder WPI gels were digested slower even though the protein content in the gels was the same. This finding is supported by many other *in vitro* studies, and it is generally agreed that a higher hardness (usually linked to a higher crosslinking density) could hinder erosion and enzymatic hydrolysis. Guo et al. (2015) found that in a dynamic *in vitro* digestion model the gastric emptying rate was slower with harder gels and propose high hardness to be the key factor for delayed gel disintegration. However, in current *in vivo* study, no statistically significant difference was found between the two gels with the same protein content but different hardness, although the mean of gastric volume content of Hard-HP was larger than the Soft-LP. This suggests that digestion rate and gastric emptying rate may not be coupled. The difference in digestion rate of food particles arise because of different hardness. However, the gastric emptying rate is not only related to the degradation rate of food particles in the stomach but is more regulated by a feedback system as the composition (in other words: nutrient density) of digesta is sensed by the small intestine. This might be a perspective that food scientists need to take into consideration when aiming to alter digestion by designing specific food structures.

Therefore, the current study shows that nutrient density is the main driver of gastric emptying of solid food, and higher hardness additionally slows gastric emptying down. Interestingly, this is similar to what has been reported with liquid meal where nutrient density was the main driver of gastric emptying, but viscosity was the second factor (Camps et al., 2016). This confirms that changing food properties, via nutrients compositions and/or food structure for example the mechanical properties, can be a promising approach to modulating gastric emptying.

Food texture is an important factor in satiation and satiety (Stribiţcaia et al., 2020). However, in the current study, no difference was found in appetite ratings and ad libitum meal intakes between the three treatments. For appetite ratings, the reason might be that the portion size of the gels was not big enough for participants to perceive the difference. The ratings are correlated with the gastric content volume (Fig. 5-S3). For ad libitum meal intake, the reason may be the long-time window between gel ingestion and meal consumption. Similarly, in other studies with a longer time interval (i.e. 90 min, 180 min) between the preload and ad libitum meal, there was no effect on food intake (Camps et al., 2016; Tsuchiya et al., 2006; Yeomans et al., 2016; Tournier & Louis-Sylvestre, 1991).

5.4.3 Interpretation of changes in T_1 and T_2

The T_1 and T_2 indicate properties of the proton environment in the stomach over time. As shown in *in vitro* studies, protons in simulated gastric fluid and protein gels have a different T_1 and T_2 (**Chapters 2 and 4**). In Fig. 5-3 and 5-4 showed a high T_1 and T_2 at baseline because the gastric content was gastric fluid. After ingestion of the protein gels, the T_1 and T_2 decrease because of the presence of protein gel mixed with the initial gastric contents. Subsequently, the T_1 and T_2 values increased over the course of digestion. This is mainly because of the decreased ratio of protein gel in the measured gastric content, which can also be observed from the maps in Fig. 5-3a and Fig. 5-4a. During gastric digestion, not only the protein gels are broken down into smaller particles by stomach contractions, but also protein is hydrolyzed by pepsin which results in peptides suspending in the gastric fluid. The concentration of protein in the stomach decreased due to the secretion of fresh gastric fluid in a combination with removal of digesta from the stomach. An early human study showed a similar result but with liquid food, where the T_2 value was associated with the dilution of the original meal by the gastric fluid (Marciani et al., 1998).

For Hard-HP, the T_2 and T_1 values of the measured stomach content were lower compared to Soft-LP. This is because the degradation of Hard-HP is slower and the retention of gel in the stomach is higher. Interestingly, the difference between treatments in T_1 is larger than that in T_2. Since the Soft-LP was digested faster, the digestion effect was stronger than Hard-HP. This stronger digestion effect reduced the T_2 more with Soft-LP than with Hard-HP, while T_1 was not affected much by the digestion effect. This may explain the larger differences in T_1 than T_2 between Soft-LP and Hard-HP.

Interestingly, at the last time points, T_1 of Hard-HP was significantly different from Soft-LP and Hard-LP while there was no statistically significant difference in the gastric content volume (Fig. 5-2a). This indicates that the ratio between gastric fluid to gel is significantly lower for Hard-HP. It also suggests that the reduction of whole gastric content may not be the same as that of meal. As the gastric emptying rate is not necessarily identical for whole gastric content or for the meal.

Our previous research showed that by combining T_1 and T_2 measurements, we could monitor the change of pH and protein concentration in the liquid phase during digestion (**Chapters 2** and **4**). That grants T_1 and T_2 as potential markers of gastric protein digestion. However, in the current study, the liquid phase (gastric fluid) and the solid phase (protein gel particles) are not distinguishable because: 1) the digesta are well-mixed in the stomach especially at the earlier time points, 2) the resolution of the images is relatively low (1.56 × 1.56 × 6 mm) while the food particles are approximately 5 mm. Thus, there are so-called partial volume effects i.e., many voxels contain a mix of liquid and solid material. Therefore, for future research, it would be crucial to further develop the MRI sequences and analysis approaches to enable tracking of changes in T_1 and T_2 of food and gastric fluid. That will enable the use of these MRI markers to measure *in vivo* digestion in more detail.

5.5 Conclusion

The current work compared gastric digestion of foods differing in structure and protein content in humans. A higher hardness, regardless of protein content, resulted in a slower eating rate; a slow eating rate across participants may probably relates with longer gastric retention time and thus likely more sufficient gastric digestion. The *in vivo* results show that the protein content is the main driver of gastric emptying, that hardness is an additional factor and that the effect of hardness is not as strong as what has been observed *in vitro*. To our knowledge, this is the first *in vivo* human study measuring T_1 and T_2 during gastric digestion of solid foods. These T_1 and T_2 measurements can provide extra information on the dilution and digestion taking place in the stomach. Further research on applying these markers to track changes in different components will be valuable to provide more detailed information on *in vivo* gastric digestion. The *in vivo* data presented here can serve as input data for tuning and validating *in vitro* and *in silico* models, specifically with regard to the physiological responses to food structure and nutrient density.

Supplementary material

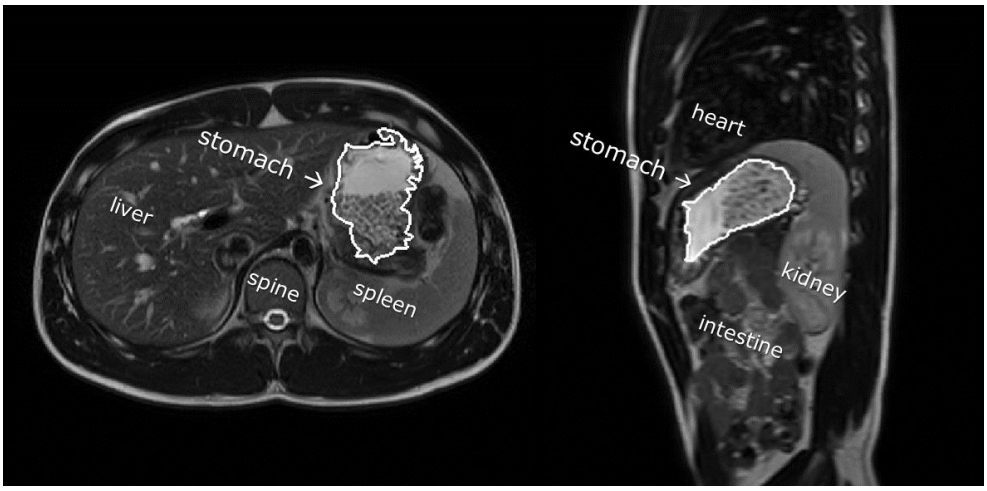

(a) (b)

Fig. 5-S1. An example of segmentation of gastric content on a transverse anatomical scan (a) and a roadmap (b). The region inside of the white line is considered as the stomach content.

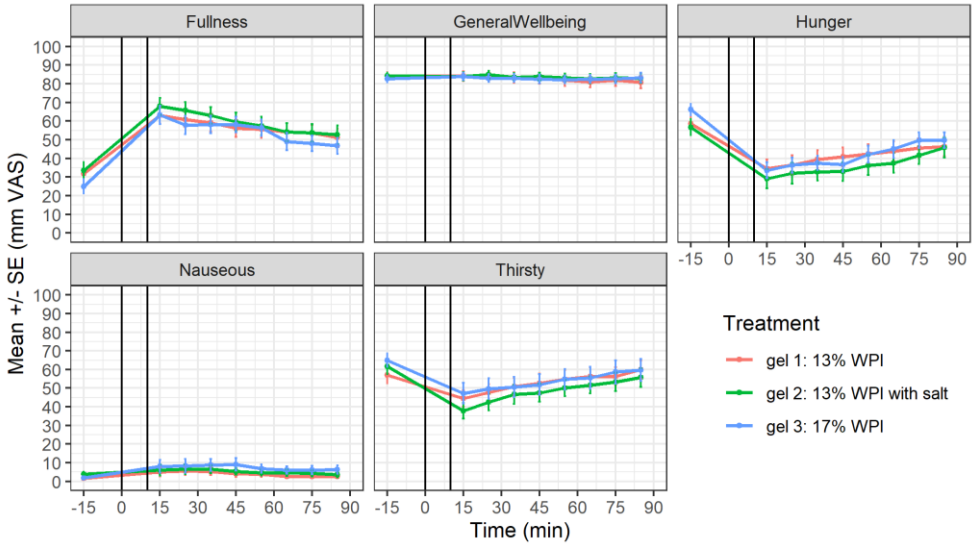

(a)

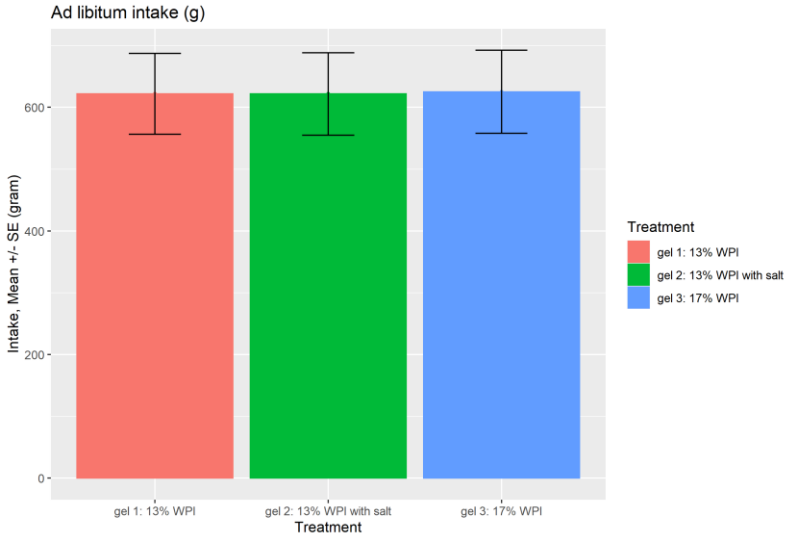

(b)

Fig. 5-S2*. Appetite and wellbeing ratings during the test session for each treatment (a, the vertical lines represent the start and the end time of ingestion of the test meal) and the ad libitum intake after the test session for each treatment (b) (means ± SEM)*

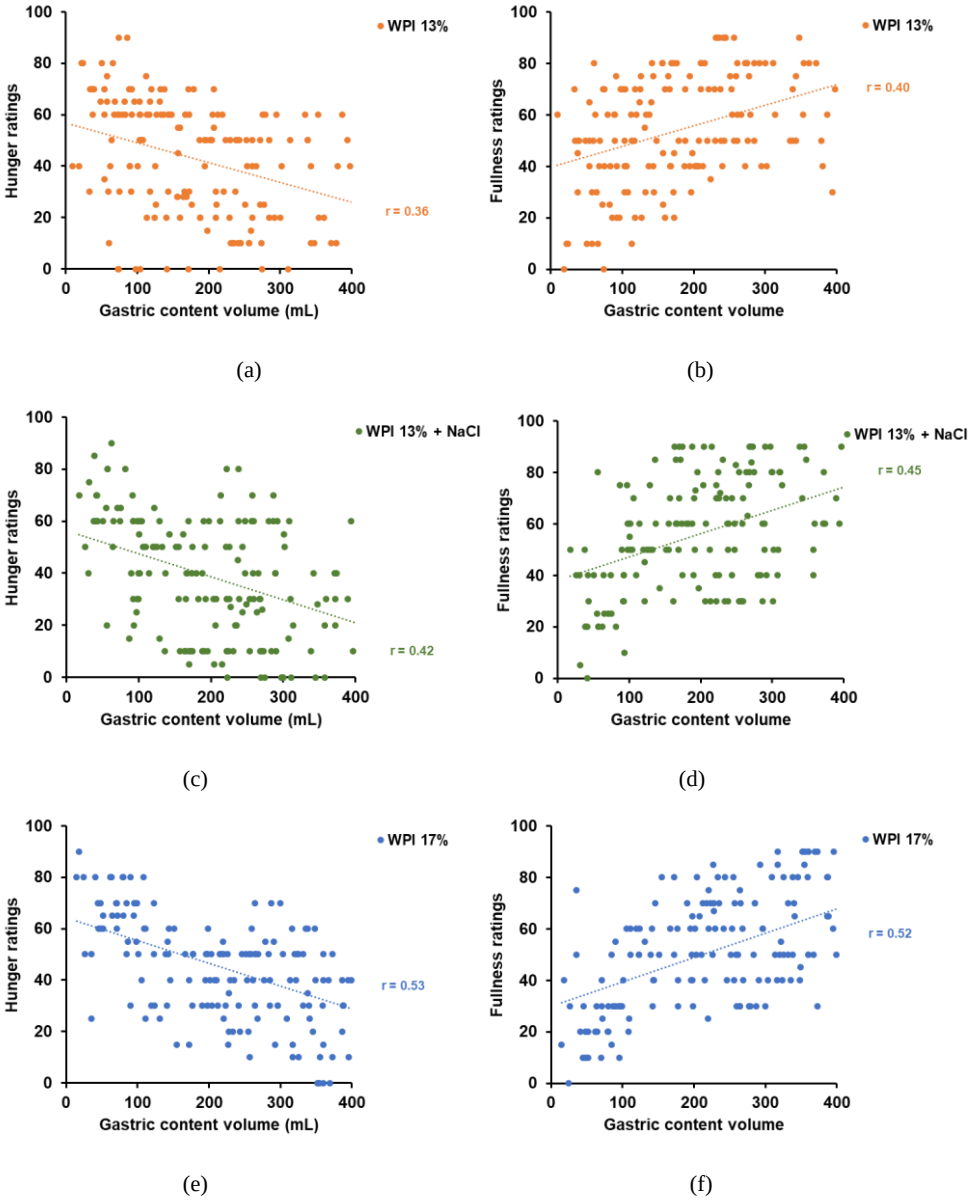

Fig. 5-S3*. Correlation between the ratings of hunger (a: treatment Soft-HP c: treatment Hard-LP, e: treatment Hard-HP) or fullness (b: treatment Soft-HP, d: treatment Hard-LP, f: treatment Hard-HP) with gastric content volume*

References

Bonny, J. M., Zanca, M., Boire, J. Y., & Veyre, A. (1996). T2 maximum likelihood estimation from multiple spin-echo magnitude images. Magnetic Resonance in Medicine. https://doi.org/10.1002/mrm.1910360216

Bornhorst, G. M., & Singh, R. P. (2014). Gastric digestion *in vivo* and *in vitro*: how the structural aspects of food influence the digestion process. Annual Review of Food Science and Technology, 5(1), 111–132. https://doi.org/10.1146/annurev-food-030713-092346

Camps, G., Mars, M., De Graaf, C., & Smeets, P. A. M. (2016). Empty calories and phantom fullness: A randomized trial studying the relative effects of energy density and viscosity on gastric emptying determined by MRI and satiety. American Journal of Clinical Nutrition, 104(1), 73–80. https://doi.org/10.3945/ajcn.115.129064

Chen, Y., Capuano, E., & Stieger, M. (2021). Chew on it: Influence of oral processing behaviour on *in vitro* protein digestion of chicken and soya-based vegetarian chicken. British Journal of Nutrition, 126(9), 1408–1419. https://doi.org/10.1017/S0007114520005176

Deng, R., Janssen, A. E. M., Vergeldt, F. J., Van As, H., de Graaf, C., Mars, M., & Smeets, P. A. M. (2020). Exploring *in vitro* gastric digestion of whey protein by time-domain nuclear magnetic resonance and magnetic resonance imaging. Food Hydrocolloids, 99, 105348. https://doi.org-/10.1016/j.foodhyd.2019.105348 *(Chapter 2 in this thesis)*

Deng, R., Seimys, A., Mars, M., Janssen, A. E. M., & Smeets, P. A. M. (2022). Monitoring pH and whey protein digestion by TD-NMR and MRI in a novel semi-dynamic *in vitro* gastric simulator (MR-GAS). Food Hydrocolloids, 125, 107393. https://doi.org/10.1016/j.foodhyd. 2021.107393 *(Chapter 4 in this thesis)*

Deng, R., Mars, M., Van Der Sman, R. G. M., Smeets, P. A. M., & Janssen, A. E. M. (2020). The importance of swelling for *in vitro* gastric digestion of whey protein gels. Food Chemistry, 330, 127182. https://doi.org/10.1016/j.foodchem.2020.127182 *(Chapter 3 in this thesis)*

Devezeaux de Lavergne, M., Derks, J. A. M., Ketel, E. C., de Wijk, R. A., & Stieger, M. (2015). Eating behaviour explains differences between individuals in dynamic texture perception of sausages. Food Quality and Preference, 41, 189–200. https://doi.org/10.1016/j.foodqual.2014.12.006

Fisher, R. S., Malmud, L. S., Bandini, P., & Rock, E. (1982). Gastric emptying of a physiologic mixed solid-liquid meal. Clinical Nuclear Medicine, 7(5), 215–221. https://doi.org/10.1097/00003072-198205000-00005

Guo, Q., Ye, A., Lad, M., Dalgleish, D., & Singh, H. (2013). The breakdown properties of heat-set whey protein emulsion gels in the human mouth. Food Hydrocolloids, 33(2), 215–224. https://doi.org/10.1016/j.foodhyd.2013.03.008

Guo, Q., Ye, A., Lad, M., Ferrua, M., Dalgleish, D., & Singh, H. (2015). Disintegration kinetics of food gels during gastric digestion and its role on gastric emptying: An *in vitro* analysis. Food and Function, 6(3), 756–764. https://doi.org/10.1039/c4fo00700j

Houghton, L. A., Read, N. W., Heddle, R., Horowitz, M., Collins, P. J., Chatterton, B., & Dent, J. (1988). Relationship of the motor activity of the antrum, pylorus, and duodenum to gastric emptying of a solid-liquid mixed meal. Gastroenterology, 94(6), 1285–1291. https://doi.org/10.1016/0016-5085(88)90665-8

Hunt, J. N., & Stubbs, D. F. (1975). The volume and energy content of meals as determinants of gastric emptying. The Journal of Physiology, 245(1), 209–225. https://doi.org/10.1113/-jphysiol.1975.sp010841

Lasschuijt, M. P., Mars, M., Stieger, M., Miquel-Kergoat, S., de Graaf, C., & Smeets, P. A. M. (2017). Comparison of oro-sensory exposure duration and intensity manipulations on satiation. Physiology and Behavior, 176, 76–83. https://doi.org/10.1016/j.physbeh.2017.02.003

Luo, Q., Borst, J. W., Westphal, A. H., Boom, R. M., & Janssen, A. E. M. (2017). Pepsin diffusivity in whey protein gels and its effect on gastric digestion. Food Hydrocolloids, 66, 318–325. https://doi.org/10.1016/j.foodhyd.2016.11.046

Marciani, L., Manoj, P., Hills, B. P., Moore, R. J., Young, P., Fillery-Travis, A., … Gowland, P. A. (1998). Echo-planar imaging relaxometry to measure the viscosity of a model meal. Journal of Magnetic Resonance, 135(1), 82–86. https://doi.org/10.1006/jmre.1998.1560

Marciani, L., Pritchard, S. E., Hellier-Woods, C., Costigan, C., Hoad, C. L., Gowland, P. A., & Spiller, R. C. (2013). Delayed gastric emptying and reduced postprandial small bowel water content of equicaloric whole meal bread versus rice meals in healthy subjects: Novel MRI insights. European Journal of Clinical Nutrition, 67(7), 754–758. https://doi.org/10.1038/ejcn.2013.78

Marciani, L Gowland, P. A., Fillery-Travis, A., Manoj, P., Wright, J., Smith, A., … Spiller, R. C. (2001). Assessment of antral grinding of a model solid meal with echo-planar imaging. American Journal of Physiology-Gastrointestinal and Liver Physiology, 280(5), G844–G849. https://doi.org/10.1152/ajpgi.2001.280.5.G844

Marciani, L, Hall, N., Pritchard, S. E., Cox, E. F., Totman, J. J., Lad, M., … Spiller, R. C. (2012). Preventing gastric sieving by blending a solid/water meal enhances satiation in healthy humans. Journal of Nutrition, 142(7), 1253–1258. https://doi.org/10.3945/jn.112.159830

Milford, D., Rosbach, N., Bendszus, M., & Heiland, S. (2015). Mono-exponential fitting in T2-relaxometry: Relevance of offset and first echo. PLoS ONE. https://doi.org/10.1371/journal.pone.0145255

Norton, I., Moore, S., & Fryer, P. (2007). Understanding food structuring and breakdown: engineering approaches to obesity. Obesity Reviews : An Official Journal of the International Association for the Study of Obesity, 8 Suppl 1(4), 83–88. https://doi.org/10.1111/j.1467-789X.2007.00324.x

Norton, J. E., Gonzalez Espinosa, Y., Watson, R. L., Spyropoulos, F., & Norton, I. T. (2015). Functional food microstructures for macronutrient release and delivery. Food and Function, 6(3), 663–678. https://doi.org/10.1039/c4fo00965g

Rémond, D., Machebeuf, M., Yven, C., Buffière, C., Mioche, L., Mosoni, L., & Mirand, P. P. (2007). Postprandial whole-body protein metabolism after a meat meal is influenced by chewing efficiency in elderly subjects. American Journal of Clinical Nutrition, 85(5), 1286–1292. https://doi.org/10.1093/ajcn/85.5.1286

Remondetto, G. E., Beyssac, E., & Subirade, M. (2004). Iron availability from whey protein hydrogels: An *in vitro* study. Journal of Agricultural and Food Chemistry, 52(26), 8137–8143. https://doi.org/10.1021/jf040286h

Sah, B. N. P., McAinch, A. J., & Vasiljevic, T. (2016). Modulation of bovine whey protein digestion in gastrointestinal tract: A comprehensive review. International Dairy Journal, 62, 10–18. https://doi.org/10.1016/j.idairyj.2016.07.003

Sarkar, A., Murray, B., Holmes, M., Ettelaie, R., Abdalla, A., & Yang, X. (2016). *In vitro* digestion of Pickering emulsions stabilized by soft whey protein microgel particles: Influence of thermal treatment. Soft Matter, 12(15), 3558–3569. https://doi.org/10.1039/c5sm02998h

Singh, H., Ye, A., & Ferrua, M. J. (2015). Aspects of food structures in the digestive tract. Current Opinion in Food Science, 3, 85–93. https://doi.org/10.1016/j.cofs.2015.06.007

Smeets, P. A. M., Deng, R., van Eijnatten, E. J. M., & Mayar, M. (2020). Monitoring food digestion with magnetic resonance techniques. Proceedings of the Nutrition Society, 1–11. https://doi.org/10.1017/S0029665120007867

Spiller, R., & Marciani, L. (2019). Intraluminal Impact of Food: New Insights from MRI. Nutrients, 11(5), 1147. https://doi.org/10.3390/nu11051147

Stribiţcaia, E., Evans, C. E. L., Gibbons, C., Blundell, J., & Sarkar, A. (2020). Food texture influences on satiety: systematic review and meta-analysis. Scientific Reports, 10(1), 1–18. https://doi.org/10.1038/s41598-020-69504-y

Tournier, A., & Louis-Sylvestre, J. (1991). Effect of the physical state of a food on subsequent intake in human subjects. Appetite, 16(1), 17–24. https://doi.org/10.1016/0195-6663(91)90107-4

Tsuchiya, A., Almiron-Roig, E., Lluch, A., Guyonnet, D., & Drewnowski, A. (2006). Higher satiety ratings following yogurt consumption relative to fruit drink or dairy fruit drink. Journal of the American Dietetic Association, 106(4), 550–557. https://doi.org/10.1016/j.jada.2006.01.004

Urbain, J. L. C., Siegel, J. A., Charkes, N. D., Maurer, A. H., Malmud, L. S., & Fisher, R. S. (1989). The two-component stomach: effects of meal particle size on fundal and antral emptying. European Journal of Nuclear Medicine, 15(5), 254–259. https://doi.org/10.1007/BF00257543

Weiner, K., Graham, L. S., Reedy, T., Elashoff, J., & Meyer, J. H. (1981). Simultaneous gastric emptying of two solid foods. Gastroenterology, 81(2), 257–266. https://doi.org/10.1016/S0016-5085(81)80056-X

Yeomans, M. R., Re, R., Wickham, M., Lundholm, H., & Chambers, L. (2016). Beyond expectations: The physiological basis of sensory enhancement of satiety. International Journal of Obesity, 40(11), 1693–1698. https://doi.org/10.1038/ijo.2016.112

ppp

ggggg

Chapter 6

General discussion

In this thesis, we studied how the properties of protein-rich solid food affect gastric digestion via *in vitro* static, *in vitro* semi-dynamic and *in vivo* (human) models using MR techniques, namely time-domain nuclear magnetic resonance (TD-NMR) and magnetic resonance imaging (MRI). In the following sections, these results will be systematically reviewed, the strengths and limitations of this work will be discussed and directions for further research will be suggested.

6.1 Main findings

In **Chapter 2**, we explored the possibility of using TD-NMR and MRI to monitor gastric digestion of whey protein solutions and gels using static *in vitro* digestion model. With both TD-NMR and MRI, we measured transverse relaxation time (T_2) and calculated the rate ($R_2 = T_2^{-1}$). For the solution, protein concentration and T_2 did not change during digestion. For the gels, supernatant and gel phases could be discriminated based on their T_2 values; protein concentration and R_2 of the supernatant increased. The results from the gels showed that R_2 correlated positively with protein concentration in the supernatant. This indicates R_2 as a promising marker to monitor protein digestion of solid food in static *in vitro* models. Besides, for data analysis, TD-NMR measurements provide detailed spectra information, namely the T_2 distribution in the system, and that contributed to interpreting the MRI data.

T_2 measurements showed that water transportation takes place during digestion, and it may be of great importance for digestion rate. Therefore, in **Chapter 3**, we focused on the effect and its underlying mechanism of water transportation (in other words, swelling) on the digestion of whey protein gels. Protein gels with different hardness and swelling properties were formulated by modulating salt concentration (0-0.1M). Low hardness and higher swelling properties were found in gels containing less salt. Protein gels with higher swelling ratios showed a higher digestion rate, which is likely due to the enhanced transportation rate of acid and pepsin into the gel particle.

The work in **Chapter 2** was performed under static conditions, i.e. it did not consider the gastric dynamics. In **Chapter 4**, we constructed a novel MRI-compatible semi-dynamic gastric simulator (MR-GAS) and used it to investigate the feasibility of using transverse (R_2) and longitudinal relaxation rates (R_1) to monitor digestion of whey protein gels in this dynamic set-up. For TD-NMR, 99% of the variance in R_2 and 96% of the variance in R_1 could be explained as a function of protein concentration and $[H^+]$. For MRI, the explained

variances were 99% for R_2 and 60% for R_1. Based on these analyses, the empirical equations enabled the prediction of protein concentration and pH by R_2 and R_1. This indicates that R_2 and R_1 can be used as markers for protein digestion of solid foods within semi-dynamic *in vitro* models.

The promising *in vitro* results provided a solid basis for a human trial described in **Chapter 5**. Gastric digestion of protein gels with different hardness and/or protein content was investigated in a randomized crossover trial with the use of MRI anatomical, T_1 and T_2 scans. The results showed that high protein content is the main factor in reducing gastric emptying and high hardness is an additional factor. The lower gastric emptying rate did not affect satiety. T_1 and T_2 measurements can provide extra information on the dilution and digestion taking place in the stomach. This study suggests the potential of the MRI parameters providing more insights on *in vivo* digestion, and the results will contribute to linking *in vitro* and *in vivo* digestion research.

Overall, this thesis builds from *in vitro* static, *in vitro* dynamic, to *in vivo* (in human) digestion studies. This work explored the possibility of MR techniques to measure both *in vitro* and *in vivo* digestion of protein-rich solid food and to bridge the link between *in vitro* and *in vivo* research.

6.2 MRI: a promising approach to study digestion

As shown in recent reviews and this thesis, MRI, a non-invasive approach, can be very useful to assess gastric processes, including gastric emptying, gastric mobility, intragastric processes (Smeets et al., 2020; Spiller and Marciani, 2019). Apart from using it as a 'camera' to observe the change in anatomy, the ambition of this thesis was to explore the possibility of using MRI to also measure digestion at the molecular level.

6.2.1 T_1 and T_2: markers to monitor protein hydrolysis

T_1 and T_2 are the most basic two among several MR markers. As introduced in **Chapter 1**, T_1 (or $R_1 = T_1^{-1}$) and T_2 (or $R_2 = T_2^{-1}$) can be used to monitor changes in water migration, food structure, and macromolecule concentration (Le Dean et al., 2004; Mariette, 2009; Peters et al., 2016; Van Duynhoven and Jacobs, 2016). This explorative work started from the idea that these changes take place during digestion as well.

We explored the use of transverse (T_2) and longitudinal (T_1) relaxation times or rates ($R_2 = T_2^{-1}$, $R_1 = T_1^{-1}$) in measuring gastric digestion at the molecular level.

For digestion of the solid model food (protein gels), *in vitro* results from **Chapters 2** and **4** showed that R_1 and R_2 can serve as markers to monitor the change in pH and protein concentration in the liquid phase. The key point is that the two phases are present during digestion of solid food, so that by monitoring the change in the liquid phase, the digestion progress of the solid food can be tracked. In **Chapter 5**, the human trial showed that *in vivo* T_1 and T_2 values of the measured gastric content changed during digestion. Although with the *in vivo* scans, it was not possible to analyze the liquid phase separately, T_1 and T_2 values can still provide extra information on the dilution and digestion taking place in the stomach. The link between *in vitro* and *in vivo* digestion will be further discussed in section 6.3.

The solid and liquid phases were not always distinguishable for the *in vivo* scans due to multiple reasons: 1) gastric motility resulting in 'well-mixing' digesta; 2) the low resolution of the image (1.56 × 1.56 × 6 mm) compared to the diameter of the food particles (5 mm); 3) motion artefacts. The *in vivo* scans suffered from a higher partial volume effect than *in vitro* scans. The partial volume effect means that many voxels contain a mix of liquid and solid material and this effect commonly takes place in MRI measurements (Angel et al., 2002). Thus, it is always a trade-off to set up the MRI sequences. For example, when

limiting the measurement time, the resolution and other parameters have to be compromised.

For liquid food, these MRI markers may not be applied in the same way as for solid food. As shown in **Chapter 2**, during digestion of the protein solution, protein concentration and R_2 remained unchanged. The reason is that R_2 values are sensitive to the change in protein concentration, while no change in protein concentration took place during digestion of protein solution. On the other hand, this may create the opportunity for these markers to indicate not only the dilution effect from the gastric secretion but also the pH change. For example, the T_2 value can be used to assess the dilution of the original meal by the gastric fluid, and to assess the viscosity during digestion (Marciani et al., 1998; Marciani et al., 2001). The main focus of this thesis is on solid food digestion, but the use of these MRI markers on informing digestion of liquid foods is valuable to be further explored.

Apart from the T_1 and T_2, several other MR techniques or markers are potential for studying digestion at the molecular level. For example, NMR spectroscopy has been used to quantify hydrolysis of carbohydrate, protein, and lipid during *in vitro* digestion(Marciani et al., 1998; Marciani et al., 2001). Magnetization transfer has been investigated to measure *in vitro* digestion kinetics of milk proteins (Mayar et al,. 2022). T_2 and $T_{1\rho}$ relaxation time dispersion measurements are also promising but underexplored MR markers on digestion (Palmer, 2014; Smeets et al., 2020; Wáng et al., 2015). Thus, further research on

6.2.2 Anatomical scans: beyond providing gastric content volume

In **Chapter 5**, we measured not only the T_1 and T_2 maps but also gastric anatomy. Such anatomical scans are well established and many studies have used them to measure gastric emptying dynamics and intragastric processes like layering and coagulation (Alyami et al., 2019; Camps, Mars, De Graaf, & Smeets, 2016; Camps, van Eijnatten, van Lieshout, Lambers, & Smeets, 2021; Marina Coletta et al., 2016; Marciani et al., 2001). For assessing gastric emptying, the analysis approach is quite straightforward: summing up the total gastric content volume in all slices from one scan, and then comparing the change of gastric content volume over time.

In most cases, researchers use the term gastric emptying half time (GE t_{50}) to indicate the speed of gastric emptying. GE t_{50} is the time from the start of the meal until 50% of the

meal has been emptied. This term is often calculated from the gastric content volume with an exponential model (Elashoff et al., 1982), as shown in Equation (6.1).

$$V_t = V_0 \cdot 2^{(-\frac{t}{t_{50}})^{\beta}} \quad (6.1)$$

Where t represents the measurement time point; V_t represents the volume at time point t; V_0 represents the initial volume; t_{50} is the fitting output GE time t_{50}; another fitting output, β, determines the shape of the gastric emptying curve, and therefore can be considered as an indicator of food types.

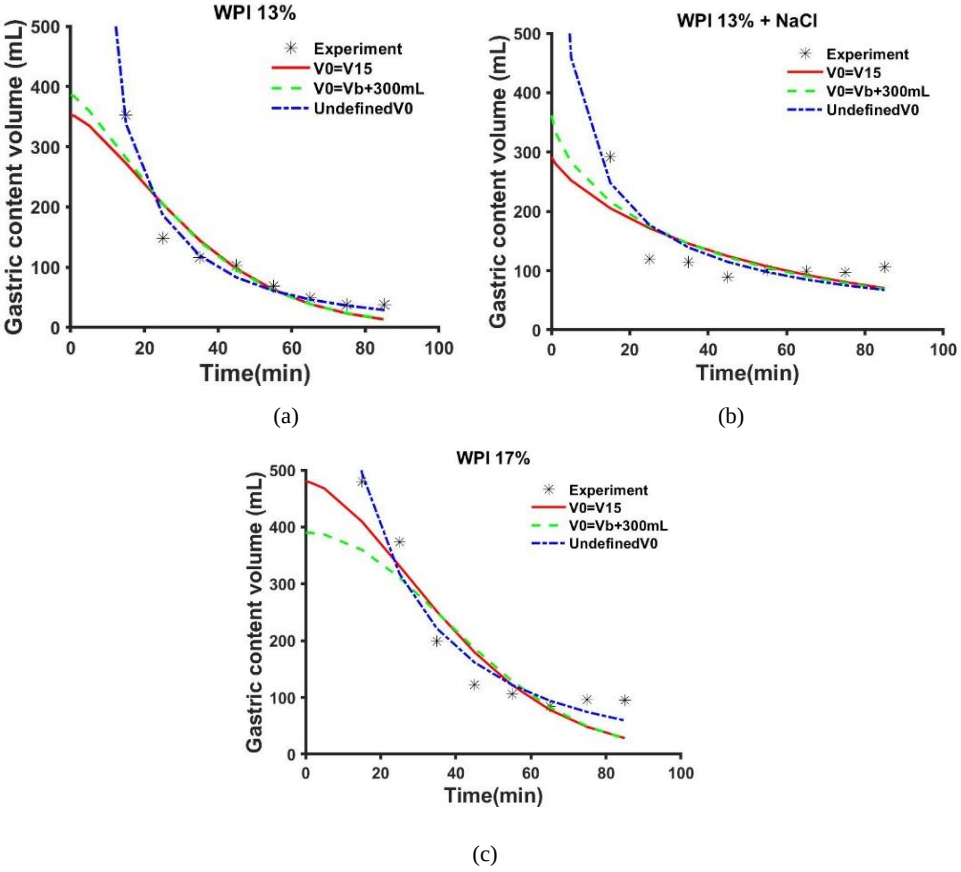

Fig. 6-1 *The experimental measured gastric content volume (scatter, experiment) and the fitting curve for gastric emptying half time with input V_0 as the volume of the first measurement point after ingestion (red line, v0 = v15), input V_0 equal to the initial amount of meal plus the basal gastric fluid (green dashed line, V0 = Vb+300), and an undefined V_0 (blue dot-dash line, UndefinedV0) based on Soft-LP (a), Hard-LP (b), and Hard-HP (c) from one participant in Chapter 5.*

In this equation, the fitting outcome t_{50} is highly dependent on the initial volume entered into the equation. V_0 is usually defined by either the measured volume of the first

measurement point after ingestion or the initial amount of meal plus the basal gastric fluid (Elashoff et al., 1982). This works well for liquid foods, as they are ingested very fast, and the oral process does not have a huge impact on the initial meal volume (V_0 in Equation (6.1)) in the stomach. However, with a solid meal, especially for foods that need long mastication and saliva lubrication effect, the saliva entering the stomach should not be neglected for defining V_0. In addition, the amount of gastric secretion triggered by chewing might also be taken into consideration. An example (Fig. 6-1, data from **Chapter 5**) showed that for fitting the same data different input V_0 provides very different fitting curves and outcome t_{50} values. The details can be found in Table 6-S1. This suggests that for solid food, presenting the actual measure of gastric content volume is more informative than showing GE t_{50} calculated from the gastric content volume.

The meaning of GE t_{50} depends on the V_t. When the gastric content volume was used as V_t, t_{50} is for the whole gastric content but not necessarily for the food (or meal). The production of gastric fluid is simultaneously taking place and the emptying rate for liquid and solid is different. Therefore, it is better to use the actual volume of the food in the stomach as V_t to calculate GE t_{50} which represents the emptying of the meal.

To acquire the volume of food in the stomach, we propose a secondary analysis of the MRI anatomical scans: by indicating a threshold intensity on the scans, the volume of food matrices and gastric fluid can be quantified. Such an analysis based on the data from **Chapter 5** provides the results shown in Fig. 6-2. In this case, the liquid component refers to gastric fluid whereas the solid component refers to the protein gel. Using information from Fig. 6-2, we can better interpret the gastric emptying behavior of the food. The change of gastric solid volume indicates the gastric emptying rate of the gels: Soft-LP > Hard-LP > Hard-HP. The gastric liquid volume is similar among the treatments. This may also be useful for other types of food, and the analysis method can be further developed. Furthermore, additional analysis can be conducted to acquire gastric secretion and emptying rates. To assess gastric secretion, the anatomical scan is practically easier than the existing T_1 mapping method in which testing meals need to be labelled (Goetze et al., 2009; Hoad et al., 2015; Treier et al., 2008).

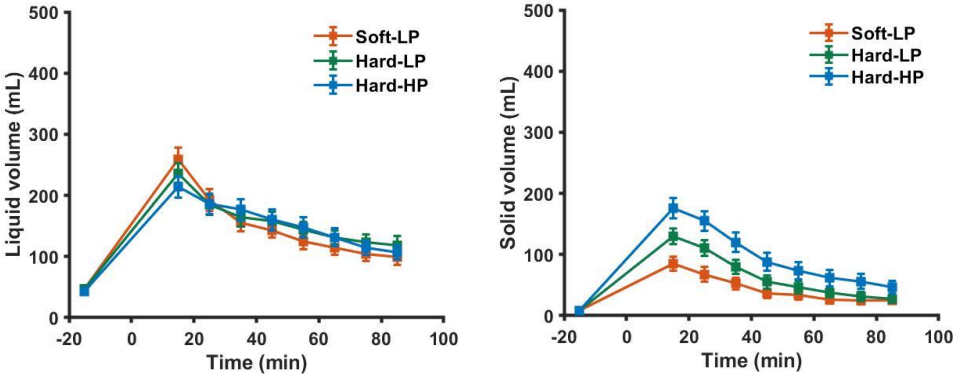

(a) (b)

Fig. 6-2 *The liquid (a) and solid (b) volume in the stomach estimated based on the anatomical scans from the human study in Chapter 5*

In summary, MR markers, for example, T_1 and T_2, showed great potential in measuring digestion both *in vitro* and *in vivo*. The *in vivo* T_1 and T_2 sequences should be further developed. The anatomical *in vivo* scans may be useful to calculate the solid and liquid volume, in addition to acquiring information on the gastric content volume.

6.3 Bridging in vitro and in vivo digestion research

In vitro studies are easy to carry out and highly reproducible, compared to *in vivo* human studies. *In vitro* models for food digestion and their standardized protocols have been rapidly developed in recent years as they can help to reduce the need for extensive *in vivo* studies (Muttakin et al., 2019). However, due to the complexity of the physiological processes during digestion, it is important to understand the limitations of each *in vitro* model, to bridge the link between *in vitro* and *in vivo* digestion research, and to validate the *in vitro* model to a good extent to represent the corresponding *in vivo* processes.

6.3.1 T_1 and T_2 as a bridge between in vitro and in vivo research

In this thesis, we proposed that T_1 and T_2 measurements may be useful to link the *in vitro* and *in vivo* results. For analyzing *in vivo* T_1 and T_2 measurements, we cannot use the same approach (namely, manual segmentation on liquid phase) as for *in vitro* ones. Because the manual segmentation is not practical for analyzing *in vivo* scans as there was no upper-lower phase separation as in *in vitro* scans. Moreover, as mentioned in Section 6.2, the solid and liquid phases were not always distinguishable for the *in vivo* scans.

To solve this problem, we made several different attempts to analyze *in vivo* images to assess the T_1 and T_2 of liquid and solid phases.

The first one was to define a boundary on the distribution curve of T_1 and T_2 in the stomach content region, as in theory voxels with pure solid would present a significant lower T_1 or T_2, compared to voxels with solely liquid. For example, in Fig. 6-3, we could set a boundary T_2 value for solid and liquid, or even two boundary values for the solid, mixture of solid and liquid, and liquid. The outcome of this approach is shown in Supplementary Fig. 6-S2. A very low volume of liquid phase was identified by this approach, which indicates that this approach failed to select the entire liquid phase. However, the question is how to define a boundary in an objective way to all the curves from different treatments and participants. Moreover, many voxels contain both solid and liquid contents due to the partial volume effect. This created more challenges for accurately selecting only the solid or liquid phase.

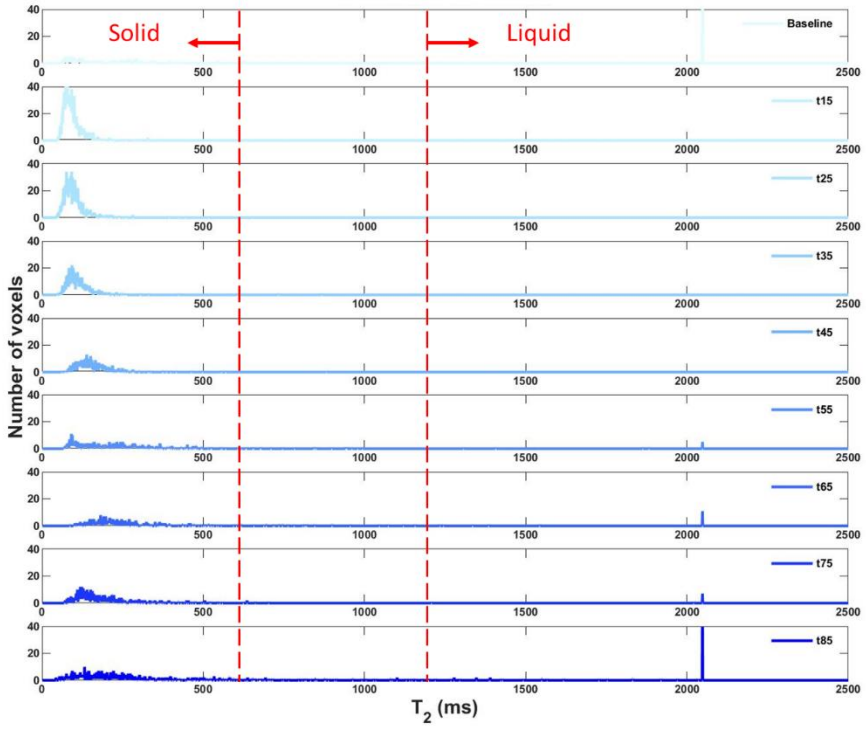

Fig. 6-3 *The example of the T_2 distribution curves in the stomach content from baseline till 85 min after ingestion and the two boundary lines to define the solid and liquid components (data from Chapter 5)*

The second approach is to first create a binary mask from an anatomical scan for one phase by applying a certain threshold, and then apply this mask on the T_1 and T_2 maps. Then the phase of interest can be selected and the average T_1 or T_2 from that phase can be calculated. However, this approach was not successful in analyzing our current *in vivo* data, due to the limited resolution and the partial volume effect.

Lots of efforts have been made to correct the partial volume effect, such as image enhancement techniques, and different models to reconstruct the information in the voxels (Erlandsson et al., 2012). Here we would like to propose another relatively simple way of analysis via mathematical calculation. The average T_1 or T_2 of the region of interest is calculated by the mean of T_1 or T_2 from all voxels. The T_1 or T_2 value from an individual voxel is determined by the composition in the voxel, in this case, the amount of solid or liquid and the T_1 or T_2 value of the pure liquid and solid phase. This is shown in the Equations (6.2-6.4). To be noted that it might be inhomogeneous distribution in the liquid

or solid phase, here we are talking about the average of T_1 or T_2 value from all protons in the liquid or solid in a voxel.

$$Mean\ T_1 = T_{1-Solid} \cdot V_{solid}\% + T_{1-liquid} \cdot V_{liquid}\% \quad (6.2)$$

$$Mean\ T_2 = T_{2-Solid} \cdot V_{solid}\% + T_{2-liquid} \cdot V_{liquid}\% \quad (6.3)$$

$$V_{solid}\% + V_{liquid}\% = 100\% \quad (6.4)$$

Where the $Mean\ T_1$ or $Mean\ T_2$ represent the mean T_1 or T_2 of an individual voxel and these are measured outcomes from the scans; $T_{1-Solid}$ or $T_{2-Solid}$ represent the average T_1 or T_2 of the solid; $T_{1-liquid}$ or $T_{2-liquid}$ represent the T_1 or T_2 of the liquid; $V_{solid}\%$ or $V_{liquid}\%$ represents the volumetric percentage of solid or liquid in the whole voxel.

In equation 6.2-6.4, $T_{1-liquid}$, $T_{1-Solid}$ and $T_{2-Solid}$ can be considered as constant parameters, which can be obtained from separate, independent MRI measurements. The $Mean\ T_1$ and $Mean\ T_2$ can be directly obtained from T_1 or T_2 maps (e.g. the measurements in **Chapter 5)**. $T_{2-liquid}$, $V_{solid}\%$ and $V_{liquid}\%$ are the calculation outcome from these three independent equations.

$T_{1-liquid}$ can be obtained from the data in **Chapter 4**. The T_1 of the liquid was not sensitive to the change of pH and protein concentration and for this reason it can be considered as a constant using the baseline T_1 value. Before being able to fit eqs 6.2-6.4, $T_{1-Solid}$ and $T_{2-Solid}$ need to be measured. This analysis may allow us to obtain more information on how T_2 and T_1 change in the different phases, and therefore help us to use these MRI markers to measure the changes during *in vivo* digestion in a more quantitative way. This analysis approach is worthwhile to be further developed, as this may be useful to analyze MRI images where partial volume effects are often an issue.

As the *in vivo* T_1 and T_2 (from **Chapter 5**) cannot be analyzed the same way as the *in vitro* data with MR-GAS (**Chapter 4**), we re-analyzed the MR-GAS data using the same way as the *in vivo* results. The mean T_2 and T_1 of the whole content in MR-GAS (based on the MRI scans in **Chapter 4**) is shown in Fig. 6-4.

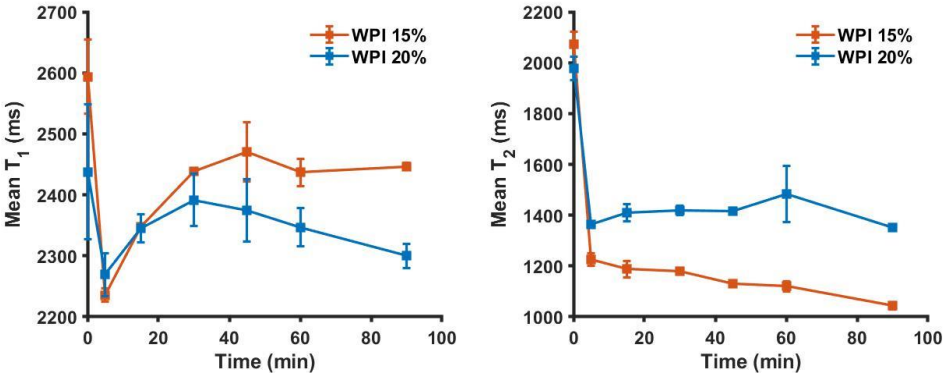

(a) (b)

Fig. 6-4 *Mean T_1 and T_2 values of the gastric compartment content in MR-GAS (re-analysis of data in Chapter 4). The bars indicates standard deviation from duplicate measurements.*

This can be compared with Fig. 5-3b and Fig. 5-4b in **Chapter 5**. Similar trends of decrease from the baseline to first measurement after gel ingestion (or addition) are observed. This is because the presence of the gel in the mixtures shortened the relaxation times. Interestingly, different trends are observed from the first measurement point onwards. *In vitro* T_1 first increased till 30 min and then decreased, while *in vivo* T_1 increased all the time. This is because T_1 is more dependent on the ratio between liquid and solid. The ratio between liquid and solid first increased from the first measurement point (t = 5 min) to 30 min and then increased. A higher liquid ratio contributes to a higher mean T_1 of the stomach content. However, for *in vivo* T_1 increased till the end. That implies that the ratio between liquid and solid increased over time. *In vitro* T_2 decreased slightly while *in vivo* T_2 increased. This is probably because the *in vivo* digestion effect was smaller than the dilution effect as described in **Chapter 5**.

This suggests that the setup in **Chapter 4** likely underestimated the amount of gastric juice production and gastric emptying of the protein gels. The *in vivo* data provided insight into the actual gastric degradation of protein gel, the secretion and emptying process, and may contribute to validating the *in vitro* model.

6.3.2 In vivo results to validate in vitro models

Apart from the information provided by T_1 and T_2 scans, the *in vivo* anatomical scans can deliver additional crucial messages to validate *in vitro* digestion models.

As discussed in Section 6.2, apart from looking at the whole stomach content, with extra analysis, the volume of solid and liquid can be analyzed from the *in vivo* anatomical scan (Fig. 6-2). Here the same approach was applied to analyze the anatomical *in vitro* images from MR-GAS (**Chapter 4**) and the result is shown in Fig.6-5a. The estimation (Fig. 6-5a) is very comparable with the actual amount of solid and liquid in the experiment (Fig. 6-5b), which confirms the feasibility and accuracy of the analysis approach.

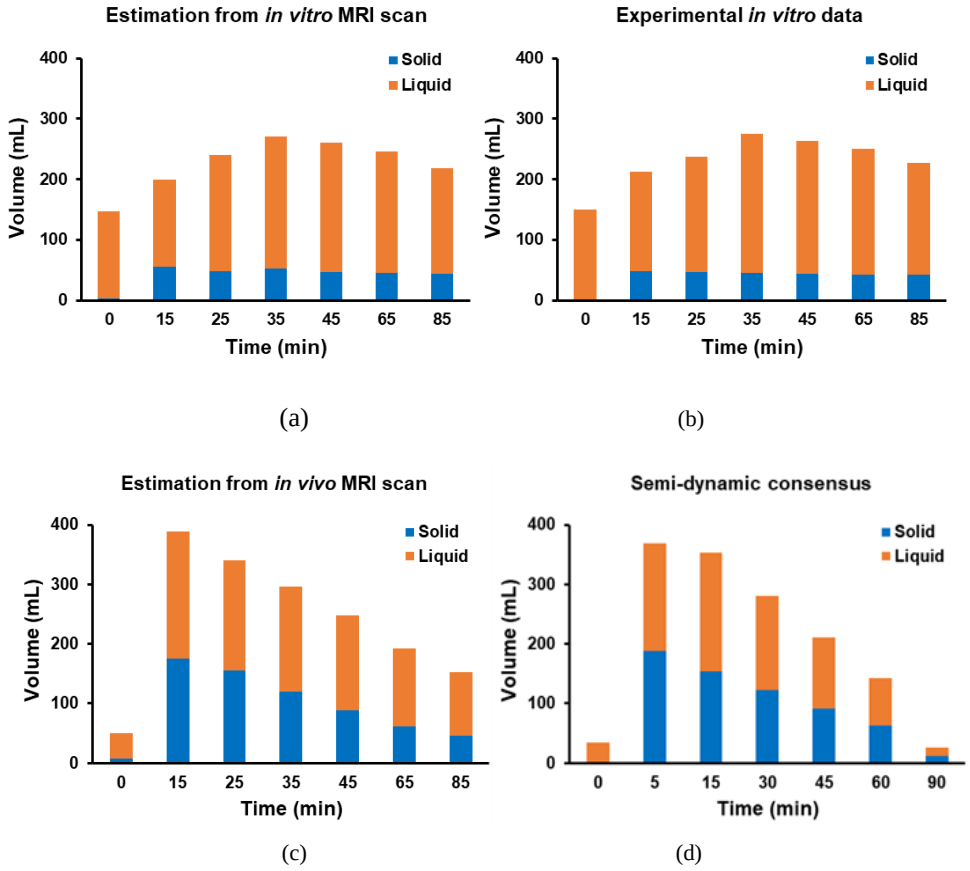

Fig. 6-5 *Comparison between estimated solid and liquid volume based on the in vitro MRI scans (a, data from Chapter 4 digestion of WPI 20% gel), the in vitro experimentally measured values (b, data from Chapter 4 digestion of WPI 20% gel), and estimated solid and liquid volume based on the in vivo MRI scans (c, data from Chapter 5 digestion of WPI 17% gel), and the estimated solid and liquid volume based on the semi-dynamic method proposed by Mulet-Cabero et al. (2020).*

The *in vitro* experiments show a different ratio between solid and liquid compared to the *in vivo* data shown in Fig. 6-5c, which indicates that the gastric dynamics we used in MR-GAS before were far from actual *in vivo* conditions. We also compared the *in vivo* results with the calculated solid and liquid volume based on the recent-proposed semi-dynamic

method (Mulet-Cabero et al., 2020). Our result here suggests that this semi-dynamic method can serve relevant gastric dynamics.

Based on the *in vivo* results, we can estimate the secretion rate of gastric fluid and the emptying rate of the food and liquid. This information is helpful to validate the *in vitro* model: As a pilot experiment, we applied the gastric secretion and emptying rates calculated from the *in vivo* results (from **Chapter 5**) on the MR-GAS. Fig. 6-6 shows the comparison of protein concentration in the supernatant during digestion between the old set-up (data from Chapter 4) and the new gastric dynamics obtained from *in vivo* results.

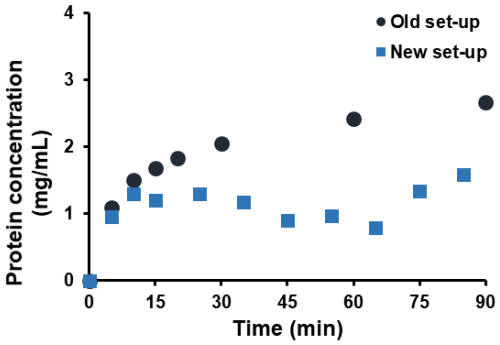

Fig. 6-6 *Protein concentration in the liquid phase during digestion in MR-GAS with the old gastric dynamic set-up (Circle scatters, dark blue) and the new set-up with gastric dynamics obtained from in vivo results (Square scatters, light blue); Protein concentration has been corrected with the amount of already-present protein in the simulated gastric fluid. Data for the old set-up was the mean of duplicates reported in Chapter 4, while data for the new set-up is the preliminary result from one measurement.*

The result with the new dynamics indicates that the protein concentration in the liquid phase did not keep increasing over time, although the protein hydrolysis progressed (because the percentage of protein released from the gel increased from 1.8% at 5 min to 4.2% at 85 min). It implies that the local protein concentration in the liquid phase *in vivo* may be low and the change in protein concentration during digestion is likely very small. This also indicates that the dilution effect of gastric fluid is significant. This may support our explanation of the difference in the T_1 and T_2 results between *in vitro* MG-GAS and *in vivo* experiments in section *6.3.1*: for *in vivo* results, dilution effect is higher than digestion effect. Although the preliminary results with adapted gastric dynamics only present the protein concentration during digestion, it shows the importance of validating the *in vitro* models based on *in vivo* data.

6.3.3 Ongoing efforts on validation

As shown in the previous section gastric dynamics significantly affect the outcomes, using validated *in vitro* parameters is essential. We are not alone in this journey. Validation and refinement of *in vitro* models using *in vivo* data is an ongoing collaborative effort in the field, see https://www.cost-infogest.eu/. For example, the *in vitro* static digestion model has been well established as the most simplified and well-controlled model (Kong and Singh, 2008; Minekus et al., 2014). These models have been validated with *in vivo* data, and they are reliable for measuring the digestibility of certain types of nutrients in a simple model food (Bohn et al., 2018). However, these models are limited to studying the digestion of complex or realistic foods whose structure change is an essential factor. Recently, various dynamic *in vitro* models have been developed, and researchers are working on the validation of these models using *in vivo* data from human trials or animal studies (Dupont et al., 2019). For example, the secretion rate of the human gastric simulator was validated by *in vivo* data from pigs (Nadia et al., 2021); the gastric transit of infant formula in the DIDGI® system showed similar results as in piglets (Ménard et al., 2014). After being programmed with physiologically-relevant parameters obtained from *in vivo* data, the dynamic *in vitro* systems may mimic the complexity of the digestion to a very good extent (Dupont et al., 2019). However, the validation with a certain food might not guarantee the relevance of the *in vitro* dynamic model for other types of food. Therefore, it will be worthwhile to further validate the dynamic *in vitro* models at least on different categories of foods with different properties.

6.3.4 Towards more physiologically relevant in vitro gastric digestion models

As described in previous sections, the information acquired from *in vivo* (human or animal) data could help to validate the *in vitro* models. For instance, in this thesis, we developed the novel MRI-compatible semi-dynamic *in vitro* gastric simulator (**Chapter 4**). It can incorporate gastric secretion, emptying, and mixing not only in a lab set-up but also in a clinical MRI scanner. However, there are several limitations of the model, and it can be further developed to be more physiologically relevant.

Firstly, the material of the ‘stomach’ was glass which is far from the real stomach. A soft material such as silicone might be more suitable and a wrinkled inner surface would also add value to make the *in vitro* ‘stomach’ closer to the real stomach (Wu and Chen, 2020).

In addition, the gastric mixing was mimicked by air bubbling in MR-GAS. This was a clever solution to solve the challenge of avoiding the use of metal. However, air bubbling for mixing may not work well if the food contains good emulsifiers, and this way of mixing is far away from the real stomach condition which is described in Section 1.2 (**Chapter 1**). Mixing mechanically without introducing any magnetic materials can be further developed.

Moreover, based on the *in vivo* data from **Chapter 5** and other *in vivo* studies, the gastric response dynamics of the *in vitro* model can be better implemented, for instance, altering secretion and emptying rating at different stages of digestion or with different types of food. In addition, for further work, it would also be interesting to include the mucus layer in the gastric model to have a more biologically relevant environment.

6.4 Effects of food properties on gastric digestion

In this thesis, we gained more insights on the effect of food properties on gastric digestion. Changes in the food properties can be a useful tool to alter overall daily energy intake and adsorption (Bolhuis et al., 2014; Forde et al., 2020; Hall et al., 2019; Mackie et al., 2017). Moreover, the properties of the food matrix are very important factors affecting gastric digestion (Bornhorst and Singh, 2014). Food structure has a straightforward impact on the digestion in the upper digestive tract, namely the oral and gastric digestion, during which the mechanical breakdown takes place. Here we would like to highlight that the effects of food properties include not only the direct effect on gastric digestion but also the effect through modulating oral processing behaviour.

In this thesis, we studied the gastric digestion of different food properties: food structure (in our case: hardness) and nutrient density (in our case: protein content). As expected, protein gels with higher protein content and/or hardness were digested slower with *in vitro* static and semi-dynamic models **(Chapters 2**, **3** and **4)**. This is in line with other *in vitro* digestion studies (Luo et al., 2015). The reason for this is that crosslinking density in the protein gel increased with a higher protein concentration or hardness and thereby the rate of enzymatic hydrolysis was reduced (Luo et al., 2017). The underlying mechanism involves the transportation behaviors of not only enzymes and acid but also water (Luo et al., 2018; Thévenot et al., 2017; van der Sman et al., 2019). As shown in **Chapter 3**, water transport (in other words: swelling or shrinking) is crucial on the mass transfer of other components, and the partitioning of the pepsin between the food matrix and gastric juice needs to be further explored to better understand the effect of microstructure on digestion.

The human trial in **Chapter 5** confirmed the effect of hardness and protein concentration on gastric emptying: protein gels with high protein content and/or high hardness were emptied slower. This is in line with many other studies where the nutrient density of the meal was found as the most important factor for gastric emptying, and the higher hardness induced a slower gastric emptying (Houghton et al., 1988; Hunt and Stubbs, 1975; Marciani et al., 2001a). Moreover, our findings also complement what has been reported with a liquid meal where nutrient density was the main driver of gastric emptying, and viscosity was the second factor (Camps et al., 2016).

Apart from the direct effect of food properties on gastric digestion, we also would like to discuss the effect through affecting oral processing. In **Chapter 5**, we observed that protein gels with higher hardness require a slower eating rate, while the nutrient density (protein content) in the protein gels did not matter. This is not a big surprise, cause the major factor on eating rate is the mechanical property of the food, such as hardness, microstructure and water content (Bolhuis and Forde, 2020; Forde et al., 2017; Witt and Stokes, 2015).

The eating rate of the protein gels was negatively associated with the gastric content area under the time curves (**Chapter 5,** Fig. 5-5). This is interesting because it may imply that a slower eating rate triggered a longer retention time in the stomach, which would promote longer gastric digestion. It may also imply that a slower eating rate triggered higher gastric juice production and therefore resulted in more retention of gastric content. The higher gastric juice production can be resulted from the longer oral exposure and/or the higher buffering capacity of the smaller gel particles after a longer eating time (Mennah-Govela et al., 2019). The underlying mechanism remains to be investigated. To be noted, the protein gels were prepared as small particles with a diameter of 5 mm to minimize variations in eating rate. Thus in real life, the effect of eating rate on gastric retention is possibly larger.

Table 6-1 *The average particle size and saliva content in the spilt-out bolus after oral processing of the whey protein gels: Soft-LP, Hard-LP, and Hard-HP*

Gels	Soft-LP	Hard-LP	Hard-HP	p value
Hardness (kPa)	67.0 ± 18.9^{a}	213.7 ± 43.2^{b}	264.9 ± 37.5^{b}	-
Particle size (mm)	4.32 ± 0.26^{a}	3.27 ± 0.12^{b}	3.34 ± 0.14^{b}	< 0.05
Saliva content (%)	10.9 ± 2.2^{a}	15.7 ± 1.9^{b}	16.1 ± 2.1^{b}	< 0.05

Mean ± SE is presented based on the incomplete data (only with 8 participants) from the in vivo Study in Chapter 5. Analysis of variance (ANOVA) tests followed by post hoc HSD Turkey test were performed to examine the difference among treatments. Different letters in the same row indicates significant differences ($p<0.05$).

In addition to the eating rate, we also collected data on the bolus properties of the spit-out gel bolus from several participants in the human trial described in **Chapter 5**. As shown in Table 6-1, with harder gels, in the spit-out bolus, the saliva content was higher and the particle size was smaller. This is in line with a longer eating time and a slower eating rate for the gels with higher hardness (shown in **Chapter 5**). The main outcome of oral processing of solid foods is to form a bolus and to lubricate the bolus to reach the swallowing threshold (Chen, 2009; Mosca and Chen, 2017). Our finding here is in good

agreement with literature in which harder gels need to fit a smaller size threshold by longer mastication (Guo et al., 2013). Thus, the eating behavior and resulting bolus properties are highly dependent on food hardness, with or without a difference in protein content.

To understand the relation between the bolus properties and gastric digestion, we conducted a pilot study on the effect of saliva content and particle size on gastric digestion of protein gels using an *in vitro* model. The results show that smaller particles and lower saliva content were associated with a faster digestion rate. In addition, the smaller particle size of the solid meal (chicken liver) increased gastric emptying (Weiner, Graham, Reedy, Elashoff, & Meyer, 1981). Based on the pilot *in vitro* finding and the early study, we would expect that the smaller particle size of harder gels (Hard-LP and Hard-HP) contribute to accelerating gastric digestion and emptying. However, in **Chapter 5**, the order of gastric emptying rate is Hard-HP < Hard-LP < Soft-LP. This indicates that the decreased bolus particle size here was likely not large enough to act against the main drivers of gastric emptying (nutrient density and hardness).

In summary, the food structure and nutrient density are both important factors for digestion in the upper digestive tract. The effect of the oral phase on subsequent gastric digestion, especially for solid food, is important to be further explored.

6.5 Future work for digestion research

The beauty of research is that it never ends. Although a lot of excitement was derived from the explorative work in this thesis, several limitations need to be addressed. First of all, the study material in this thesis was focused on whey protein gel, which is a protein-rich solid system. The MRI approaches need to be validated by the application in studying digestion of more complex food in the future. In addition, the feasibility of these approaches on studying liquid food is unclear as the phase separation between food and digestive fluid will not take place during digestion in most cases. Secondly, the role of water together with digestive enzymes need to be better understood, for example, the partitioning behavior of pepsin. Thirdly, the semi-dynamic MRI compatible gastric simulator (MG-GAS) that we developed can still be further improved. The gastric dynamics (including mixing, gastric secretion and emptying) should be validated based on the *in vivo* data. Moreover, the MRI sequences and the analysis approach remain lots of room for improvement to better measure the target outcome and interpret the data. Apart from what has been mentioned in the previous sections, we would like to highlight several aspects for future research work.

6.5.1 The connection between different phases

Nowadays research mostly focuses on specific digestion phases. It would be great if we can better understand the connection between different phases by combining different expertises. For example, how oral processing (including salivation, mastication) affect gastric digestion and other subsequent digestion phases by combining the perspectives of not only nutrient breakdown and absorption but also hormonal and neural responses. In addition, the connection between upper digestion and adsorption in the small intestinal and fermentation in the colon can be further investigated. For example, we may design food toward a better feeding of gut microbiota (Ercolini and Fogliano, 2018). By connecting the knowledge from between different phases, we can understand better how to utilize the nutrient composition and how to modulate the extent of digestion and absorption.

6.5.2 MRI to measure nutrient breakdown

This thesis is the first to show the potential of MR techniques in studying nutrient breakdowns from *in vitro* to *in vivo* research. However, one PhD thesis is clearly not enough to dive into all the possibilities of this promising approach.

The T_1 and T_2 measurements can be further explored for measuring digestion of other nutrients such as carbohydrate and fat, or mixed model foods, and then move forward to the real meal. In this thesis, the focus is mainly on the changes of the supernatant (or liquid) phase. The changes of T_1 and T_2 in the solid food are worthwhile to be further investigated, as they will provide more insight on the (macro- or even micro-)structure change of the food during digestion. Moreover, other promising markers mentioned in Section 6.2 are worthwhile to be further investigated (Smeets et al., 2020). The application of MRI on studying digestion in different contexts needs more interdisciplinary effort from food technologists, nutritionists, physicians and MRI technologists. Such joint efforts will advance this field of research.

6.5.3 Human physiologically-based modelling

In this thesis, the *in vitro* and *in vivo* human studies were conducted for studying digestion. Here we would also like to address the great potential of *in silico* modelling, which is a sustainable approach as it can reduce the use of lab material, animals or human participants. Mathematical modelling may serve as a powerful tool to mimic physiological responses, to integrate the complex stream of mechanisms that must be considered, and to retrieve a full picture of the digestion process from mouth to the colon (Le Feunteun et al., 2021). The *in silico* models in pharmacy have been extensively developed to predict the dissolution and absorption of oral-administrated drugs; for example, physiologically-based pharmacokinetic (PBPK) models can predict plasma drug concentration-time profiles (Brown et al., 1997; Kostewicz et al., 2014). However, compared to drug formulations, foods are much more complex. Some *in silico* models have been developed, but most of them are more compatible with a liquid meal and better models for solid food with different structures need to be further developed (Le Feunteun et al., 2021).

The existing data from various *in vitro* and *in vivo* experiments can be re-used to improve *in silico* models. For this, efforts to carefully review and categorize the existing data and to build a systematic database will be appreciated. Especially the *in vivo* MRI human data can be useful. For example, the fluid dynamics model in the human stomach is a great tool to understand the gastric mixing process (Ferrua and Singh, 2010); MRI data on the digestion of solid food may validate this model for wider application. *In vivo* MRI data from different studies such as **Chapter 5** may serve as input data for developing in-silico models on the

aspect of food structure because it provides information about the gastric response to solid foods with different food properties.

Hopefully, current human physiologically based *in silico* models can be further developed. They will contribute to describing or predicting complete model food transit and absorption, and to designing healthier foods and supporting the development of personalized nutrition.

6.6 Concluding remarks

To conclude, this thesis investigated the use of MR techniques to study how solid food properties affect gastric digestion via *in vitro* models and a human trial, and laid a foundation for further digestion research with the use of MRI.

From this thesis, the food properties (including hardness and protein content) have shown their significant impact on the gastric digestion rate *in vitro*, while *in vivo* protein content is more effective in delaying gastric emptying compared to hardness. The role of water transportation during digestion should be taken into account. MR techniques are promising approaches to study both *in vitro* and *in vivo* digestion. TD-NMR can serve as a good supplementary approach for interpreting MRI data. In addition to macroscopic structural information, MR techniques can provide molecular-level and quantitative information on protein hydrolysis through the use of T_1 and T_2 measurements. The *in vivo* MRI data can be used to compare with the *in vitro* MRI data, and can contribute to informing and validating *in vitro* and *in silico* digestion models.

Besides T_1 and T_2, several MR approaches are worthwhile to be explored on their application for digestion research. The ongoing efforts with *in vitro*, *in vivo*, and *in silico* digestion studies in better understanding the complex processes of food digestion and absorption will contribute to designing healthier foods, to supporting the development of personalized nutrition, and to improving the health of people wordwide.

Supplementary material

Table 6-S1 *Fitting outcome of gastric emptying half time (GE t50) of three gels with input V_0 using the volume of the first measurement point after ingestion ($V_0 = V_{t=15}$), input V_0 equal to the initial amount of meal plus the basal gastric fluid ($V_0 = V_{bsseline} + 300$), and an undefined V_0*

	$V_0 = V_{t=15}$			$V_0 = V_{bsseline} + 300$			Undefined V_0		
Gels	t_{50} (min)	beta	V_0 (mL)	t_{50} (min)	beta	V_0 (mL)	t_{50} (min)	beta	V_0 (mL)
Soft-LP	29.5	1.5	352.7	26.8	1.4	386.3	0.1	0.3	12383.8
Hard-LP	34.9	0.8	291.5	23.2	0.7	361.8	0.0	0.2	5341.2
Hard-HP	36.5	1.7	479.8	43.6	2.0	390.1	3.3	0.5	2201.6

As shown in Table 6-S1, using the first measurement point as V_0, GE $t_{50\ of}$ the Hard-LP is longer than that of Soft-LP; while contrary results can be found when using the initial amount of meal plus the basal gastric fluid V_0.

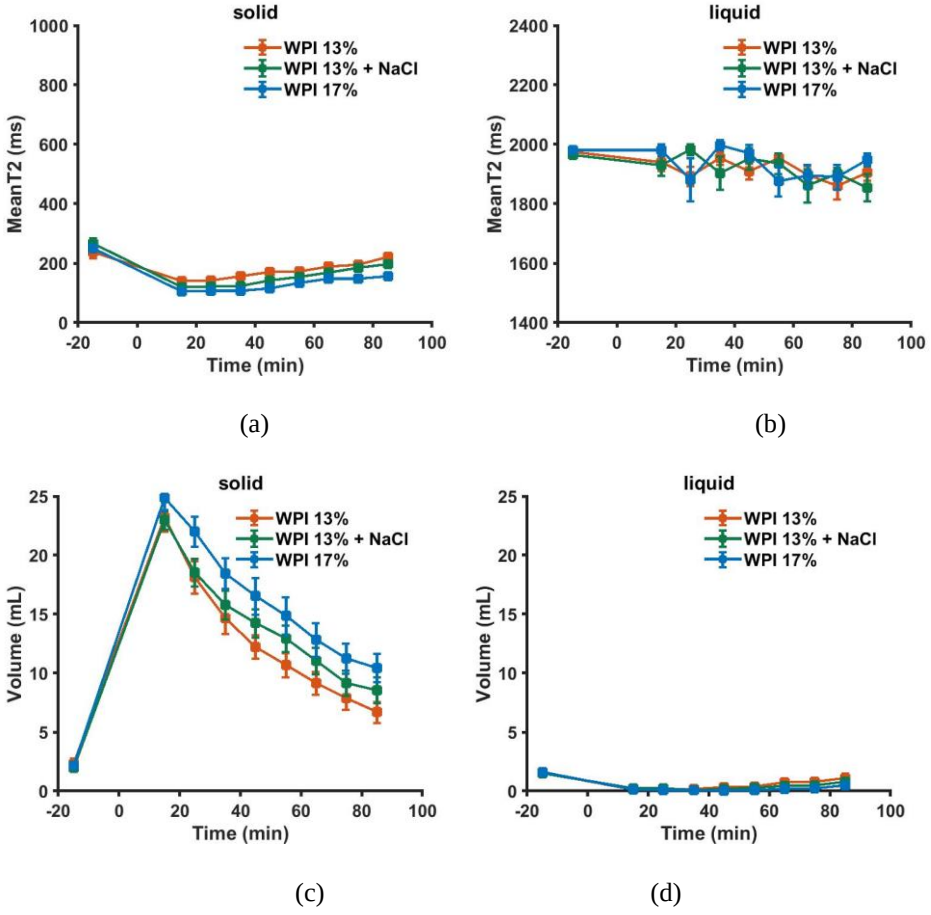

Fig. 6-S2 *Mean $T_2 \pm$ SE of the solid (a) and liquid (b) phases and the volume of solid (c) and liquid (d) phases; Data is from the T_2 map acquired in Chapter 5. To be noted, the T_2 map did not cover the whole stomach. The different phases were defined by the approach illustrated by Fig. 6-2 in the section 6.3.1.*

References

Alyami, J., Whitehouse, E., Yakubov, G. E., Pritchard, S. E., Hoad, C. L., Blackshaw, E., … Marciani, L. (2019). Glycaemic, gastrointestinal, hormonal and appetitive responses to pearl millet or oats porridge breakfasts: a randomised, crossover trial in healthy humans. British Journal of Nutrition, 122(10), 1142–1154. https://doi.org/10.1017/S0007114519001880

Angel, M., Zisserman, A. P., & Brady, M. (2002). Estimation of the partial volume effect in MRI, 6, 389–405.

Barclay, T., Ginic-Markovic, M., Johnston, M., Cooper, P., & Petrovsky, N. (2012). Analysis of the hydrolysis of inulin using real time H-1 NMR spectroscopy. Carbohydrate Research, 352, 117–125. https://doi.org/10.1016/j.carres.2012.03.001

Bohn, T., Carriere, F., Day, L., Deglaire, A., Egger, L., Freitas, D., … Dupont, D. (2018, September). Correlation between *in vitro* and *in vivo* data on food digestion. What can we predict with static *in vitro* digestion models? Critical Reviews in Food Science and Nutrition. Taylor & Francis. https://doi.org/10.1080/10408398.2017.1315362

Bolhuis, D. P., & Forde, C. G. (2020). Application of food texture to moderate oral processing behaviors and energy intake. Trends in Food Science and Technology, 106(June), 445–456. https://doi.org/10.1016/j.tifs.2020.10.021

Bolhuis, D. P., Forde, C. G., Cheng, Y., Xu, H., Martin, N., & De Graaf, C. (2014). Slow food: sustained impact of harder foods on the reduction in energy intake over the course of the day. PLoS ONE, 9(4), 1–7. https://doi.org/10.1371/journal.pone.0093370

Bornhorst, G. M., & Singh, R. P. (2014). Gastric digestion *in vivo* and *in vitro*: how the structural aspects of food influence the digestion process. Annual Review of Food Science and Technology, 5(1), 111–132. https://doi.org/10.1146/annurev-food-030713-092346

Brown, R. P., Delp, M. D., Lindstedt, S. L., Rhomberg, L. R., & Beliles, R. P. (1997). Physiological parameter values for physiologically based pharmacokinetic models. Toxicology and Industrial Health, 13(4), 407–484.

Camps, G., Mars, M., De Graaf, C., & Smeets, P. A. M. (2016). Empty calories and phantom fullness: A randomized trial studying the relative effects of energy density and viscosity on gastric emptying determined by MRI and satiety. American Journal of Clinical Nutrition, 104(1), 73–80. https://doi.org/10.3945/ajcn.115.129064

Camps, G., van Eijnatten, E. J. M., van Lieshout, G. A. A., Lambers, T. T., & Smeets, P. A. M. (2021). Gastric emptying and intragastric behavior of breast milk and infant formula in lactating mothers. The Journal of Nutrition, 151(12), 3718–3724. https://doi.org/10.1093/jn/nxab295

Chen, J. (2009). Food oral processing-A review. Food Hydrocolloids, 23(1), 1–25. https://doi.org/10.1016/j.foodhyd.2007.11.013

Coletta, M., Gates, F. K., Marciani, L., Shiwani, H., Major, G., Hoad, C. L., … Spiller, R. C. (2016). Effect of bread gluten content on gastrointestinal function: A crossover MRI study on healthy humans. British Journal of Nutrition, 115(1), 55–61. https://doi.org/10.1017/S0007114515004183

Deng, R., Janssen, A. E. M., Vergeldt, F. J., Van As, H., de Graaf, C., Mars, M., & Smeets, P. A. M. (2020). Exploring *in vitro* gastric digestion of whey protein by time-domain nuclear magnetic resonance and magnetic resonance imaging. Food Hydrocolloids, 99, 105348. https://doi.org/10.1016/j.foodhyd.2019.105348 *(Chapter 2 in this thesis)*

Deng, R., Seimys, A., Mars, M., Janssen, A. E. M., & Smeets, P. A. M. (2022). Monitoring pH and

whey protein digestion by TD-NMR and MRI in a novel semi-dynamic *in vitro* gastric simulator (MR-GAS). Food Hydrocolloids, 125, 107393. https://doi.org/10.1016/j.foodhyd.2021.107393 *(Chapter 4 in this thesis)*

Deng, R., Mars, M., Van Der Sman, R. G. M., Smeets, P. A. M., & Janssen, A. E. M. (2020). The importance of swelling for *in vitro* gastric digestion of whey protein gels. Food Chemistry, 330, 127182. https://doi.org/10.1016/j.foodchem.2020.127182 *(Chapter 3 in this thesis)*

Dupont, D., Alric, M., Blanquet-Diot, S., Bornhorst, G., Cueva, C., Deglaire, A., … Van den Abbeele, P. (2019). Can dynamic *in vitro* digestion systems mimic the physiological reality? Critical Reviews in Food Science and Nutrition, 59(10), 1546–1562. https://doi.org/10.1080/10408398.2017.1421900

Elashoff, J. D., Reedy, T. J., & Meyer, J. H. (1982). Analysis of Gastric Emptying Data. Gastroenterology, 83(6), 1306–1312. https://doi.org/10.1016/S0016-5085(82)80145-5

Ercolini, D., & Fogliano, V. (2018). Food Design to Feed the Human Gut Microbiota. Journal of Agricultural and Food Chemistry, 66(15), 3754–3758. https://doi.org/10.1021/acs.jafc.8b00456

Erlandsson, K., Buvat, I., Pretorius, P. H., Thomas, B. A., & Hutton, B. F. (2012). A review of partial volume correction techniques for emission tomography and their applications in neurology, cardiology and oncology. Physics in Medicine and Biology. https://doi.org/10.1088/0031-9155/57/21/R119

Ferrua, M. J., & Singh, R. P. (2010). Modeling the fluid dynamics in a human stomach to gain insight of food digestion. Journal of Food Science, 75(7), 151–162. https://doi.org/10.1111/j.1750-3841.2010.01748.x

Forde, C. G., Leong, C., Chia-Ming, E., & McCrickerd, K. (2017). Fast or slow-foods? Describing natural variations in oral processing characteristics across a wide range of Asian foods. Food and Function, 8(2), 595–606. https://doi.org/10.1039/c6fo01286h

Forde, Ciarán G., Mars, M., & De Graaf, K. (2020). Ultra-processing or oral processing? A role for energy density and eating rate in moderating energy intake from processed foods. Current Developments in Nutrition, 4(3), 1–7. https://doi.org/10.1093/cdn/nzaa019

Goetze, O., Treier, R., Fox, M., Steingoetter, A., Fried, M., Boesiger, P., & Schwizer, W. (2009). The effect of gastric secretion on gastric physiology and emptying in the fasted and fed state assessed by magnetic resonance imaging. Neurogastroenterology and Motility, 21(7), 725–734. https://doi.org/10.1111/j.1365-2982.2009.01293.x

Guo, Q., Ye, A., Lad, M., Dalgleish, D., & Singh, H. (2013). The breakdown properties of heat-set whey protein emulsion gels in the human mouth. Food Hydrocolloids, 33(2), 215–224. https://doi.org/10.1016/j.foodhyd.2013.03.008

Hall, K. D., Ayuketah, A., Brychta, R., Cai, H., Cassimatis, T., Chen, K. Y., … Zhou, M. (2019). Ultra-processed diets cause excess calorie intake and weight gain: An Inpatient Randomized Controlled Trial of Ad Libitum Food Intake, 30(1), 67–77. https://doi.org/10.1016/j.cmet.2019.05.008.Ultra-processed

Hoad, C. L., Parker, H., Hudders, N., Costigan, C., Cox, E. F., Perkins, A. C., … Gowland, P. A. (2015). Measurement of gastric meal and secretion volumes using magnetic resonance imaging. Physics in Medicine and Biology, 60(3), 1367–1383. https://doi.org/10.1088/0031-9155/60/3/1367

Houghton, L. A., Read, N. W., Heddle, R., Horowitz, M., Collins, P. J., Chatterton, B., & Dent, J. (1988). Relationship of the motor activity of the antrum, pylorus, and duodenum to gastric emptying of a solid-liquid mixed meal. Gastroenterology, 94(6), 1285–1291. https://doi.org/10.1016/0016-5085(88)90665-8

Hunt, J. N., & Stubbs, D. F. (1975). The volume and energy content of meals as determinants of gastric emptying. The Journal of Physiology, 245(1), 209–225. https://doi.org/10.1113/jphysiol.1975.sp010841

Kong, F., & Singh, R. P. (2008). A model stomach system to investigate disintegration kinetics of solid foods during gastric digestion. Journal of Food Science, 73(5), 202–210. https://doi.org/10.1111/j.1750-3841.2008.00745.x

Kostewicz, E. S., Aarons, L., Bergstrand, M., Bolger, M. B., Galetin, A., Hatley, O., … Dressman, J. (2014). PBPK models for the prediction of *in vivo* performance of oral dosage forms. European Journal of Pharmaceutical Sciences, 57(1), 300–321. https://doi.org/10.1016/j.ejps.2013.09.008

Le Dean, A., Mariette, F., & Marin, M. (2004). 1H nuclear magnetic resonance relaxometry study of water state in milk protein mixtures. Journal of Agricultural and Food Chemistry, 52(17), 5449–5455. https://doi.org/10.1021/jf030777m

Le Feunteun, S., Al-Razaz, A., Dekker, M., George, E., Laroche, B., & Van Aken, G. (2021). Physiologically based modeling of food digestion and intestinal microbiota: state of the art and future challenges. An INFOGEST Review. Annual Review of Food Science and Technology, 12, 149–167. https://doi.org/10.1146/annurev-food-070620-124140

Luo, Q., Boom, R. M., & Janssen, A. E. M. (2015). Digestion of protein and protein gels in simulated gastric environment. LWT - Food Science and Technology, 63(1), 161–168. https://doi.org/10.1016/j.lwt.2015.03.087

Luo, Q., Borst, J. W., Westphal, A. H., Boom, R. M., & Janssen, A. E. M. (2017). Pepsin diffusivity in whey protein gels and its effect on gastric digestion. Food Hydrocolloids, 66, 318–325. https://doi.org/10.1016/j.foodhyd.2016.11.046

Luo, Q., Zhan, W., Boom, R. M., & Janssen, A. E. M. (2018). Interactions between acid and proteins under *in vitro* gastric condition-a theoretical and experimental quantification. Food and Function, 9(10), 5283–5289. https://doi.org/10.1039/c8fo01033a

Mackie, A. R., Bajka, B. H., Rigby, N. M., Wilde, P. J., Alves-Pereira, F., Mosleth, E. F., … Salt, L. J. (2017). Oatmeal particle size alters glycemic index but not as a function of gastric emptying rate. American Journal of Physiology - Gastrointestinal and Liver Physiology, 313(3), G239–G246. https://doi.org/10.1152/ajpgi.00005.2017

Marciani, L., Manoj, P., Hills, B. P., Moore, R. J., Young, P., Fillery-Travis, A., … Gowland, P. A. (1998). Echo-planar imaging relaxometry to measure the viscosity of a model meal. Journal of Magnetic Resonance, 135(1), 82–86. https://doi.org/10.1006/jmre.1998.1560

Marciani, L, Gowland, P. a, Spiller, R. C., Manoj, P., Moore, R. J., Young, P., & Fillery-Travis, a J. (2001). Effect of meal viscosity and nutrients on satiety, intragastric dilution, and emptying assessed by MRI. American Journal of Physiology. Gastrointestinal and Liver Physiology, 280(6), G1227–G1233. https://doi.org/10.1152/ajpgi.2001.280.6.G1227

Marciani, L, Gowland, P. A., Fillery-Travis, A., Manoj, P., Wright, J., Smith, A., … Spiller, R. C. (2001). Assessment of antral grinding of a model solid meal with echo-planar imaging. American Journal of Physiology-Gastrointestinal and Liver Physiology, 280(5), G844–G849. https://doi.org/10.1152/ajpgi.2001.280.5.G844

Marciani, L, Gowland, P. A., Spiller, R. C., Manoj, P., Moore, R. J., Young, P., & Fillery-Travis, A. J. (2001). Effect of meal viscosity and nutrients on satiety, intragastric dilution, and emptying assessed by MRI. American Journal of Physiology - Gastrointestinal and Liver Physiology, 280(6 43-6), 1227–1233. https://doi.org/10.1152/ajpgi.2001.280.6.g1227

Mariette, F. (2009). Investigations of food colloids by NMR and MRI. Current Opinion in Colloid and Interface Science, 14(3), 203–211. https://doi.org/10.1016/j.cocis.2008.10.006

Mayar, M., Miltenburg J., Hettinga, K., Smeets, P., van Duynhoven, J. & Terenzi, C.. (2022). Non-invasive monitoring of *in vitro* gastric milk protein digestion kinetics by 1H NMR magnetization transfer. Food Chemistry, under review.

Ménard, O., Cattenoz, T., Guillemin, H., Souchon, I., Deglaire, A., Dupont, D., & Picque, D. (2014). Validation of a new *in vitro* dynamic system to simulate infant digestion. Food Chemistry, 145, 1039–1045. https://doi.org/10.1016/j.foodchem.2013.09.036

Mennah-Govela, Y. A., Singh, R. P., & Bornhorst, G. M. (2019). Buffering capacity of protein-based model food systems in the context of gastric digestion. Food & Function, 10(9), 6074–6087. https://doi.org/10.1039/C9FO01160A

Minekus, M., Alminger, M., Alvito, P., Ballance, S., Bohn, T., Bourlieu, C., … Brodkorb, A. (2014). A standardised static *in vitro* digestion method suitable for food-an international consensus. Food and Function, 5(6), 1113–1124. https://doi.org/10.1039/c3fo60702j

Mosca, A. C., & Chen, J. (2017). Food-saliva interactions: mechanisms and implications. Trends in Food Science and Technology, 66, 125–134. https://doi.org/10.1016/j.tifs.2017.06.005

Mulet-Cabero, A. I., Egger, L., Portmann, R., Ménard, O., Marze, S., Minekus, M., … Mackie, A. (2020). A standardised semi-dynamic: *in vitro* digestion method suitable for food-an international consensus. Food and Function, 11(2), 1702–1720. https://doi.org/10.1039/c9fo01293a

Muttakin, S., Moxon, T. E., & Gouseti, O. (2019). *In vivo*, *In vitro*, and *In silico* Studies of the GI Tract. In O. Gouseti, G. M. Bornhorst, S. Bakalis, & A. Mackie (Eds.), Interdisciplinary Approaches to Food Digestion (pp. 29–67). Cham: Springer International Publishing. https://doi.org/10.1007/978-3-030-03901-1_3

Nadia, J., Olenskyj, A. G., Stroebinger, N., Hodgkinson, S. M., Estevez, T. G., Subramanian, P., … Bornhorst, G. M. (2021). Tracking physical breakdown of rice-and wheat-based foods with varying structures during gastric digestion and its influence on gastric emptying in a growing pig model. Food and Function, 12(10), 4349–4372. https://doi.org/10.1039/d0fo02917c

Nieva-Echevarría, B., Goicoechea, E., Manzanos, M. J., & Guillén, M. D. (2015). Usefulness of 1H NMR in assessing the extent of lipid digestion. Food Chemistry, 179, 182–190. https://doi.org/https://doi.org/10.1016/j.foodchem.2015.01.104

Palmer, A. G. (2014). Chemical exchange in biomacromolecules: Past, present, and future. Journal of Magnetic Resonance, 241, 3–17. https://doi.org/10.1016/J.JMR.2014.01.008

Peters, J. P. C. M., Vergeldt, F. J., Van As, H., Luyten, H., Boom, R. M., & van der Goot, A. J. (2016). Time domain nuclear magnetic resonance as a method to determine and characterize the water-binding capacity of whey protein microparticles. Food Hydrocolloids, 54, 170–178. https://doi.org/10.1016/j.foodhyd.2015.09.031

Smeets, P. A. M., Deng, R., van Eijnatten, E. J. M., & Mayar, M. (2020). Monitoring food digestion with magnetic resonance techniques. Proceedings of the Nutrition Society, 1–11. https://doi.org/10.1017/S0029665120007867

Spiller, R., & Marciani, L. (2019). Intraluminal Impact of Food: New Insights from MRI. Nutrients, 11(5), 1147. https://doi.org/10.3390/nu11051147

Sundekilde, U. K., Jarno, L., Eggers, N., & Bertram, H. C. (2018). Real-time monitoring of enzyme-assisted animal protein hydrolysis by NMR spectroscopy – An NMR reactomics concept. Lwt, 95(January), 9–16. https://doi.org/10.1016/j.lwt.2018.04.055

Thévenot, J., Cauty, C., Legland, D., Dupont, D., & Floury, J. (2017). Pepsin diffusion in dairy gels depends on casein concentration and microstructure. Food Chemistry, 223, 54–61. https://doi.org/10.1016/j.foodchem.2016.12.014

Treier, R., Steingoetter, A., Goetze, O., Fox, M., Fried, M., Schwizer, W., & Boesiger, P. (2008). Fast and optimized T1 mapping technique for the noninvasive quantification of gastric secretion. Journal of Magnetic Resonance Imaging, 28(1), 96–102. https://doi.org/10.1002/jmri.21400

van der Sman, R. G. M., Houlder, S., Cornet, S., & Janssen, A. (2019). Physical chemistry of gastric digestion of proteins gels. Current Research in Food Science, 1–26. https://doi.org/10.1016/j.crfs.2019.11.003

Van Duynhoven, J. P. M., & Jacobs, D. M. (2016). Assessment of dietary exposure and effect in humans: The role of NMR. Progress in Nuclear Magnetic Resonance Spectroscopy, 96, 58–72. https://doi.org/10.1016/j.pnmrs.2016.03.001

Wáng, Y.-X. J., Zhang, Q., Li, X., Chen, W., Ahuja, A., & Yuan, J. (2015). T1ρ magnetic resonance: basic physics principles and applications in knee and intervertebral disc imaging. Quantitative Imaging in Medicine and Surgery, 5(6), 858–885. https://doi.org/10.3978/j.issn.2223-4292.2015.12.06

Witt, T., & Stokes, J. R. (2015). Physics of food structure breakdown and bolus formation during oral processing of hard and soft solids. Current Opinion in Food Science, 3, 110–117. https://doi.org/10.1016/j.cofs.2015.06.011

Wu, P., & Chen, X. (2020). On designing biomimic *in vitro* human and animal digestion track models: ideas, current and future devices. Current Opinion in Food Science, 35, 10–19. https://doi.org/10.1016/j.cofs.2019.12.004

Summary

A better understanding of the gastric digestion of solid food will allow for a more thorough exploration of the relationship between food properties and the physiological mechanisms underlying the digestion of nutrients. The breakdown of food structures has mainly been studied via *in vitro* models, which can provide detailed information about the effects of enzymatic processes on the physical and chemical characteristics of food structures. However, these results have been verified only to a limited extent *in vivo*. This limitation necessitates the investigation of the potential use of non-invasive approaches to bridge the link between *in vivo* and *in vitro* digestion research. Thus, the objective of this thesis was to investigate the potential of magnetic resonance (MR) techniques in monitoring gastric digestion of solid food in static, (semi-)dynamic *in vitro* models and in humans.

The work began with a well-controlled *in vitro* static digestion model in **Chapter 2**. With this model, we explored the use of time-domain nuclear magnetic resonance (TD-NMR) and magnetic resonance imaging (MRI) to monitor the gastric digestion of whey protein (solution and gel). During digestion, free amino groups ($-NH_2$ groups) and protein concentrations in the supernatant were measured. Transverse relaxation time (T_2) values of the digestion mixture were determined by TD-NMR and MRI, and transverse relaxation rate ($R_2 = T_2^{-1}$) was calculated. Subsequently, relative amplitudes (TD-NMR) for different T_2 values and T_2 distribution (MRI) were determined. For the solution, protein concentration and T_2 did not change during digestion. For the gels, water in the both supernatant and gel phase could be discriminated on the basis of their T_2 values. During digestion, R_2 of the supernatant correlated positively with the protein ($-NH_2$ groups) concentration in the supernatant. In contrast, the relative amplitude of the gel fraction had a negative linear correlation with the supernatant protein concentration. MRI T_2-mapping showed similar associations between R_2 of supernatant and protein ($-NH_2$ groups) concentration. Thus, R_2 was shown to be a useful marker to monitor *in vitro* gastric digestion of whey protein gels and TD-NMR measurements contributed to interpreting the MRI data.

TD-NMR results from **Chapter 2** showed that water transportation (namely swelling) took place during digestion and may be of great importance for digestion rate. Therefore, we investigated the effect of swelling on gastric digestion of protein gels in **Chapter 3**. Whey protein gels with NaCl concentrations of 0-0.1 M were used as model foods. Young's modulus, swelling ratio, acid uptake and digestion rate of the gels were measured. Pepsin

transport was monitored by confocal laser scanning microscopy using green fluorescent protein (GFP), which has a similar size as pepsin. We observed that an increase of NaCl in gels corresponded with increased Young's modulus, reduced swelling and slower digestion. Additionally, a reduction of acid transport was observed, as well as a reduction of GFP both at the surface and in the gels. This shows that swelling affects digestion rate not only by enhancing acid diffusion but also by modulating the partitioning of pepsin at the food-gastric fluid interface and thereby the total amount of pepsin in the food particle. This perspective on swelling provides new insight for designing food with a specific digestion rate for targeted dietary demands.

The work in **Chapter 2** was performed under static conditions, i.e., it did not consider the dynamic circumstances in the human body, such as gastric secretion and gastric emptying. To account for this, further work was conducted in **Chapter 4**. We developed a novel MRI-compatible semi-dynamic gastric simulator (MR-GAS) that includes controlled gastric secretion, emptying and mixing at body temperature, and applied it to investigate the potential of relaxation rates on monitoring digestion under the dynamic set-up. During protein gel digestion, pH and protein hydrolysis were measured. R_2 and R_1 (= T_1^{-1}) of the supernatant were measured by time-domain nuclear magnetic resonance (TD-NMR). The stomach chamber of the MR-GAS was scanned with MRI to measure R_2 and R_1. With TD-NMR, 99% of the variance in R_2 and 96% of the variance in R_1 could be explained as a function of protein concentration and [H^+]. With MRI, the explained variances were 99% for R_2 and 60% for R_1. From these analyses, the obtained equations enabled the prediction of protein concentration and pH with measured R_2 and R_1 values. The normalised root mean squared deviation of the predictions for protein concentration were 0.15 (NMR) and 0.18 (MRI), and for pH were 0.12 (NMR) and 0.29 (MRI). This shows that the MR-GAS model may be used in a clinical MRI scanner to monitor gastric digestion under *in vitro* dynamic circumstances, by measuring R_2 and R_1. These results underscored the potential of MRI to monitor nutrient hydrolysis and pH changes in *in vivo* studies. Therefore, in **Chapter 5**, we conducted a human randomized cross-over trial in which we assessed the effect of food hardness and protein content on gastric emptying and additionally investigated the application of the T_1 and T_2 to monitor *in vivo* gastric digestion.

The trial was conducted with 18 healthy males who were provided with three gels differing in hardness and protein content: a soft gel with low protein content (Soft-LP), a hard gel

with low protein content (Hard-LP), and a hard gel with high protein content (Hard-HP). Before and after ingestion, abdominal MRI scans and appetite and well-being ratings were obtained until t = 85 min after the start of ingestion. At t = 100 min participants ate an ad libitum lunch. Overall, gastric content volume was different among the treatments: High-HP < Soft-HP < Soft-LP,. After all treatments, mean T_2 and T_1 of the measured stomach content decreased after ingestion from baseline and then gradually increased from 15 min onwards. The treatments resulted in different T_1 and T_2 values: Hard-HP < Soft-HP < Soft-LP, although not all the time points differed significantly. The high protein content was the main factor in delaying gastric emptying and high hardness was the secondary factor. Lower gastric emptying rate did not affect subsequent food intake. T_1 and T_2 measurements can provide extra information on the dilution and digestion taking place in the stomach. This study suggests the potential of MRI parameters for providing more insights on *in vivo* digestion, and its results may contribute to linking *in vitro* and *in vivo* digestion research.

Finally, **Chapter 6** discusses findings from *in vitro* models to *in vivo* human trials in this thesis. It provides an overview of the application of MR techniques to measure gastric digestion, the added value of MRI measurements for digestion research, and the effects of food properties on gastric digestion. To conclude, MR techniques can provide molecular-level and quantitative information on protein hydrolysis in solid food through T_1 and T_2 measurements. Moreover, the findings from this thesis can aid in informing *in vitro* and *in silico* models and bridging the link between *in vitro* and *in vivo* digestion research.

Acknowledgement

Acknowledgement

Time flies by...When I am writing the acknowledgement, my PhD journey is almost to the end. I am so lucky that I am always surrounded by a group of intelligent, supportive and lovely people. Therefore, I would like to take the chance to express my gratitude to everyone who has inspired, guided, and supported me during these years.

First and foremost, I would like to sincerely thank my supervisors. Kees, we first met in China in 2016 when I was in the last year of my MSc study. Thank you for introducing me to this awesome PhD project and building a brilliant supervision team for me. Monica, thank you for your support, not only on the project but also on my well-being with all the personal talks. Thank you for helping me with statistics and for valuable input from a nutritionist's point of view. Thank you Paul for your guidance on my research work and scientific writing, I truly appreciate and enjoy spending time with you for MRI data collection and analysis. I will never forget the late afternoon/evenings that we spent in the hospital for the scanning. Anja, thank you for being constantly supportive and always helpful with the challenges I faced with. I admire and learned a lot from your work attitude as a researcher, a teacher, and a supervisor. I am grateful for your being supportive not only on my project but also in my personal life. Thank you for helping me to move during the pandemic in the summer of 2020. I always feel lucky to have such a luxury supervision team as you gave me the freedom to explore and provided me with crucial guidance from different perspectives. Remko, although you are not officially my supervisor, thank you for taking the time to have meetings with me from time to time. Your innovative ideas always inspire me a lot.

I would also like to thank all other co-authors. Frank and Henk, thank you for the discussion at the beginning of my PhD, You are so patient to help me with the difficulties that I encountered with TD-NMR. Ruud, thank you for the discussion and input on the swelling paper. Aurimas, it was great to work together with MRI in the evenings and weekends in the hospital. Together we built our Mr. GAS digestion model. Much Appreciated!

I would also like to thank my thesis committee Prof. Vincenzo Fogliano, Prof. Alan Mackie, Prof. Ad Masclee and Dr Tim Lambers for reading my thesis and being present at my defence.

Thank you Frank for instructing me on the Maran (TD-NMR) and for your great patience to answer all my questions. Thank you Arjen for training me to use the MRI scanner in the hospital (Ziekenhuis Gelderse Vallei), and for helping us improve the MRI sequences. My appreciation to Paul de Bruin, thank you for being patient to help me optimize the MRI sequences on the Philips scanner and working with me sometimes even till late evenings.

Thank you, Morwarid, Elise, Julia, and Dan for the chats and the meetings. I enjoyed your company on the journey of investigating gastric digestion with MRI. Thank you, Ciáran, Marlou, Lise, Yong for working together on the OffR study after I handed in the reading version of my thesis. The sandwiches and pizza tasting made my post PhD defence days much busier but more fun!

During my PhD, I received a lot of support from people at the laboratory of Food Process Engineering (FPE). I would like to start with Jos, Maurice, Jarno, and Wouter, thank you for solving lab problems for me and my students. Wanqing, Sicong, Lu, Konstantina, Isabel, Sirinan, Boxin, Qinhui, Qi, Jun, Zhaojun, Eric, Jilu, Katharina, Andrea, Anna, Anouk, Nattawan, Eric, Joanna, Hilda, Yizhou, Lingfeng, Yifeng, Zhaoxiang, Mingzhao, Thank you for the time in the lab, the dinners, chats, and all other activities we had together.

My dear colleagues from HNH, I would like to thank you all for creating an enjoyable working environment! Jasmijn and Gea, thank you for your help with solving countless problems regarding the visa, reimbursement, course registration etc. Els and Corrine, thank you for arranging for me to use the human unit research facility. Asrullah, Marion, Charlotte, Giulia, Marielle, Pauline, Guido, Marlou, Eva Ketel, Eva Cad, Matjaz, Lennke, Rachelle, Elbrich, Santiago, Eva, Romain, Katherine, Duong, Mashina, Danny, Mingjuan, Hongyi, Thank you all for creating a pleasant environment to discuss work or non-work related topics. We shared a lot of nice memories. Thank all the PhD tour numbers for an awesome trip in Canada in the autumn of 2019.

I would like to thank all my students during my PhD: Yusi, Karen, Isabella, Renee, Aurimas, Naska, Ilja, Keita, Eliana, Yoshinta. It was a great pleasure to work with you. I learned a lot from you as well as from the supervision process.

My lovely officemates, Apple, Vera, Marie, Elly, Pol, Desiree, Xinmeng, Cong, Peiheng, Son, Carina, Gerdine. Thank you for all the nice chats and coffee (/tea) breaks, dinners, Sinterklaas celebration and game nights. Back in the autumn of 2017, you guys helpt me a lot to integrate into the new environment.

Tsitsi and Polly, thank you for being my paranymphs. Tsitsi, it was awesome to go through my PhD journey with your accompany. We are so different but so similar. You can always understand my happiness and struggles. Although we fought for certain things, it never stops us from being good friends. Polly, I always come to you when I lack courage. Your advice and your amazing food can cure me immediately. Thank you for all the beautiful memories you add to my life. To dear amigas, Maria J., Maria S., Lupita, Liangzi, Thank you for the fun time we had, the holiday trips, the cycling trips, the dinners, game or movie nights. Your hugs always make me feel safe and at home. Thank you Kamalita and Xiaolin for the delicious (Korean and other) food we had and the great chats, which gave me great mental support. Thank you Inga for being so kind and always supportive and for your always wise advice. Thank you Claudia for your encouragement and house-sitting period which made me more efficient on thesis writing. Thank you Son, Tesfaye, and Max, I enjoyed the dinners and coffee breaks that we had together and appreciate all the life tips that I receive from you.

Thank you, Sjoerd for teaching me Dutch, the nice chats and the lovely day trips we had. Thank you Jingrui, you encouraged me a lot when I was down. I appreciate your presence which helpt me grow up. Qi and Guangyuan, you always care about me not only from a friend's perspective but also more like my family, thank you for the dinners and the trips and the wise words, I truly cherish your presence in my life. Thank you Yuting and Jiahong, we are connected no matter where we are. Thank you Yu for always being an angel for me. Countless dinners and fun activities together, you saw all my tears and laughter. Sherly and Andreas, it was lovely to meet you in Copenhagen, thank you for showing up in my life before I finish my thesis writing. Thank you Youfeng for bringing me lots of fun time during and after my intense thesis writing stage and helping me to proof-read the booklet :)

Of course, I would not have come this far without the love and support from my family. 谢谢所有家人们，即便你们远在国内，你们的关心和牵挂都给我了无限的力量。妈妈爸爸，谢谢你们一直以来的支持，我从来都觉得自己是最幸运的小孩，遇上了世界上最棒的父母。即便你们不能认同我的所有观点，你们依旧支持我追求梦想，我很感激，我爱你们!

With love,

About the author

About the Author

Ruoxuan Deng (邓若璇) was born on June 27th 1995, in Henan Province, China. With strong interests in mathematics, chemistry and biology, she decided to study life science at the university.

From 2011 to 2017, She followed a BSc-MSc joint program in life science majoring in Food Science and Technology at Jiangnan University in China. Since her MSc, she started digestion research on "the effect of cellulose on the *in vitro* digestion rate of food matrix". With the curiosity to experience different cultures and research interest in food digestion, she started her PhD in Wageningen Univerisity & Research (WUR) in September 2017.

In WUR, She conducted her PhD project in the chair of Sensory Science and Eating Behaviour under the Division of Human Nutrition & Health and Laboratory of Food Process Engineering. This multi-disciplinary research project aims to investigate *in vitro* and *in vivo* (human) protein digestion by magnetic resonance imaging (MRI). The result of this research is presented in this thesis. During her PhD, she attended several international conferences and courses. She was awarded as the Best Young Researcher Speaker in Food Structures, Digestion & Health 6th International Conference. She was involved in teaching and supervising Bachelor's and Master's students. After submitting her thesis, Ruoxuan works as a postdoctoral researcher in WUR while awaiting her defence.

Contact her: ruoxuandeng@gmail.com

List of publications

Publications in peer reviewed journals

R. Deng, A.E.M. Janssen, F. J. Vergeldt, H. Van As, C. de Graaf, M. Mars, P.A.M. Smeets. (2020). Exploring *in vitro* gastric digestion of whey protein by time-domain nuclear magnetic resonance and magnetic resonance imaging. ***Food Hydrocolloids***, 99. https://doi.org/10.1016/j.foodhyd.2019.105348 (this thesis)

R. Deng, M. Mars, R. van der Sman, C. de Graaf, P.A.M. Smeets, A.E.M. Janssen. (2020). The importance of swelling: *in vitro* gastric digestion of whey protein gels. ***Food Chemistry***, 330, 127182. https://doi.org/10.1016/j.foodchem.2020.127182 (this thesis)

R. Deng, A. Seimys, M. Mars, A.E.M. Janssen, P.A.M. Smeets (2022). Monitoring pH and whey protein digestion by TD-NMR and MRI in a novel semi-dynamic *in vitro* gastric simulator. **Food Hydrocolloids**, 125. https://doi.org/10.1016/j.foodhyd.2021.107393 (this thesis)

P.A.M. Smeets, **R. Deng**, E. Van Eijnatten, M. Mayar, (2021). Monitoring food digestion with magnetic resonance techniques. ***Proceedings of the Nutrition Society***, 80(2), 148–158. https://doi.org/10.1017/S0029665120007867 (this thesis)

Submitted papers

L. Chen, **R. Deng**, W. Yokoyama, F. Zhong. Investigation of the effect of nanocellulose on the *in vitro* digestion of macronutrients.

Papers in preparation for submission

R. Deng, A.E.M. Janssen, M. Mars, P.A. M. Smeets. Gastric digestion of whey protein gels in human: an MRI study. (this thesis)

Abstracts and presentations

R. Deng, A.E.M. Janssen, M. Mars, P.A.M. Smeets. Gastric digestion of whey protein gels in human: an MRI study, Food Structures, Digestion & Health (FSDH) 6th International Conference, Australia (attending online), 2021. (*Oral* presentation, awarded as the Best Young-Researcher Speaker)

R. Deng, A.E.M. Janssen, M. Mars, P.A.M. Smeets. Monitoring pH and whey protein digestion by TD-NMR and MRI in a novel semi-dynamic *in vitro* gastric simulator Virtual International Conference on Food Digestion, Youtube, 2021. (*Oral* presentation)

R. Deng, A.E.M. Janssen, C. de Graaf, M. Mars, P.A.M. Smeets. The importance of swelling: *in vitro* gastric digestion of whey protein gels. European Federation of Food Science and Technology (EFFoST) 33rd International Conference, the Netherlands, 2019. (*Oral* presentation)

R. Deng, A.E.M. Janssen, C. de Graaf, M. Mars, P.A.M. Smeets. Monitoring gastric digestion of whey protein gel by MRI. European Federation of Food Science and Technology (EFFoST) 33rd International Conference, the Netherlands, 2019. (Nominated the best *poster* presentation)

R. Deng, A.E.M. Janssen, C. de Graaf, M. Mars, P.A.M. Smeets. Gastric digestion of structured food: combining *in vitro* and *in vivo* approaches. PhD trip, Canada, 2019. (*Oral* presentations)

R. Deng, A.E.M. Janssen, F. J. Vergeldt, H. Van As, C. de Graaf, M. Mars, P.A.M. Smeets. Exploring *in vitro* gastric digestion of whey protein by time-domain nuclear magnetic resonance and magnetic resonance imaging. 6th International Conference of Food Digestion, Granada, Spain, 2019. (*Oral* presentation)

R. Deng, A.E.M. Janssen, C. de Graaf, M. Mars, P.A.M. Smeets. Gastric digestion of structured food: combining *in vitro* and *in vivo* approaches. 5th Wageningen PhD Symposium, Wageningen, the Netherlands, 2018. (*Poster* presentation)

Overview of completed trainning activities

Discipine specific courses and activities		
In vivo NMR course	Utrecht, NL	2017
Healthy Food Design	Wageningen, NL	2018
Sensory Perception & Food Preference	Wageningen, NL	2018
Wageningen 5th PhD symposium	Wageningen, NL	2018
6th International Conference on Food Digestion	Granada, SP	2019
European Federation of Food Science and Technology 33rd International Conference	Rotterdam, NL	2019
Plant-based Foods and Protein Summit	online	2020
Virtual Internation Conference on Food Digestion	online	2021
Food Structures, Digestion & Health 6th International Conference	online	2021
Human Digestion and Absorption	Copenhagen, DK	2021
General courses and activities		
VLAG PhD week	Baarlo, NL	2017
Philosophy and Ethics of Food Science and Technology	Wageningen, NL	2018
Data Management	Wageningen, NL	2018
The Essentials of Scientific Writing and Presenting	Wageningen, NL	2018
Pitch training	Wageningen, NL	2019
Supervising thesis student	Wageningen, NL	2019
Scientific writing	Wageningen, NL	2020
Start to teach	Wageningen, NL	2021
Career perspective	Wageningen, NL	2021
Write grant proposal	Wageningen, NL	2021

Option courses and activities		
Preparation of research proposal	Baarlo, NL	2017
PhD study tour to Canada	CA	2019
Tasty talk (research chair group meeting)	Wageningen, NL	2017-2020
FPE group meeting	Wageningen, NL	2017-2020
Teaching: Supervising practicals in *FPE-32306 Food Digestion: Ingestion and Structure Breakdown*) Supervising MSc- and BSc- students	Wageningen, NL	2018-2022

This research described in this thesis was carried out at the division of Human Nutrition and Health and the laboratory of Food Process Engineering at Wageningen University. The research is supported by Chinese Scholarship Council.

Financial support from Wageningen Univerisity for printing this thesis is gratefully acknowledged.

About the cover

Want to watch a live show of stomach as a VIP? MRI is the right candidate to closely observe what's happening in real-time in the human stomach. Many other *in vivo* approaches can be used to measure human digestion as well, while most of them are invasive and/or indirect. That is why in the back of the cover, they are a bit further to the stage, among all the approaches, you can find there three example characters: blood parameters, gastric aspirate and appetite questionnaires. If you can give your attention to the left corner, three characters sit on the top platform further away from the main stage, those stand for analytical and physio-chemical approaches that can only be used to study *in vitro* gastric digestion. Again among all the approaches, three characters are given as examples: microscopy, rheology, and chemical analysis (from left to right). The design of the cover was inspired by dr. Guangyuan Jin and the cover was designed together with Jinhui Ye (Wuguan Design).